Zero-crossing Intervals of Gaussian and Symmetric Stable Processes

Yufei Cao, MSc

Thesis submitted to The University of Nottingham

for the degree of Doctor of Philosophy

Sep 2016

To my parents.

Abstract

The zero-crossing problem is the determination of the probability density function of the intervals between the successive axis crossings of a stochastic process. This thesis studies the properties of the zero-crossings of stationary processes belonging to the symmetric-stable class of Gaussian and non-Gaussian type, corresponding to the stability index $\nu = 2$ and $0 < \nu < 2$ respectively.

The statistical properties of zero-crossing intervals of Gaussian processes are strongly influenced by the form of their autocorrelation function. The thesis examines two broad classes of autocorrelation functions. One is exponentially bounded for large delay time, and the other one has a power-law asymptote. These cases respectively represent processes with short-term and long-term correlation memory. It is found that, on comparison with numerical simulations, zero-crossing intervals of short-term correlated Gaussian processes can be approximated by assuming that they form independent random variables. The general morphologies presented by the interval probability density function, and the moments associated with it, are identified qualitatively and determined quantitatively in terms of the smoothness of the underlying process and the rate at which the autocorrelation function decays. The asymptote of the probability density function for large intervals τ is a simple exponential $\sim \exp(-\theta\tau)$, where the 'persistence parameter' θ is a non-trivial constant involving the parameter of the autocorrelation function, and which is calculated quantitatively and compared with simulation

results.

For autocorrelation functions with power-law decaying tails, it is found that the approximation that zero-crossing intervals are independent random variables is not valid. The independence model shows that the tail of the interval density function is of power-law form, but simulation results show that it remains of exponential type provided that the power-law index γ is not too small compared with unity. Claims appearing in extant literature (Eichner et al., Physical Review E **75**, 011128 (2007)) that the asymptote of the large interval τ becomes a stretched exponential function are examined critically, and it is shown that processes with $\gamma \leq 1$ have infinite power and so are inadmissible. This can be corrected if the autocorrelation function possesses a cut-off at large delay times, whereupon the large τ asymptote for the density function once again becomes a simple exponential. The behaviours presented in terms of the properties of the cut-off are examined using theory and simulation.

This programme is continued to consider the zero-crossing intervals of symmetric stable non-Gaussian processes. These processes have infinite variance and consequently do not possess an autocorrelation function. Nevertheless, there is a quantity, termed 'coherence' which imbues 'memory', is defined for these processes and which maps continuously to a function of the Gaussian autocorrelation function when $\nu = 2$. Classes of coherence function corresponding to the exponential and power-law bounded autocorrelation functions are considered within the assumption that the intervals are independent. The properties of the interval density function and its moments are calculated as functions of the properties of the coherence function and the stability index $0 < \nu < 2$. It is shown that the general morphology of the interval density functions behave as for the Gaussian case.

Acknowledgements

I would like to thank my first supervisor Keith Hopcraft who suggested the topic of this thesis to me, and gave all necessary help in all the steps of this thesis. I truly value his advice and encouragement. I also would like to thank my second supervisor Eric Jakeman, who supervised this work during my studies.

I also would like to thank Guta Madalin and Frank Ball for being my internal assessors and discussing the subject during my annual reviews.

I would also like to thank all of my friends who supported me, especially Bosichan Gong.

Finally, I would like to thank my parents for always being there for me. Words cannot express how grateful I am to my parents. Without their constant support, I could not reach the end of this project. I thank my Mum for her unconditional love and my Dad for constant encouragement.

Contents

Chapter 1

Introduction

1.1 Background

Natural and economic disasters, such as floods, droughts, earthquakes, and economic recession, occur intermittently and bring enormous damages to life and property in human society. Hence, it is profitable to study their properties of occurrence and develop technique related to their prediction regarding the frequency of the events in a given period, and the time intervals between the events. These are, by their nature, random variables and so the machinery of stochastic processes is a tool that can be utilised for their study. There are extensive literatures concentrated on issues of the occurrence and properties of such catastrophic events. For example, the classical extreme value theory shows the distribution of extreme maximal values of a given random variable [1].

In contrast to the classical extreme value theory, another way to consider extreme events is to investigate the distributions of returns/occurrence intervals *between* these events. That is the so-called the zero/level-crossing analysis of random processes, whose the main aim is to determine the probability distribution of zero/level-crossing intervals. This problem is illustrated in Figure 1.1, and has been researched extensively since the pioneering works
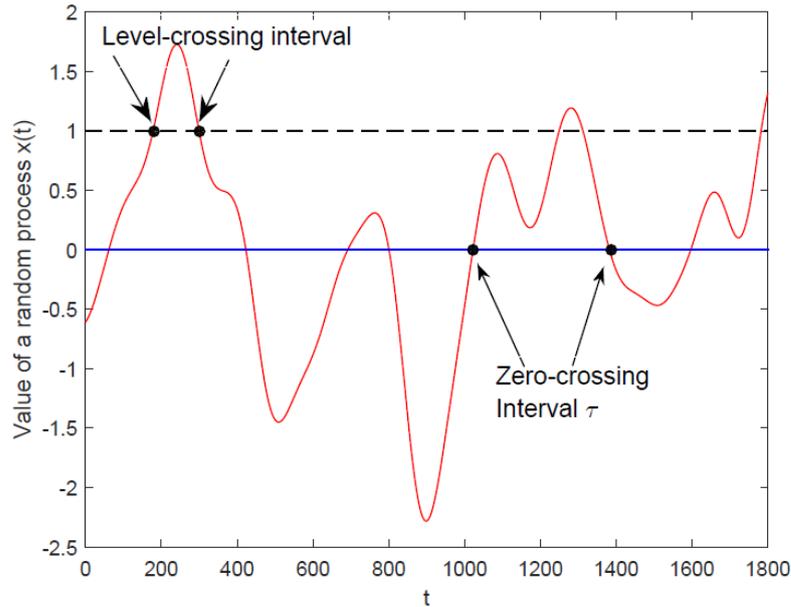
Figure 1.1: This figure shows that the goal in the zero/level-crossing analysis is to determine the probability density function of the zero-crossing interval τ.

of Kac [2] and Rice [3, 4]. Although the study dates back to the 1940s, there are few rigorous and exact solutions to the entire problem. So far, the mean of the zero-crossing interval τ has been obtained, but its probability density function is still unknown in all generality. Such a problem is not only of physical and theoretical importance but is also of practical importance. For example, the related fields of the zero-crossing problem include signal processing [5, 6], communications [7], reliability [8, 9], stock market [10], and oceanography [11, 12]. More applications of the zero-crossing analysis can be found in Blake and Lindsey [13].

For the most commonly studied random processes, a Gaussian process with an arbitrary autocorrelation function, the probability density function of zero crossing intervals cannot be derived explicitly by analytical methods. Hence, the thesis investigates zero-crossing intervals of Gaussian processes through numerical methods and simulations before using these results to inform a theoretical description. The thesis is motivated by wide applications of Gaussian distributions and is to analyse statistical properties of zero-

crossing intervals of Gaussian processes.

In 1924, Paul Lévy investigated the sum of independent and identical random variables, and defined the notion of stable random variables and processes [14], which will be reviewed later. He pointed out that the Gaussian random variable is a special case in the class of stable random variables. Most results of the zero-crossing problem are known for the Gaussian process. Hence, it is natural to generalise such results to the non-Gaussian stable case. A few results concern the zero-crossing problem of the stable processes, and these will be described in Chapter 5 and 6 of this thesis. These two chapters investigate the zero-crossing problem of the *symmetric* stable non-Gaussian process. Such a process introduces the concept of the coherence function [15], which measures the 'correlations' between two different time lags of the process. These two chapters consider the zero-crossing intervals when the underlying process with the coherence function has either the exponential or the power-law asymptotic behaviour since it will be seen later that the properties of zero-crossing intervals are influenced by the structure of the coherence function. The methodology is inherited from the Gaussian case.

1.2 Literature review

The research literature, which has an effect on the thesis, includes two parts. The first part reviews the zero-crossing interval problem, and then stable random variables are introduced.

1.2.1 The zero-crossing analysis

The zero/level-crossing problem of random processes began with the work of Kac [2] and Rice [3, 4]. The major review regarding the zero/level-crossings of random processes was given by Blake and Lindsey [13].

Chapter 1

In 1945, Rice derived the formula for the mean rate of zero-crossings per unit time (namely, the zero-crossing rate β) for Gaussian processes

$$\beta = \frac{1}{\pi} \sqrt{-\rho''(0)},$$

where $\rho(t) = \langle x(t')x(t'+t) \rangle$ is the autocorrelation function of the Gaussian process $\{x(t)\}$ with zero mean and unit variance. Others [16–18] also derived the same formula. Rice's formula is very simple and only requires that the second derivative of $\rho(t)$ evaluated at the origin is finite. This condition also implies that the underlying Gaussian process has to be smooth and differentiable. If the second derivative of $\rho(t)$ at the origin does not exist, it means that the number of zero-crossings per unit time is infinite and that the zero-crossing intervals are infinitesimally small. Hence, this thesis considers the zero-crossing problem with the finite zero-crossing rate. Rice's formula is important for the zero-crossing problem because the approach Rice developed can be generalised to other random processes [19].

Another significant contribution by Rice was that he obtained an approximation to the probability density function of zero-crossing intervals. Others [11, 20] tried to improve Rice's approximation. The only known exact analytical result of the probability density function of zero-crossing intervals was obtained by Wong [21] for the Gaussian process with a specific autocorrelation function. Wong expressed this density function in terms of complete elliptic integrals, and one can use this closed form result for verification of computer codes when simulating the zero-crossing problem.

McFadden [22, 23] focused on the same problem without assuming the underlying process is Gaussian distributed. Parts of his results are reviewed in Chapter 2.

The zero-crossing problem is closely related to another problem: the persistence probability, which measures how long the process stays above/below a set level. The precise definition of persistence is as follows. Consider a

random process $x(t)$, the persistence probability $\Pr(t)$ is that $x(t')$ remains below (or above) a given level L for all times $t' \in [0, t]$. Namely, $\Pr(t) = \text{Prob}\{x(t') < L, \ t' \in [0, t]\}$. This problem has been researched by mathematicians and physicists, e.g. [24–26], but exact expressions for the persistence probability have been obtained only for a very limited number of cases [21, 27]. Hence, an alternative problem is considered. That is, to determine the large-time asymptotic behaviours of the persistence probability, which leads to the definition of the *persistence parameter* [25, 28, 29]. It can be shown [28, 30] that for the stationary Gaussian process, $\Pr(t) \sim \exp(-\theta t)$ for large t, where θ is termed as the persistence parameter. It will be seen in Chapter 2 that θ describes the tail behaviour of the probability density function of zero-crossing intervals. The question to determine θ turns out to be a hard unsolved problem [4, 31, 32]. By assuming that the successive zero-crossing intervals are independent and identically distributed random variables, Majumdar et al. [28] and Derrida et al. [25] found that the independence assumption could produce the persistence value θ which is close to the simulation results for a particular class of autocorrelation functions that decay to zero rapidly.

The statistics of zero-crossings has also been considered. Steinberg et al. [33] developed a method for calculating the second order moment of the number of zero-crossings occurring in an interval. Furthermore, they derived an exact formula for the variance of the number of zero-crossing points. Smith et al. [34] considered the zero-crossings of Gaussian processes as a stochastic point process, and showed that the distribution of the number of zero-crossings in the asymptotically large interval regime is approximately negative-binomial or binomial according to the smoothness of the process.

Hopcraft and Jakeman [15] derived the zero-crossing rate formula for the symmetric stable process, and showed that this formula reverts to Rice's formula when the underlying process is the Gaussian case.

In recent years, there is growing evidence and interest in many examples of natural phenomena, which shows the 'long-term' memory. For example, heartbeat records [35], daily temperature [36], DNA sequences [37] etc. The long-term memory means that the autocorrelation function is of power-law type $\rho(t) \sim t^{-\gamma}$, for large t, where $\gamma > 0$ is a constant. Altmann [38] and Eichner et al. [39] argued that if the autocorrelation function of the Gaussian process is of power-law form with $0 < \gamma < 1$, then the tail of the probability density function of zero-crossing intervals is approximately given by a stretched exponential distribution $\exp(-t^{\gamma})$. They obtained this result from simulations but did not give an analytical proof. Olla [40] applied an ϵ-expansion for $\gamma = 1 - \epsilon$ and claimed to obtain the stretched exponential distribution. This issue will be investigated in Chapter 4.

1.2.2 Stable random variables and processes

In 1924, Paul Lévy introduced the notion of the stable random variable, and realised that a powerful technique to study the stable random variable is its characteristic function, which is the Fourier transform of a random variable, and summarised his main results in [41]. Since then papers on the theory and applications of stable random variables and processes are published by many authors. Analysis of stable distributions and processes and their theoretical proof can be found in Samorodnitsky and Taqqu [42]. A review in this area from a statistical perspective is provided by a collection of papers edited by Cambanis et al. [43]. One monograph focused on the one-dimensional stable distribution was written by Zolotarev [44]. Various applications of the stable distributions are contained in Adler et al. [45], and Mittnik et al. [46].

A random variable X is said to stable if for any positive constants a and b, there exists positive constants c, and d, such that $aX_1 + bX_2$ has the same distribution as $cX + d$, where X_1 and X_2 are independent copies of X [47]. The stable distribution is a generalisation of the Gaussian case. The epithet

'stable' used in this thesis means the non-Gaussian stable random variable. Three commonly seen stable random variables are the Gaussian distribution, the Cauchy distribution, and the Lévy distribution, whose probability density functions are known in closed forms [42]. More closed expressions of probability density functions of stable random variables can be found in [48]. The more elegant way to define a stable random variable is the characteristic function, and more details can be found in [42]. Chapter 5 and 6 concentrate on the *symmetric* stable process, whose characteristic function has a very simple form $\langle \exp(i\lambda X) \rangle = e^{-A|\lambda|^{\nu}}$, where $A > 0$ is a scale parameter and $0 < \nu \leq 2$. When $\nu = 2$, it corresponds to the Gaussian case. A statistical model based on the class of the bivariate symmetric stable distributions and processes will be reviewed and exploited in Chapter 5.

The stable distributions have power-law tails, such that $P(x) \sim |x|^{-\nu-1}$ for large x with $0 < \nu < 2$. There is much evidence to show that stable distributions can be used to model impulsive signals and noise, financial data, and fluctuations of highly correlated systems. For example, a large number of financial institutions collapsed during the global financial crisis of 2007-2008, including Lehman Brothers and Merrill Lynch. By studying six daily total return indices (ISEQ, CAC40, DAX30, FTSE100, Dow Jones Composite and S&P500) from 31 December 1987 to 31 January 2008, Frain [49] used the stable distributions to fit the daily returns on these indices, as he found a larger number of extreme values from the data set and stable distributions allow the heavy tails.

The applications of the stable distributions also appear in the physics literature. Bak et al. [50] introduced the notion of the sandpile model, which is a system to count numbers of falling sand grains onto a pile. Once the pile becomes too steep, the pile will collapse like an avalanche until the pile is again stable. They repeated the sandpile model and found that the size and frequency of avalanches followed power-law tails with index in the sta-

ble range. They introduced the concept of self-organized criticality, where systems evolve naturally to their critical points.

1.3 Outline of thesis

The thesis is divided into six further chapters: five chapters of results and one providing a summary of conclusions and suggestions for further work. At the end of each results chapter, its findings are summarized.

Chapter 2 first reviews mathematical models of zero-crossing intervals of stationary random processes, which will be utilised throughout this thesis. Then zero-crossing intervals of Gaussian processes with three different autocorrelation functions are considered. One is of the exponentially bounded form, and the others are of power-law type. Results obtained in this chapter are derived by assuming that successive zero-crossing intervals are independent. The independence assumption is simple to use, but its validity needs to be examined by comparison with the simulation experiment.

Results of Chapter 3 largely depend on numerical simulations, and the aim is to examine the independence assumption. This chapter shows simulation results of zero-crossing intervals of Gaussian processes with the autocorrelation functions considered in Chapter 2. Chapter 3 first introduces simulation algorithms, then the simulation results are compared with that in Chapter 2. It is found that the independence assumption is valid for the exponentially bounded autocorrelation function, but not for the power-law types. The simulation result for the power-law autocorrelation function seems to support the work of Eichner et al. [39], and is discussed in detail in Chapter 4.

Chapter 4 investigates the results of Eichner et al. [39] by considering the spectral density function of the power-law autocorrelation function and the finite size of the data stream. Based on this analysis, the cut-off power-

law autocorrelation function is motivated. Then the thesis argues that the tail of the zero-crossing interval is of exponential form, not the stretched exponential form, which was claimed by Eichner et al.

Chapter 5 considers zero-crossing intervals of the symmetric stable process, which is a generalisation of the Gaussian process. Such a process introduces the coherence function, which plays the similar role as the autocorrelation function of the Gaussian process, but is *not* the autocorrelation function, rather is a generalisation of a structure function. The exact definition of the coherence function can be found in Chapter 5. Specifically, this chapter investigates zero-crossing intervals given the exponential coherence function.

In Chapter 6, zero-crossing intervals with the power-law coherence function are considered first. Then, motivated by the cut-off power-law autocorrelation function, this chapter obtains the properties of zero-crossing intervals given the cut-off power-law coherence function. The main aim is to show that given the cut-off term, the tail of the zero-crossing interval is of exponential form.

Conclusions are drawn in Chapter 7. Suggestions are given as to how these results might be furthered and exploited.

Chapter 2

Zero-crossing Intervals of Gaussian Processes

2.1 Introduction

This chapter investigates zero-crossing intervals of the Gaussian process with different autocorrelation functions. Mathematical background required to understand this is reviewed first, then statistical properties of the zero crossing intervals are presented. Due to lack of any other effective model for incorporating correlations among the crossing intervals, results shown in this chapter are obtained by assuming that successive zero-crossing intervals are independent. The independence assumption is an approximation only, but it is a simple and analytically tractable choice. The results of this chapter will be compared with simulation results of zero-crossing intervals in Chapter 3. This chapter also serves to set up various notations that will be used throughout this thesis.

2.2 Mathematical background

This section reviews the fundamental identities given by McFadden [22, 23] and Rice [3, 4]. Their results provide the general way to investigate zero-crossing intervals of any arbitrary stationary random process.

2.2.1 Zero-crossing intervals of the stationary process

Let $x(t)$ describe a stationary random process with zero mean. The autocorrelation function of $x(t)$ is denoted by $r(t) = \langle x(t')x(t'+t) \rangle$. The average $\langle x(t')x(t'+t) \rangle$ is independent of t' since $x(t)$ is a stationary process. The clipped process $y(t)$ is defined as

$$
y(t) = \begin{cases} 1, & x(t) \geq 0 \\ -1, & x(t) < 0. \end{cases}
\tag{2.1}
$$

Let the autocorrelation function of $y(t)$ denote as $R(t) = \langle y(t')y(t'+t) \rangle$. The process $y(t)$ is of interest because it preserves information about the zero-crossings.

Let $p(n,t)$ describe the probability of finding exactly n zeros in the given interval $(t', t'+t)$. Now consider the possible values of $\langle y(t')y(t'+t) \rangle$. The product $\langle y(t')y(t'+t) \rangle$ is 1 if there are an even number of zero-crossings in the interval $(t', t'+t)$, and -1 if there are an odd number of crossings in the interval $(t', t'+t)$. Then it leads to the infinite series

$$
R(t) = \langle y(t')y(t'+t) \rangle = \sum_{n=0}^{\infty} (-1)^n p(n,t),
\tag{2.2}
$$

which is first given by Rice [4].

Let τ be a random variable, which describes the lengths of intervals between two successive zero-crossings, and denote $P_0(\tau)$ as the probability density function of the zero-crossing interval τ. The main aim of zero-

crossing analysis is to determine $P_0(\tau)$. Then define $P_n(\tau)$, $n = 0, 1, 2, \cdots$, as the probability density functions of crossing intervals between the mth and $(m + n + 1)$st zeros, where $m = 1, 2, \cdots$. In other words, $P_0(\tau)$ is the probability density function of the zero-crossing interval τ; $P_1(\tau)$ is the probability density function of the sum of *two* successive zero-crossing intervals; $P_2(\tau)$ is the probability density function of the sum of *three* successive zero-crossing intervals, and so on.

Let β be the expected number of zero-crossings per unit time. Consider the mean $\langle \tau \rangle$ of the zero-crossing interval τ. Given a very long time interval T, there will be βT zeros and βT intervals; then it implies that $\langle \tau \rangle = T/(T\beta) = 1/\beta$. The analytical proof can be found in [39] and [51], and is verified below. Although this argument is heuristic, the mean $\langle \tau \rangle$ is unaffected by whether or not there are correlations between successive zero-crossing intervals [39].

The contribution of McFadden is that he connected the function $p(n, t)$, which is already seen before, with the probability density function $P_n(\tau)$, and derived the recursion relationships between them:

$$p''(0, \tau) = \beta P_0(\tau) \tag{2.3}$$

$$p''(1, \tau) = \beta[P_1(\tau) - 2P_0(\tau)] \tag{2.4}$$

$$p''(n, \tau) = \beta[P_n(\tau) - 2P_{n-1}(\tau) + P_{n-2}(\tau)] \quad n \geq 2, \tag{2.5}$$

where primes denote differentiation with respect to τ. These relationships are derived in the Appendix A. Differentiating (2.2) twice with respect to t and then inserting Equations (2.3)-(2.5) leads to

$$\frac{R''(\tau)}{4\beta} = \sum_{n=0}^{\infty} (-1)^n P_n(\tau), \tag{2.6}$$

which implies that the clipped autocorrelation function $R(t)$ and the crossing

rate β are required for the zero-crossing analysis to be effected.

McFadden then used the Laplace transform to derive moments of the zero-crossing interval τ. The Laplace transform of a function $h(t)$ is [52]

$$\mathcal{L}\{h(t)\} = \int_0^\infty e^{-st} h(t)\, \mathrm{d}t.$$

Now denote the following notations

$$g(s) = \mathcal{L}\left\{\frac{R''(\tau)}{4\beta}\right\}, \tag{2.7}$$

$$p_n(s) = \mathcal{L}\{P_n(\tau)\}.$$

Then transforming Equation (2.6) gives

$$g(s) = \sum_{n=0}^{\infty}(-1)^n p_n(s). \tag{2.8}$$

The thesis investigates the probability density function $P_0(\tau)$ of zero-crossing intervals under the assumption that successive axis-crossing intervals are statistically independent. This is a rough approximation and may not be in accordance with the practice problem. However, in the absence of any other definitive model for the correlations among zero-crossing intervals, this is a simple and analytically tractable choice. Furthermore, it will be seen in Chapter 3 that the independence approximation is *adequate* for certain types of autocorrelation functions. Based on this argument, if it is presumed that successive axis-crossing intervals are statistically independent, then the probability density functions of the sums of the crossing intervals are given by the convolution of $P_0(\tau)$, or in terms of the transform $p_n(s) = p_0^{n+1}(s)$. Inserting this into Equation (2.8) allows the sum to be evaluated

$$p_0(s) = \frac{g(s)}{1 - g(s)}. \tag{2.9}$$

The advantage of the independence assumption is that one can sum up the infinite series on the right-hand side of Equation (2.8) in the Laplace space. Theoretically, the full probability density function $P_0(\tau)$ of the zero-crossing interval τ can be revealed by the inversion of Laplace transform of Equation (2.9). The zero-crossing problem can also be investigated from the renewal theory, as one can consider each zero-crossing as a 'renewal' of the process. A similar structure can be found in [24, 53].

According to the definition of the Laplace transform, moments of the zero-crossing interval τ may be obtained from the derivatives of $p_0(s)$, evaluated at $s = 0$. Then McFadden [23] evaluated the following quantities:

$$g(0) = \frac{1}{2} \tag{2.10}$$

$$\langle \tau \rangle = \frac{1}{\beta} \tag{2.11}$$

$$\sigma^2 = \frac{2}{\beta} \int_0^\infty R(t) \, \mathrm{d}t, \tag{2.12}$$

which are derived in Appendix B. Note that given (2.9), Equation (2.10) confirms that $p_0(0) = 1$, which states that $P_0(\tau)$ is correctly normalised.

The model (2.9) is based on the independence assumption, which makes the analysis possible, but does not reflect the reality in general. Therefore, the independence assumption has to be tested by comparing with simulation experiments when possible. It can be seen that the independence model (2.9) requires the knowledge of the clipped autocorrelation function $R(t)$ and the zero-crossing rate β to obtain the Laplace transform $g(s)$. The next two sections outline the principle methodology to derive these two quantities for the Gaussian process.

2.2.2 The Van Vleck theorem

Define the rectified telegraph signal $\chi(t)$ of the clipped process $y(t)$ as:

$$\chi(t) = \frac{1}{2}(1 + y(t)) = \begin{cases} 1, & y(t) \geq 0 \\ 0, & y(t) < 0. \end{cases} \tag{2.13}$$

Now consider the autocorrelation function $\langle \chi(t')\chi(t' + t) \rangle$. Let $m_2(x, y)$ denote the bivariate probability density function of the underlying process $x(t)$. Then the average $\langle \chi(t')\chi(t' + t) \rangle$ is either zero or unity, thus by stationary it follows that

$$\langle \chi(0)\chi(t) \rangle = \int_0^\infty \int_0^\infty m_2(x, y)\,\mathrm{d}x\,\mathrm{d}y, \tag{2.14}$$

which depends on the specific form of the joint density function $m_2(x, y)$.

Take the most familiar Gaussian process with zero mean and unity variance as an example. Let $x = x(t')$ and $y = x(t' + t)$, then its autocorrelation function is defined as $\rho(t) = \langle x(t')x(t'+t) \rangle$, and the joint distribution function is

$$m_2(x, y) = \frac{1}{2\pi(1 - \rho^2)^{1/2}} \exp\left(-\frac{x^2 + y^2 - 2xy\rho(t)}{2(1 - \rho^2)}\right). \tag{2.15}$$

Then evaluating Equation (2.14) gives a closed expression:

$$\langle \chi(0)\chi(t) \rangle = \frac{1}{4} + \frac{1}{2\pi} \arcsin(\rho(t)).$$

Then, following Equation (2.13), it obtains a quite simple form

$$R(t) = \frac{2}{\pi} \arcsin(\rho(t)), \tag{2.16}$$

which is known as the Van Vleck theorem or the arcsine law formula [54].

The above analysis shows that if the autocorrelation function $R(t)$ of the clipped process is required to be determined, one needs the proper defined *bivariate* probability density function $m_2(x, y)$ of the underlying process. It

will be seen in Chapter 5 that for the symmetric stable process, the derivation of the joint density function $m_2(x, y)$ is obtained, which enables the Van Vleck theorem to be generalised.

2.2.3 Rice's formula

This section reviews the mean zero-crossings rate of a Gaussian process, which was was first derived by Rice [4]. Let $x(t)$ be a continuous and differentiable random process. Namely, its sample path is continuous and differentiable. Now consider its behaviour in the time interval $(t_1, t_1 + \mathrm{d}t)$. If $\mathrm{d}t$ is chosen to be so small that $x(t)$ can be treated as a straight line in $(t_1, t_1 + \mathrm{d}t)$. For simplicity, let $x = x(t_1)$ at time t_1. Suppose it passes a zero in $(t_1, t_1 + \mathrm{d}t)$, then its intercept on $x(t) = 0$ is

$$t = t_1 - \frac{x}{\dot{x}}, \tag{2.17}$$

where the time derivative is defined as

$$\dot{x} = \dot{x}(t_1) = \lim_{\mathrm{d}t \to 0} \frac{x(t_1 + \mathrm{d}t) - x(t_1)}{t_1},$$

where the limit is to be interpreted in the mean square sense [55]. Equation (2.17) implies that x and $\dot{x}$ have opposite signs, and there is a relation

$$t_1 < t_1 - \frac{x}{\dot{x}} < t_1 + \mathrm{d}t. \tag{2.18}$$

Consider the positive slopes ($\dot{x} > 0$), then Equation (2.18) becomes

$$-\dot{x}\,\mathrm{d}t < x < 0. \tag{2.19}$$

Let $q_2(x, \dot{x})$ denote the joint probability density function of x and $\dot{x}$, then the probability of x and $\dot{x}$ satisfying the inequality (2.19) is

$$\int_0^\infty \mathrm{d}\dot{x} \int_{-\dot{x}\,\mathrm{d}t}^0 q_2(x, \dot{x})\,\mathrm{d}x$$

$$= \mathrm{d}t \int_0^\infty \dot{x}\, q_2(0, \dot{x})\,\mathrm{d}\dot{x}, \tag{2.20}$$

where we have made use of the fact that $\mathrm{d}t$ is so very small that x is effectively zero. Similar analysis yields

$$- \,\mathrm{d}t \int_{-\infty}^0 \dot{x}\, q_2(0, \dot{x})\,\mathrm{d}\dot{x}, \tag{2.21}$$

as the probability of x and $\dot{x}$ satisfying the inequality (2.18) when $\dot{x} < 0$. Combining (2.20) and (2.21) leads to the zero-crossing rate per unit time formula

$$\beta = \int_{-\infty}^\infty |\dot{x}|\, q_2(0, \dot{x})\,\mathrm{d}\dot{x}, \tag{2.22}$$

which is first obtained by Rice [4].

The above derivation is the main procedure to calculate the zero-crossing rate for a continuous and differentiable process, but to proceed further requires knowing the *bivariate* probability density function $q_2(x, \dot{x})$. Note that $q_2(x, \dot{x})$ is not the same as $m_2(x, y)$ in the previous section, but $m_2(x, y)$ can be used to determine $q_2(x, \dot{x})$ through the following transformation. Let $x = x(t')$ and $y = x(t' + t)$. For sufficient small t, then there exists the transform pair $x = x$ and $y = x + \dot{x}t$. After changing variables from x and y to x and $\dot{x}$, and note that the Jacobian of the transform is

$$\left| \frac{\partial(x, y)}{\partial(x, \dot{x})} \right| = t,$$

it leads to

$$q_2(x, \dot{x}) = \lim_{t \to 0} t\, m_2(x, x + \dot{x}t). \tag{2.23}$$

The implication of Equation (2.23) is that to determine the joint density function $q_2(x, \dot{x})$, one needs to know $m_2(x, y)$, which is the joint density function of the underlying process.

Rice [4] evaluated Equation (2.23) for the Gaussian process with the joint density function $m_2(x, y)$ given by (2.15), and found that

$$q_2(x, \dot{x}) = \frac{1}{2\pi\sqrt{-\rho''(0)}} \exp\left(-\frac{1}{2}\left(x^2 + \frac{\dot{x}^2}{-\rho''(0)}\right)\right), \qquad (2.24)$$

which means that x and $\dot{x}$ are joint-Gaussian distributed and independent of each other. Then inserting Equation (2.24) into Equation (2.22), Rice showed that the zero-crossing rate

$$\beta = \frac{1}{\pi}\sqrt{-\rho''(0)}. \qquad (2.25)$$

Note that Equation (2.25) is only applied to when the second derivative of $\rho(t)$ exists, which means that the expansion of $\rho(t)$ near the origin is $\rho(t) = 1 - \rho''(0)t^2/2 + \cdots$. This restriction is generalised when it comes to investigating the zero-crossing rate for the symmetric stable process. It can be seen that calculating the zero-crossing rate also requires knowledge of the joint density function $m_2(x, y)$. Rice's formula (2.25) is generalised to the symmetric stable case in Chapter 5 by using a similar method.

2.2.4 Autocorrelation functions $\rho(t)$

Equation (2.16) indicates that the behaviour of the clipped autocorrelation function $R(t)$ is influenced by the structure of the autocorrelation function $\rho(t)$ of the Gaussian process, then it will affect the probability density functions $\{P_n(\tau)\}$ by Equation (2.6). Two classes of correlations often encountered in random processes and time series analysis are considered in this thesis.

Chapter 2

1. *Short-term memory correlations* where values are correlated with one
   another at short lags in time ([56]; [57]). That is the autocorrela-
   tion function for short-range correlations is bounded by an exponential
   decay $\rho(t) \sim \exp(-\alpha_1 t)$, as $t \to \infty$ where α_1 is a constant. Random pro-
   cesses with short-term correlation functions can be found in practical
   applications such as river flows [58], ecology [59] and telecommuni-
   cation networks [60].

2. *Long-term memory correlations* where values are correlated with one
   another at very long lags in time ([61]; [62]). That is the autocor-
   relation function has a power-law asymptote $\rho(t) \sim t^{-\gamma}$, as $t \to \infty$,
   where $\gamma > 0$ is a constant. Long-term correlations have been found in
   the physiological records [35], DNA sequences [37] and musical pitch,
   rhythms, and loudness fluctuations ([63], [64] and [65]).

To explore the effects that changes in the autocorrelation function $\rho(t)$ have
on the probability density function $P_0(\tau)$ of the zero-crossing interval τ, the
thesis considers three specific models.

The first one is the exponentially bounded autocorrelation function, cor-
responding to the short-term memory,

$$\rho_e(t) = \frac{2 \exp(-at)}{1 + \exp(-2at)}, \tag{2.26}$$

where $a > 0$ is a time-scale parameter. $\rho_e(t)$ is of interest since it is generated
from the exponential coherence function of the symmetric stable process,
which has the asymptotic form $\exp(-at)$ for large t. The detail will be seen
in Chapter 5 of the thesis. The expansion of $\rho_e(t)$ near the origin is

$$\rho_e(t) = 1 - \frac{a^2}{2}t^2 + \frac{5a^4}{24}t^4 + O(t^6),$$

implying that the mean rate β of zero-crossings of the process exists by Rice's

formula (2.25).

The second autocorrelation function is power-law bounded, corresponding to the long-term memory,

$$\rho_\gamma(t) = (1 + a^2 t^2/\gamma)^{-\gamma/2}, \qquad (2.27)$$

where $a > 0$ is the time-scale parameter and $\gamma > 0$ is the long-term memory index. The expansion of this model for small t always contains *even* terms:

$$\rho_\gamma(t) = 1 - \frac{a^2}{2}t^2 + \frac{a^4(2+\gamma)}{8\gamma}t^4 + O(t^6),$$

implying the existence of the zero-crossing rate. Note that as $\gamma \to \infty$, $\rho_\gamma(t) \to \exp(-a^2 t^2/2)$, which is the Gaussian type autocorrelation function [34].

The final model for the autocorrelation function that will be considered is still long-term correlated

$$\phi_\gamma(t) = \frac{2(1 + a|t|/\gamma)^\gamma}{1 + (1 + a|t|/\gamma)^{2\gamma}}. \qquad (2.28)$$

The expansion of $\phi_\gamma(t)$ near the origin includes both *even* and *odd* terms:

$$\phi_\gamma(t) = 1 - \frac{a^2}{2}t^2 + \frac{a^3}{2\gamma}|t|^3 + \frac{a^4(5\gamma^2 - 11)}{24\gamma^2}t^4 + O(|t|^5).$$

Clearly, the zero-crossing rate exists according to Rice's formula (2.25). Note that, as $\gamma \to \infty$, $\phi_\gamma(t) \to \rho_e(t)$, which implies that $\phi_\gamma(t)$ is reflected the power-law coherence function, which is discussed in Chapter 6.

Both the power-law autocorrelation functions are with asymptote $t^{-\gamma}$ for large t, but it will be seen later that the initial behaviour of the probability density function $P_0(\tau)$ of the zero-crossing interval τ shows the different property. A key difference between these two power-law models $\phi_\gamma(t)$ and $\rho_\gamma(t)$ is that $\phi_\gamma(t)$ is known as a 'sub-fractal' ([66], [67]). Because the fourth derivative at the origin is singular corresponding to the process having a

derivative that is continuous but not differentiable ([34], [68]), however $\rho_\gamma(t)$ is smooth to all orders.

2.3 The exponentially bounded autocorrelation model $\rho_e(t)$

This section considers zero-crossing intervals of the Gaussian process with the exponentially bounded autocorrelation function $\rho_e(t)$, given by Equation (2.26). The aim is to show statistical properties of the zero-crossing interval τ, when the Gaussian process is short-term correlated.

2.3.1 Mean and variance of zero-crossing intervals

The calculation for the mean $\langle \tau \rangle$ and variance σ^2 of the zero-crossing interval τ is simple. By using Rice's formula (2.25), it gives $\beta = a/\pi$, therefore by Equation (2.11), the mean $\langle \tau \rangle$ is π/a. According to Equation (2.12), the variance σ^2 is

$$\sigma^2 = \frac{2}{\beta} \int_0^\infty \frac{2}{\pi} \arcsin[\rho_e(t)]\, \mathrm{d}t.$$

The numerical evaluation of the integral gives $\sigma^2 \approx 7.32/a^2$. It will be seen in Chapter 5 that these values for $\langle \tau \rangle$ and σ^2 can be obtained from the general symmetric stable case.

2.3.2 The persistence parameter

The second quantity to be calculated is the persistence parameter θ, which describes the tail behaviour of zero-crossing intervals. The independence assumption plays an important role to determine θ. The Laplace transform of the probability density function $P_0(\tau)$ of the zero-crossing interval τ is given by Equation (2.9), which has a pole satisfying $1 - g(s) = 0$, where $g(s)$ is given by Equation (2.7). Note that for $s \geq 0$, $0 < g(s) \leq 1/2$, which means

that the pole is located on the negative s-axis. Hence the pole we are after is the least negative solutions to this equation. If let $s = -\theta$ denote the location of the pole, where $\theta > 0$, then the expansion of $g(s)$ around $s = -\theta$ is

$$g(s) = g(-\theta) + g'(-\theta)(s + \theta) + \frac{g''(-\theta)}{2}(s + \theta)^2 + \cdots.$$

With $g(-\theta) = 1$, inserting Equation (2.9) gives that, for $s = -\theta$

$$p_0(s) \approx \frac{-1}{g'(-\theta)(s + \theta)}.$$

Furthermore, by using the property of Laplace transform, then it gives that $P_0(\tau) \sim \exp(-\theta\tau)$ for large τ. This result implies that the existence of the persistence parameter θ gives the exponential tail of the zero-crossing interval τ.

Now evaluate the Laplace transform $g(s) = \mathcal{L}\{R''(t)/(4\beta)\}$. For the exponentially bounded autocorrelation function $\rho_e(t)$, which is given by (2.26), we evaluate that

$$R''(t) = \frac{2a^2}{\pi} \operatorname{sech}(at) \tanh(at).$$

Then with the constant $\beta = a/\pi$, the Laplace transform of $R''(t)/(4\beta)$ is

$$g(s) = \frac{1}{4\beta} \int_0^\infty \frac{2a^2}{\pi} \operatorname{sech}(at) \tanh(at) \mathrm{e}^{-st} \, \mathrm{d}t, \qquad (2.29)$$

which implies that a is only a scaling constant if we introduce the variable $p = at$. Evaluating Equation (2.29) gives that

$$g(s) = \frac{1}{4a} \left[2a + s \left(\psi(\frac{s + a}{4a}) - \psi(\frac{s + 3a}{4a}) \right) \right], \qquad (2.30)$$

where $\psi(\cdot)$ is the logarithmic derivative of the gamma function:

$$\psi(x) = \frac{\mathrm{d}}{\mathrm{d}x} \ln \Gamma(x) = \frac{\Gamma'(x)}{\Gamma(x)}.$$

Given the closed form of $g(s)$ (2.30), now we can evaluate the persistence parameter θ. As a is a time-scale factor, for computational simplicity, let $a = 1$. Then the solution of $1 - g(-\theta) = 0$ gives that $\theta = 0.37$. This result implies that the tail of the zero-crossing interval τ is of exponential form $\exp(-\theta\tau)$ for large τ, and this result is verified in the following section.

2.3.3 Probability density functions

The main interest of the zero-crossing problem is to determine the probability density function $P_0(\tau)$ of the zero-crossing interval τ. The thesis uses numerical inversion of Laplace transform to obtain $P_0(\tau)$. That is to invert Equation (2.9) by a proper numerical algorithm, once we know the exact form $g(s)$.

The Tablot method

The formal inverse Laplace transform formula [69] is given by

$$h(t) = \mathcal{L}^{-1}\{\tilde{h}(s)\} = \frac{1}{2\pi i} \int_{x-i\infty}^{x+i\infty} \tilde{h}(s)e^{st}\,ds, \tag{2.31}$$

where x is real and greater than the real parts of all singularities of $\tilde{h}(s)$. In practice, the integral in (2.31) is evaluated by considering the Bromwich contour [70], which is composed of the vertical line $s = x$ parallel to the imaginary axis and the arc of a circle with centre at the origin.

There are several algorithms available for the numerical inversion of Laplace transforms. One of the best ways for numerical inversion of the Laplace transform is to deform the Bromwich integral [71–73]. One of the methods in this direction is given by Tablot [74]. With the Cauchy theorem [70], Tablot deformed the Bromwich contour with

$$s(\eta) = x\eta(\cot(\eta) + i), \tag{2.32}$$
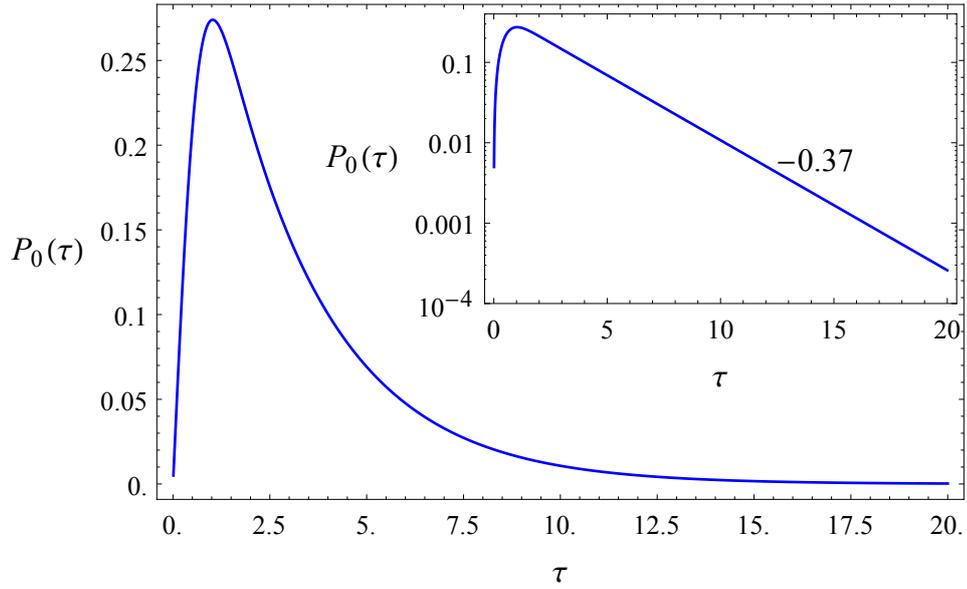
Figure 2.1: The probability density function $P_0(\tau)$ of the zero-crossing interval τ of the Gaussian process with the exponentially bounded autocorrelation function $\rho_e(t)$, given by Equation (2.26). This figure is obtained by using the Tablot method. The inset log-linear plot suggests that the tail of the zero-crossing interval τ is exponential: $P_0(\tau) \sim \exp(-A\tau)$, where $A = 0.37$ is consistent with the persistence parameter θ obtained by solving equation $1 - g(-\theta) = 0$, where $g(s)$ is given by Equation (2.30).

where $-\pi < \eta < \pi$. Replace the contour in (2.31) with (2.32), then

$$h(t) = \frac{1}{2\pi i} \int_{-\pi}^{\pi} \exp(ts(\eta))\tilde{h}(s(\eta))s'(\eta)\,d\eta, \qquad (2.33)$$

where $s'(\eta) = x(i + \cot(\eta) - \eta\csc^2(\eta))$. Then Tablot used the trapezoidal rule to approximate Equation (2.33).

The Tablot method has been coded in the mathematical software package, e.g. *Mathematica*. Abate and Valkó [71] implemented the Tablot method and provided the command 'FT[$F\_$, $t\_$]' in *Mathematica*, where F is the inverse Laplace transform function for a given time point t. This thesis obtains the probability density function $P_0(\tau)$ of the zero-crossing interval τ by using this function in *Mathematica*.

The probability density function

For the exponentially bounded model $\rho_e(t)$ (2.26), $g(s)$ is given by Equation (2.30), so there is no need to approximate the function $g(s)$. By using the Tablot method, Figure 2.1 shows the probability density function $P_0(\tau)$ of the zero-crossing interval τ of the Gaussian process with $\rho_e(t)$. It can be seen that the initial value $P_0(0) = 0$, and a peak is located off-axis, which implies that the zero-crossings have a tendency to stay apart from one another. This behaviour is called 'anti-bunching' [34, 48], referring zero-crossings are repelled from each other. The inner log-linear plot shows that the tail is a straight line, indicating that the zero-crossing interval τ follows an exponential tail: $P_0(\tau) \sim \exp(-A\tau)$, where $A = 0.37$ is obtained from numerical data and is approximately equal to the persistence parameter θ, which is calculated from solving the pole with the aid of Equation (2.30) in the last section. The agreement implies that θ can be obtained from two methods. This result shows that the existence of θ means that the tail of zero-crossing intervals is of exponential form and that θ describes the tail behaviour. Figure 2.1 will be compared with the simulation experiment in Chapter 3.

2.4 The power-law model $\rho_\gamma(t)$

This section considers zero-crossing intervals of the Gaussian process with the power-law autocorrelation function $\rho_\gamma(t)$, which is given by Equation (2.27). Section 2.2 presumed successive zero-crossing intervals are statistically independent. This is a gross approximation, but it turns out to be a analytically tractable choice. Therefore, based on this argument, this section considers the independent model analytically for the power-law bounded model $\rho_\gamma(t)$. Results derived from the independent approximation will be compared with that of simulations in Chapter 3, if the analytical results of this chapter are not inconsistent with simulations, the assumption of inde-

pendence should be rejected.

2.4.1 Mean and variance of zero-crossing intervals

For the power-law model $\rho_\gamma(t)$ (2.27), the crossing rate β is a/π, so the mean $\langle\tau\rangle$ of the zero-crossing interval τ is still π/a, implying that $\langle\tau\rangle$ does not depend on the memory index γ. The variance σ^2, however, is not always finite, which is given by (2.12):

$$\sigma^2 = \frac{4}{\beta\pi} \int_0^\infty \arcsin\left[(1 + a^2t^2/\gamma)^{-\gamma/2}\right] \, \mathrm{d}t. \tag{2.34}$$

If $\gamma \leq 1$, Equation (2.34) does not converge by the comparison test [75], and for other γ, it is solved numerically. The normalised variance $\sigma^2/\langle\tau\rangle^2$ is considered, since $\sigma^2/\langle\tau\rangle^2$ shows the fluctuations of the lengths of the zero-crossing intervals. Figure 2.2 plots $\sigma^2/\langle\tau\rangle^2$ as a function of γ. It can be seen that $\sigma^2/\langle\tau\rangle^2$ is finite for $\gamma > 1$. Otherwise, it is infinite. This result indicates that the variance σ^2 depends on the value γ. In practice, the variance σ^2 cannot be infinite, and this issue will be discussed in Chapter 4.

2.4.2 The persistence parameter

We have already seen that the persistence parameter θ can be determined by solving the equation $1 - g(-\theta) = 0$, where $g(s) = \mathcal{L}\{R''(t)/(4\beta)\}$. For the power-law autocorrelation function $\rho_\gamma(t)$ (2.27), we can calculate that

$$\frac{R''(t)}{4\beta} = \frac{a\left(2 - h + (\gamma(h-1) + h - 2)h^\gamma\right)}{2h^2\left(h^\gamma - 1\right)^{3/2}} \tag{2.35}$$

where $h = 1 + a^2t^2/\gamma$. It can be seen that Laplace transforming Equation (2.35) does not converge for negative s values, which implies that there does *not* exist the persistence parameter θ. This fact implies that the probability density function $P_0(\tau)$ of the zero-crossing interval τ does not have an
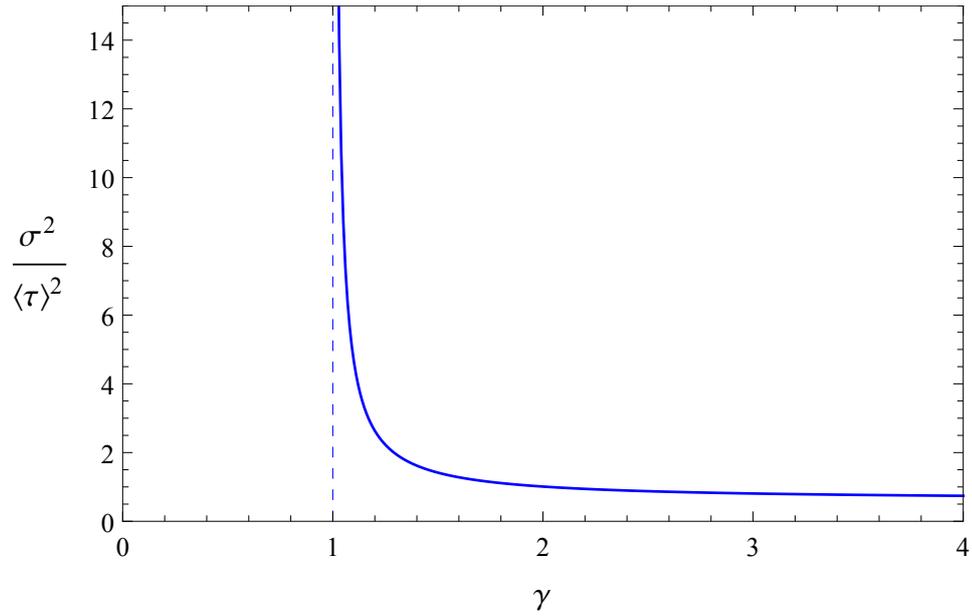
Figure 2.2: This figure shows the normalised variance $\sigma^2/\langle\tau\rangle^2$ of the zero-crossing interval τ against the index γ for the Gaussian process with the power-law autocorrelation function $\rho_\gamma(t)$, which is given by Equation (2.27). It can be seen that the variance σ^2 becomes infinite if γ is equal to or less than 1, implying that the zero-crossing interval τ is related to the value of γ.

exponential tail. If it had, then the variance σ^2 would be finite. This result is different with that for the exponentially bounded autocorrelation function $\rho_e(t)$, which is shown in previous section.

Another way to show the same result is to consider the asymptotic behaviour of the Laplace transform of Equation (2.35). In asymptotic analysis, the symbol '$\sim$' means that for two functions $w(t)$ and $f(t)$, $\lim_{t\to\infty} w(t)/f(t) = 1$. Hence, for large t, Equation (2.35) behaves like

$$\frac{R''(t)}{4\beta} \sim \frac{c}{(t+1)^{\gamma+2}}, \tag{2.36}$$

where c is a constant $\gamma^{1+\gamma/2}(\gamma+1)a^{1-\gamma}/2$. By the property of the Laplace transform [76], then Laplace transforming Equation (2.36) gives the small s behaviour

$$g(s) = \mathcal{L}\left\{\frac{R''(t)}{4\beta}\right\} \sim c\,e^s\,\mathrm{E}_{2+\gamma}(s), \tag{2.37}$$

where the exponential integral [77] is defined as

$$E_{2+\gamma}(s) = \int_1^\infty \frac{e^{-st}}{t^{2+\gamma}}\, dt.$$

Note that the expansion of $E_{2+\gamma}(s)$ for small s depends on whether the index γ is an integer or not. If γ is an integer, then it gives the *logarithmic* case:

$$E_{2+\gamma}(s) = c_0 s^{1+\gamma} \ln(s) + c_1 + c_2 s + \cdots + c_i s^{1+\gamma} + O(s^{2+\gamma}),$$

where $\{c_i\}$ are constants. If γ is not an integer, then it has the *fractional* form:

$$E_{2+\gamma}(s) = b_0 s^{1+\gamma} + b_1 + b_2 s + b_3 s^2 + O(s^3),$$

where $\{b_i\}$ are constants. These two expansions for $E_{2+\gamma}(s)$ imply that Equation (2.9)

$$p_0(s) = \frac{g(s)}{1 - g(s)}$$

will also have two expansion forms for small s.

Now we expand the function $p_0(s)$ for small s. Taking into $g(0) = 1/2$ and $g'(0) = 1/(4\beta)$ (Appendix B) into account, we can write

$$g(s) = \frac{1}{2} - \frac{1}{4\beta}s + U(s),$$

where $U(s)$ has either the logarithmic term $s^{1+\gamma} \ln(s)$ or the fractional term $s^{1+\gamma}$ depending on whether γ is an integer or not, according to the expansion of $E_{2+\gamma}(s)$. If γ is an integer, then

$$U(s) = v_0 s^{1+\gamma} \ln(s) + v_1 s^2 + \cdots + v_j s^{1+\gamma} + O(s^{2+\gamma}),$$

where $\{v_i\}$ are constants. If γ is not an integer, then

$$U(s) = w_0 s^{1+\gamma} + w_1 s^2 + O(s^3),$$

where $\{w_i\}$ are constants. Therefore, if we expand $p_0(s)$ for small s, it either gives

$$p_0(s) = 1 - \frac{1}{\beta}s + u_0 s^{1+\gamma} \ln(s) + u_1 s^2 + \cdots + u_j s^{1+\gamma} + O(s^{2+\gamma})$$

or

$$p_0(s) = 1 - \frac{1}{\beta}s + l_0 s^{1+\gamma} + l_1 s^2 + O(s^3),$$

where $\{u_i\}$ and $\{l_i\}$ are constants. These two expansions for $p_0(s)$ imply that the zero-crossing interval τ always has the finite mean $\langle\tau\rangle = 1/\beta$, but its higher order moments do not always exist, indicating that the tail of the zero-crossing interval τ does not follow the exponential tail. As a consequence, it implies that the persistence parameter θ does not exist.

It has to be mentioned that the above two expansions for $p_0(s)$ are not the same as the McFadden's assumption [23]:

$$p_0(s) = 1 - \langle\tau\rangle s + \frac{\langle\tau^2\rangle}{2}s^2 - \cdots,$$

where he assumed that all moments of the zero-crossing interval τ exist and are finite. It can be shown that given the independence model, the tail now is of power-law form with the index $\gamma + 2$:

$$p_0(s) = \frac{g(s)}{1 - g(s)} \approx g(s) + O(g(s)^2),$$

then the inverse Laplace transform leads to $P_0(\tau) \sim \tau^{-(\gamma+2)}$ for large τ. This behaviour is consistent with the fact that the existence of the variance σ^2 depends on whether $\gamma > 1$ or not.

2.4.3 Probability density functions

This section is to evaluate the probability density function $P_0(\tau)$ of the zero-crossing interval τ and its initial value $P_0(0)$. The initial behaviour of $P_0(\tau)$ is related to the concept of the anti-bunching and bunching, by which is meant that the zero-crossings are respectively repelled or attracted to one-another [34], [48].

The initial value $P_0(0)$

The initial value theorem [76] can be used to determine $P_0(0)$. That is

$$\lim_{\tau \to 0} P_0(\tau) = \lim_{s \to \infty} s\, p_0(s),$$

where $p_0(s)$ is given by Equation (2.9). For the power-law model $\rho_\gamma(t)$, $g(s)$ refers to the Laplace transform of Equation (2.35). The theorem requires to know the large s behaviour of $g(s)$, which is related to the small t behaviour of Equation (2.35). If we expand Equation (2.35) near the origin for small t, it yields

$$\frac{R''(t)}{4\beta} = \frac{a^2(\gamma + 3)}{4\gamma}t - \frac{a^4(\gamma^2 + 30\gamma + 65)}{48\gamma^2}t^3 + O(t^5),$$

implying the leading order of s-term is

$$g(s) = \frac{a^2(\gamma + 3)}{4\gamma}\frac{1}{s} - \frac{a^4(\gamma^2 + 30\gamma + 65)}{8\gamma^2}\frac{1}{s^4} + O(s^{-6}).$$

Then by the initial value theorem, it gives that

$$\lim_{\tau \to 0} P_0(\tau) = \lim_{s \to \infty} s\, p_0(s)$$

$$= \lim_{s \to \infty} \frac{a^2(\gamma + 3)\, s}{4\gamma s^2 - a^2(\gamma + 3)}$$

$$= 0.$$

It can be seen that the initial value $P_0(0)$ is always zero for all γ. If applying the initial value theorem twice to $P_0'(\tau)$, it yields

$$
\begin{aligned}
\lim_{\tau \to 0} P_0'(\tau) &= \lim_{s \to \infty} s(sp_0(s) - P_0(0)) \\
&= \lim_{s \to \infty} \frac{a^2(\gamma + 3)s^2}{4\gamma s^2 - a^2(\gamma + 3)} \\
&= \frac{a^2(\gamma + 3)}{4\gamma} > 0.
\end{aligned}
$$

The analytical result of $P_0'(0)$ indicates that zero-crossings tend to repel by each other, namely the anti-bunched behaviour, which is similar to that for the exponentially bounded model $\rho_e(t)$ given by Equation (2.26). The results of $P_0(0) = 0$ and $P_0'(0) > 0$ indicate that the probability density function $P_0(\tau)$ will increase from the origin, and this fact is to be verified in the next section.

Probability density functions

This section shows three examples of the probability density function $P_0(\tau)$ of the zero-crossing interval τ for the cases $\gamma = 2/5, 1$ and 2. The aim is to find the influence of the index γ on the zero-crossing intervals. Based on the previous analysis, the cases $\gamma = 2/5$ and 1 correspond to that the mean $\langle \tau \rangle$ of the zero-crossing interval τ is finite, but the variance and higher order moments are not. As for $\gamma = 2$, it represents the mean and variance are finite, but the third and higher order moments are not.

The numerical method for inverting the Laplace transform $p_0(s)$ is still the Tablot method. Hence, it requires an analytical form for $g(s)$. For $\gamma = 1$, the closed form for $g(s)$ is shown below, but for the rest two cases, the closed forms are not known yet. In order to fill this gap, an approximation function $G(s)$, which combines the asymptotic large and small behaviours of $\mathcal{L}\{R''(t)/(4\beta)\}$, will be used. As the constant a is a time scale parameter, shown in Appendix D, so set $a = 1$ as before.

Chapter 2

When $\gamma = 1$, the Laplace transform of Equation (2.35) is

$$g(s) = \frac{1}{4a}\left[2a - 2s\,\mathrm{Ci}\left(\frac{s}{a}\right)\sin\left(\frac{s}{a}\right) - s\cos\left(\frac{s}{a}\right)\left(\pi - 2\mathrm{Si}\left(\frac{s}{a}\right)\right)\right], \qquad (2.38)$$

where the cosine-integral [77] is

$$\mathrm{Ci}(x) = \zeta + \ln(x) + \int_0^x \frac{\cos(q) - 1}{q}\,\mathrm{d}q,$$

where $\zeta = 0.5772\cdots$ is the Euler constant [77], and the sine-integral [77] is

$$\mathrm{Si}(x) = \int_0^x \frac{\sin(q)}{q}\,\mathrm{d}q.$$

Inserting Equation (2.38) into Equation (2.9) and expanding $p_0(s)$ near the origin for small s lead to

$$p_0(s) = 1 - \frac{\pi}{a}s + \frac{1}{2a^2}(4 - 4\zeta + \pi^2 + 4\ln(a) - 4\ln(s))s^2 + O(s^3),$$

which implies that $\langle\tau\rangle$ is π/a and that the existence of the second and higher order moments depends on γ. As $\gamma = 1$ is an integer, so the expansion has the singularity $\ln(s)$ term, so the variance does not exist, as illustrated in Figure 2.2. This expansion justifies the asymptotic analysis in the previous section.

For the cases $\gamma = 2/5$ and 2, the closed forms for $g(s) = \mathcal{L}\{R''(t)/(4\beta)\}$ are not known. Hence, the thesis approximates $g(s)$ by considering its asymptotic large and small behaviours. In time t space, the large t behaviour of $R''(t)/(4\beta)$ is given by the Equation (2.36), and the small t behaviour is obtained by expanding Equation (2.35) near the origin:

$$\frac{R''(t)}{4\beta} = \frac{a^2(\gamma + 3)}{4\gamma}t + O(t^3).$$

Transforming these two behaviours into the Laplace s space, then the ap-

proximation function $G(s)$ to $g(s)$ has the general form

$$G(s) = \frac{1}{Ws^2 + Ms + 2(u(0) + Q)}(u(s) + Q), \qquad (2.39)$$

where W, M and Q are constants, and can be determined from the data of numerical calculating the Laplace transform of $R''(t)/(4\beta)$, so that to furnish the correct asymptotic form for $g(s)$ at small and large values of s respectively. Note that the fact that $G(0)$ is $1/2$ results in $p_0(0) = 1$, which provides the right normalisation. The function $u(s)$ is given by Equation (2.37). As $s \to \infty$, the fact that $u(s) \to 0$ ensures that the asymptotic large behaviour of $G(s)$ is s^{-2}, which agrees with the small t expansion of $R''(t)/(4\beta)$.

The probability density function $P_0(\tau)$ of the zero-crossing interval τ now is determined by numerically inverting Equation (2.9) by using the Tablot method. To justify the validity of the approximation function $G(s)$, Figure 2.3 compares the probability density function $P_0(\tau)$ for the case $\gamma = 1$. The solid-blue curve represents $P_0(\tau)$ produced by using the closed form $g(s)$ (2.38), and the dashed-black one is obtained from by using the asymptotic approximation function $G(s)$ (2.39). It can be seen that this asymptotic approximation method well matches the analytical result. The precise form of $G(s)$ is found in Appendix F.

Figure 2.4 shows the probability density function $P_0(\tau)$ of the zero crossing interval τ for three γ. From top to bottom, it is for $\gamma = 2, 1$ and $\gamma = 2/5$ respectively. Appendix F shows the approximation function $G(s)$. It can be seen that the probability density function $P_0(\tau)$ shows the similar shape for all γ, and has a single peak off-axis, implying that zero-crossings tend to stay away from each other. The initial value is zero, which is consistent with the analysis. The inner figure is plotted on a log-log scale, and the straight line indicates that the tail of the zero-crossing interval τ is of power-law form $P_0(\tau) \sim \tau^{-\alpha}$, where $\alpha = 2 + \gamma$ for all examples. This result agrees with the asymptotic analysis shown in the previous section. These three examples will
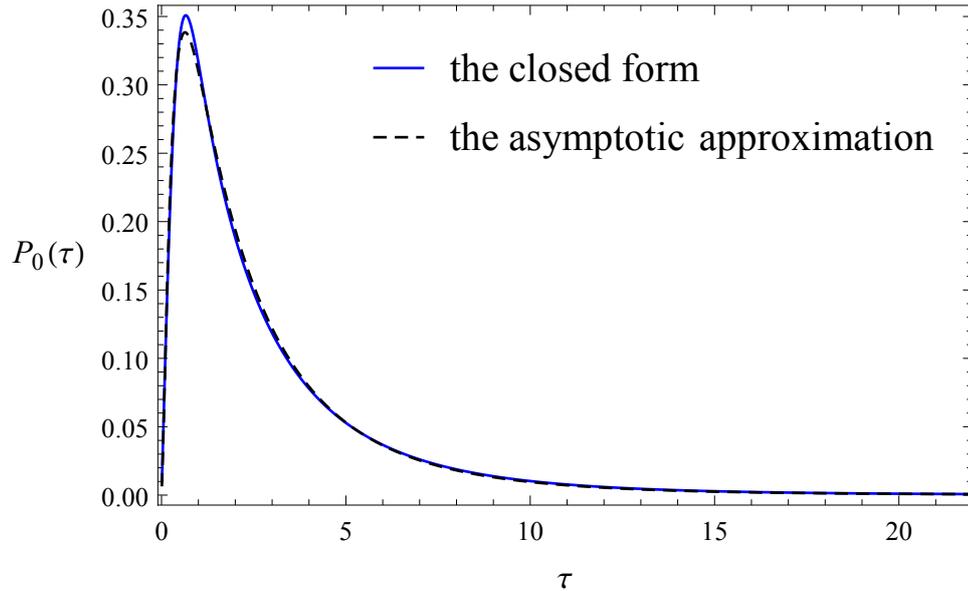
Figure 2.3: Verification of the approximation function $G(s)$ for the case $\gamma = 1$. This figure compares the probability density function $P_0(\tau)$, which is obtained from either the analytical or asymptotic method. The closed form for $g(s)$ (Equation (2.38)) is used for produced the solid-blue curve, and the approximation function $G(s)$ is for the dashed-black one.

be compared with the simulation results in the next chapter.

2.5   The power-law model $\phi_\gamma(t)$

This section considers zero-crossing intervals of the Gaussian process with the power-law autocorrelation function $\phi_\gamma(t)$, which is given by Equation (2.28). The two power-law models $\rho_\gamma(t)$ and $\phi_\gamma(t)$ have the same asymptote $t^{-\gamma}$ for large t, but it is shown in this section that the full structure of the power-law autocorrelation function affects the initial behaviour of the probability density function $P_0(\tau)$ of the zero-crossing interval τ. This section uses the similar method to derive statistical properties of the zero-crossing interval τ under the independence assumption, which was introduced in Section 2.2. The analytical results serve as the benchmark, which will be compared with simulations in Chapter 3. If simulations are not in accordance with
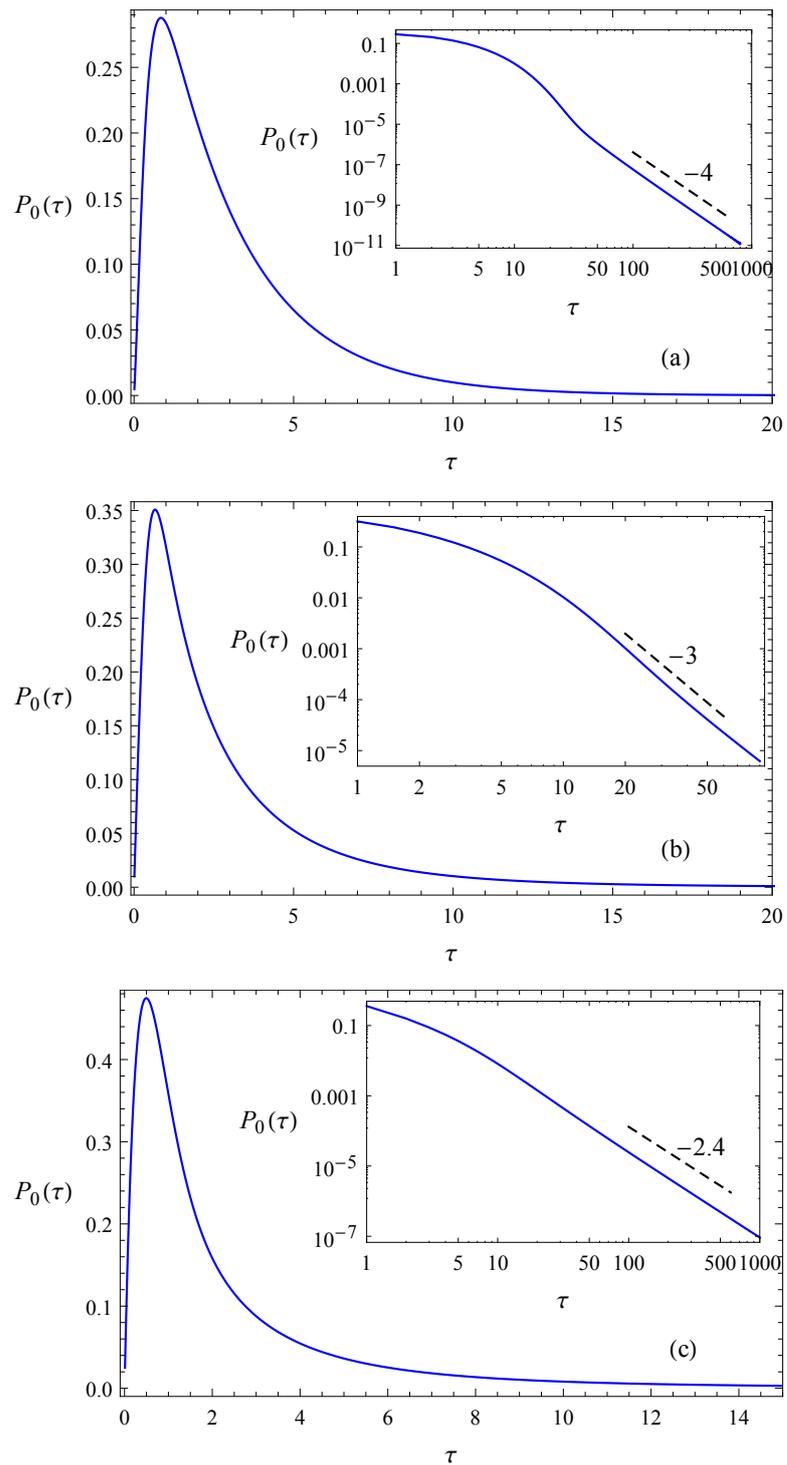
Figure 2.4: The probability density function $P_0(\tau)$ of the zero-crossing interval τ for the Gaussian process with the power-law autocorrelation function $\rho_\gamma(t)$. These curves are obtained from the independence assumption by numerical inverting Equation (2.9). From top to bottom, it corresponds to $\gamma = 2$, 1 and $2/5$ respectively.

analytical results, the assumption of independence should be rejected.

2.5.1 Mean and variance of zero-crossing intervals

The mean $\langle \tau \rangle$ of the zero-crossing interval τ is still π/a, and the variance σ^2 is calculated by Equation (2.12). By using the comparison test [75], it is found that σ^2 is infinite when $0 < \gamma \leq 1$, and shows the similar shape like that for the power-law model $\rho_\gamma(t)$, which is given by Equation (2.27).

2.5.2 The persistence parameter

The persistence parameter θ is calculated by solving the pole of the Laplace transform of the probability density function in Equation (2.9). That is, to determine θ, which satisfies the equation $1 - g(-\theta) = 0$, where $g(s) = \mathcal{L}\{R''(t)/(4\beta)\}$. For the power-law autocorrelation function $\phi_\gamma(t)$, it is easy to obtain that

$$\frac{R''(t)}{4\beta} = \frac{a}{\gamma} \frac{(1 + at/\gamma)^\gamma (1 - \gamma + (1 + \gamma)(1 + at/\gamma)^{2\gamma})}{(1 + at/\gamma)^2 (1 + (1 + at/\gamma)^{2\gamma})^2}, \qquad (2.40)$$

which does not converge for negative s values when evaluating the Laplace transform, implying that θ does not exist. This fact indicates that the tail of the zero-crossing interval τ is not of exponential form, and higher order moments of the zero-crossing interval τ are not always finite. This result is consistent with the infinite variance when $0 < \gamma \leq 1$. Note that the non-existence of the persistence parameter θ is similar to that for the power-law autocorrelation function $\rho_\gamma(t)$ (2.27).

2.5.3 Probability density functions

This section is to evaluate the probability density function $P_0(\tau)$ of the zero-crossing interval τ and its initial value $P_0(0)$. The aim is to show that given

different power-law autocorrelation functions, the initial behaviour $P_0(0)$ shows various forms.

The initial value $P_0(0)$

It has been seen that the initial behaviour of $P_0(\tau)$ provides information about zero-crossings, which can be used to determine whether zero-crossings are anti-bunching or bunching. The initial value theorem [76] is used again to investigate $P_0(0)$. For the power-law model $\phi_\gamma(t)$, if we expand Equation (2.40) for small t, it gives that

$$\frac{R''(t)}{4\beta} = \frac{a}{2\gamma} + \frac{a^2(\gamma^2 - 2)}{2\gamma}t + O(t^2),$$

which implies that the large s behaviour of $g(s) = \mathcal{L}\{R''(t)/(4\beta)\}$ is

$$g(s) = \frac{a}{2\gamma}\frac{1}{s} + \frac{a^2(\gamma^2 - 2)}{2\gamma}\frac{1}{s^2} + O(s^{-3}).$$

Inserting this expansion into the initial value theorem leads to

$$\begin{aligned}
\lim_{\tau \to 0} P_0(\tau) &= \lim_{s \to \infty} s\,p_0(s) \\
&= \lim_{s \to \infty} \frac{sg(s)}{1 - g(s)} \\
&= \frac{a}{2\gamma},
\end{aligned} \tag{2.41}$$

which indicates that $P_0(0)$ is determined by the time-scale constant a and the memory index γ. As $\gamma \to \infty$, then $\phi_\gamma(t) \to \rho_e(t)$, and the limit of Equation (2.41) is zero, which is consistent with the initial behaviour shown in Figure 2.1. Equation (2.41) implies that $P_0(0)$ is not zero for all finite γ, which differs from that for the power-law autocorrelation function $\rho_\gamma(t)$.

It has been seen that zero-crossings whether bunched or anti-bunched

depend on the sign of $P_0'(0)$, so using the initial value theorem twice yields

$$
\begin{aligned}
\lim_{\tau \to 0} P_0'(\tau) &= \lim_{s \to \infty} s(sp_0(s) - P_0(0)) \\
&= \lim_{s \to \infty} s\left(\frac{sg(s)}{1 - g(s)} - \frac{a}{2\gamma}\right) \\
&= \frac{a^2(\gamma^2 - 2)}{2\gamma}.
\end{aligned}
\tag{2.42}
$$

If $\gamma > \sqrt{2}$, zero-crossings are anti-bunched (repelled by each other), otherwise, they are bunched (attracted to each other). When $\gamma \to \infty$, Equation (2.42) is positive, which agrees with that for the exponentially bounded model $\rho_e(t)$ shown in Figure 2.1, because $\phi_\gamma(t) \to \rho_e(t)$.

We conclude that although the autocorrelation functions $\rho_\gamma(t)$ and $\phi_\gamma(t)$ have the same asymptote $t^{-\gamma}$ for large t, the probability density function $P_0(\tau)$ of the zero-crossing interval τ has different initial behaviours.

The probability density function

This section shows the probability density function $P_0(\tau)$ of the zero-crossing interval τ for the power-law autocorrelation function $\phi_\gamma(t)$. Let $\gamma = 1$ and $a = 1$ in Equation (2.40), then the Laplace transform of $R''(t)/(4\beta)$ is

$$
g(s) = \frac{1}{2}\left(i\,e^{(1-i)s}\,s\,\Gamma(0, (1-i)s) - i\,e^{(1+i)s}\,s\,\Gamma(0, (1+i)s) + 1\right),
$$

where the incomplete Gamma function [77] is

$$
\Gamma(\alpha, x) = \int_x^\infty t^{\alpha-1} e^{-t}\, dt,
$$

and i is the imaginary unit. By using the Tablot method to inverse Equation (2.9), Figure 2.5 plots the probability density function $P_0(\tau)$ for the case $\gamma = 1$. It can be seen that the initial value $P_0(0)$ is $1/2$, which is consistent with Equation (2.41), and that $P_0'(0) < 0$ because $\gamma - \sqrt{2} < 0$, which is in
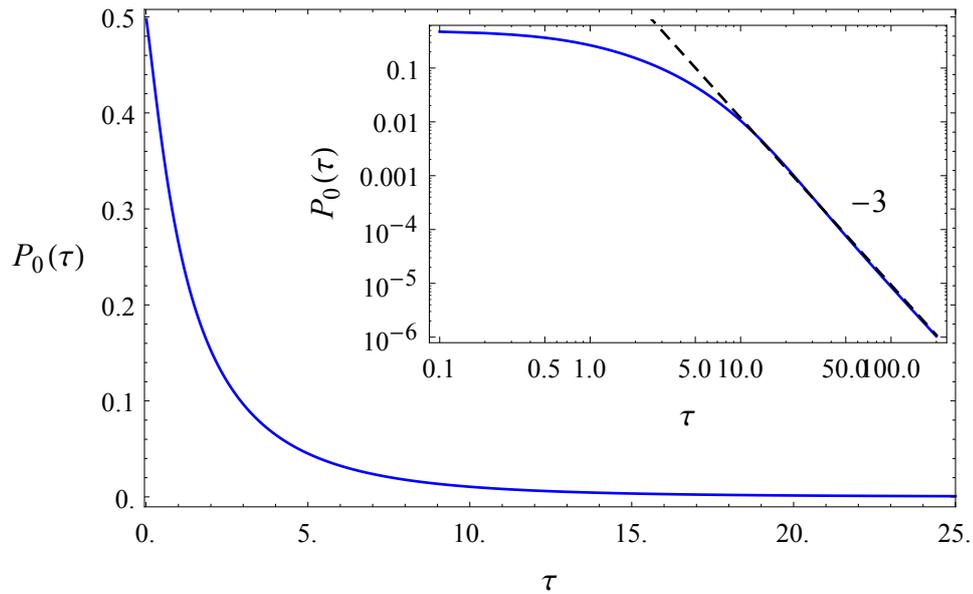
Figure 2.5: This figure shows the probability density function $P_0(\tau)$ of the zero-crossing interval τ for the power-law model $\phi_\gamma(t)$ for the case $\gamma = 1$ under the independence assumption. The initial value $P_0(0)$ is $1/2$, and the inner log-log plot indicates that the tail of the zero-crossing interval τ is of power-law form $P_0(\tau) \sim \tau^{-(\gamma+2)}$ for large τ.

accord with (2.42). The inset log-log plot shows that the tail is of power-law form $P_0(\tau) \sim \tau^{-(\gamma+2)}$ for large τ. Comparing with Figure 2.4 (b), which is the case $\gamma = 1$ for the power-law model $\rho_\gamma(t)$, one concludes that the probability density function $P_0(\tau)$ of the zero-crossing interval τ is influenced by the entire structure of the autocorrelation function.

2.6 Summary

Chapter 2 considered zero-crossing intervals of correlated Gaussian processes under the assumption that successive zero-crossing intervals are statistically independent. This is a rough approximation though and in the absence of any other known model for the correlations among zero-crossing intervals, this is an analytically tractable choice. Based on this argument, results in this chapter are obtained analytically, and will serve as the benchmark to com-

pare with the simulations in Chapter 3. Three different models for the autocorrelation functions were investigated. One is the exponentially bounded type (short-term memory): $\rho_e(t)$, and the other two are the power-law form (long-term memory): $\rho_\gamma(t)$ and $\phi_\gamma(t)$. If results of simulations in Chapter 3 do not consist with analytical results shown in Chapter 2, the independence approximation to zero-crossing intervals should be rejected.

For the exponentially bounded autocorrelation function $\rho_e(t)$, it is found that the mean $\langle \tau \rangle$ of the zero-crossing interval τ is π/a, and the variance σ^2 is finite. The persistence parameter θ is obtained analytically, which is about 0.37. The existence of θ implies that the tail of the zero-crossing interval τ is of exponential form $P_0(\tau) \sim \exp(-\theta\tau)$ for large τ. This fact is justified by determining the full probability density function of $P_0(\tau)$, which is plotted in Figure 2.1.

For the power-law autocorrelation functions $\rho_\gamma(t)$ and $\phi_\gamma(t)$, it is found that the mean $\langle \tau \rangle$ is π/a; the variance σ^2 is finite if $\gamma > 1$ but becomes infinite if $\gamma \leq 1$. The implication of this result is that the persistence value θ does not exist, and two different methods are used to show this fact. The asymptotic analysis shows that the expansion of $p_0(s)$ for small s consists of terms either $s^{\gamma+1}\ln(s)$ or $s^{\gamma+1}$ depending on whether or not γ is an integer. These singularity terms imply that not only the variance could be infinite, but also higher order moments. The tail of the zero-crossing interval τ follows $P_0(\tau) \sim \tau^{-(\gamma+2)}$ for large τ, which agrees with the fact that σ^2 is infinite when $\gamma \leq 1$. The tail behaviour is justified by plotting the full probability density functions, which are shown in Figure 2.4 and 2.5. The initial value of $P_0(\tau)$ is considered analytically by using the initial value theorem, and it is found that $P_0(0)$ is zero for the model $\rho_\gamma(t)$, but it is not for $\phi_\gamma(t)$. This result implies that the entire structure of the autocorrelation function affects the initial behaviour of $P_0(\tau)$.

It has to be noted that results of zero-crossing intervals in this chapter

are derived from the independence assumption. Hence, in the next chapter, these results will be compared with the simulation results, so that to examine the validity of the independence assumption.

Chapter 3

Simulation Results of Zero-crossing Intervals

3.1 Introduction

Chapter 2 investigated zero-crossing intervals of Gaussian processes, and results were obtained by assuming that the successive zero-crossing intervals are statistically independent. The aim of this chapter is to examine the validity of the independence assumption by comparison with simulations.

This chapter first introduces simulation algorithms, which consist of two steps. The first step is to generate the Gaussian process with the specific autocorrelation function, and the second is to locate zero-crossings so that to determine the lengths of zero-crossing intervals. These two steps can be coded in the computer software, for example, *MatLab*. Therefore, the results of this chapter heavily depend on numerical simulations. The autocorrelation functions used for simulations are the same as those considered in Chapter 2, including the exponentially bounded autocorrelation function $\rho_e(t)$, and two power-law autocorrelation functions $\rho_\gamma(t)$ and $\phi_\gamma(t)$.

3.2   Simulation algorithms

This section reviews the simulation procedures. To simulate the correlated Gaussian process, the Fourier filtering method [78] is used. A summary of methods of simulating correlated Gaussian processes can be found in [79]. The algorithm for finding zero-crossings was demonstrated by Smith [68].

3.2.1   Correlated Gaussian processes

To simulate the correlated Gaussian process is the first step. We want to generate a Gaussian random process with the autocorrelation function $\rho(t)$ and with a Fourier transform

$$S(\omega) = \int_{-\infty}^{\infty} \rho(t) \mathrm{e}^{-\mathrm{i}\omega t} \, \mathrm{d}t.$$

In signal analysis, $S(\omega)$ is called as the spectral density function [80]. In this section, we briefly outline the Fourier filter method, and more details can be found in [78], [81] and [82]. In simulations, the processes are discrete, so the discrete Fourier transform is used [83]:

$$F_k = \frac{1}{\sqrt{N}} \sum_{j=0}^{N-1} f_j \exp\left(\frac{2\pi\mathrm{i}j}{N}k\right)$$

where f_j is the jth component of the N elements to be transformed, and F_k are the N transformed numbers. The inverse discrete Fourier transform is defined as

$$f_j = \frac{1}{\sqrt{N}} \sum_{k=0}^{N-1} F_k \exp\left(\frac{-2\pi\mathrm{i}k}{N}j\right).$$

When N is large enough, the transformation pair is an accurate approximation to the continuous Fourier transform. The exact value N used for simulations in this thesis is seen in the next section.

Now consider a sequence $\{u_j\}_{j=1,2,\ldots,N}$ of uncorrelated Gaussian random

numbers with zero mean and unit variance, and the autocorrelation function $\rho(t)$ sampled at N intervals: $\{\rho_j\}$. The Fourier filter method includes the following three steps:

a. Compute the discrete Fourier transform of $\{u_j\}$, denoted as $\{U_k\}$.

b. Compute the discrete Fourier transform of the sampled autocorrelation function $\{\rho_j\}$, denoted as $\{S_k\}$.

c. Multiply them together

$$Y_k = \sqrt{S_k}\, U_k,$$

and calculate the discrete inverse Fourier transform of $\{Y_k\}$ to obtain $\{y_j\}$, which is the required Gaussian process with the desired autocorrelation function $\rho(t)$.

Many numerical programming packages provide the built-in functions to compute the discrete Fourier transform and its inverse, for instance, MatLab provides the command 'fft' and 'ifft', which make the Fourier filter method is simple to code. Given the correlated process $\{y_j\}$, then we have to locate the zero-crossing points so that to obtain data for zero-crossing intervals.

3.2.2   Lengths of zero-crossing intervals

We are now in a position that given a correlated series and need to locate its zero-crossings. It has to mention that the process is discrete in simulations, so it is necessary to define what is exactly meant by zero-crossings in a discrete series.

Zero-crossings in a discrete process

Given a discrete series $\{y_j\}$, $j = 1, 2, \ldots, N$, first consider a series $\{h_j\}$ defined by

$$
h_j = \begin{cases} 1 & y_j \geq 0 \\ 0 & y_j < 0. \end{cases} \tag{3.1}
$$

Let d_j be an indicator function $d_j = (h_{j+1} - h_j)^2$. Then d_j is 0 or 1. When $d_j = 1$, we say that a zero-crossing occurs at time j. This definition implies that the length of one zero-crossing interval is determined by the difference between two successive zero-crossing times and that there cannot have infinite zero-crossings.

Lengths of zero-crossing intervals

An efficient method to detect the zero-crossings was demonstrated by Smith [68]. As an illustration of his method, consider the following series:

0.2	-0.2	-0.1	-0.3	0.3	0.1	0.3	-0.1	0.2

The first step is to take the sign of the series:

1	-1	-1	-1	1	1	1	-1	1

Next, create a new array which is the above sign array multiplies one which the sign array shifts every element to right one place, and ignore the elements where they do not overlap:

1	−1	−1	−1	1	1	1	−1	1	
×									
	1	−1	−1	−1	1	1	1	−1	1
=									
	−1	1	1	−1	1	1	−1	−1	

The last step is to subtract one from each element in the above series, and divide by minus two:

1	0	0	1	0	0	1	1

The corresponding train of zeros and ones gives the locations of the zero crossings. The Smith's method is quick to count zero-crossings in very long streams of data. Once we know locations of the zero-crossing points, with the help of MatLab's built-in 'find' function, the locations of zero-crossings can be identified:

1	0	0	1	0	0	1	1
Find							
		1	4	7	8		

Then we can obtain the data for lengths of zero-crossing intervals by difference:

Lengths of Zero-Crossing interval	3	3	1

MatLab allows operations to be performed on entire vectors, so in general, there is no need to calculate in an element-by-element fashion.

3.3 Simulation results

We simulate the Gaussian process with the specific autocorrelation function by the Fourier filter method. The first considered autocorrelation function is

$$\rho_e(t) = \frac{2\exp(-at)}{1+\exp(-2at)},\tag{3.2}$$

the second one is

$$\rho_\gamma(t) = (1+a^2t^2/\gamma)^{-\gamma/2}\tag{3.3}$$

and the last one is

$$\phi_\gamma(t) = \frac{2(1+a|t|/\gamma)^\gamma}{1+(1+a|t|/\gamma)^{2\gamma}}.\tag{3.4}$$

Here $\gamma > 0$ is the memory index, and a is the correlation scale-length, which is taken to be 0.01 in the simulations. The correlation length can be interpreted as the resolution of the process: decreasing it allows the process to be resolved in more detail so that to expect the number of zero-crossings agree with Rice's formula (2.25).

For the exponentially bounded model $\rho_e(t)$ (3.2), the simulations are formed by averaging 5000 realisations each with length up to 2^{18}, which is an adequate length, because $\rho_e(t) \sim \exp(-t)$ for large t and has a rapid decay.

The power-law models $\rho_\gamma(t)$ and $\phi_\gamma(t)$ given by Equation (3.3) and (3.4) require longer and more realisations to achieve the accuracy for the mean of the zero-crossing intervals, predicted by the reciprocal of Rice's formula (2.25). For generating longer data arrays, the Fourier transform takes longer times to evaluate, but it still can be run. When $\gamma > 1$, each realisation with 2^{20} is sufficient, but must be increased to 2^{24} when $\gamma \leq 1$. For all considered γ, the simulated results are averaged over 10^5 realisations.
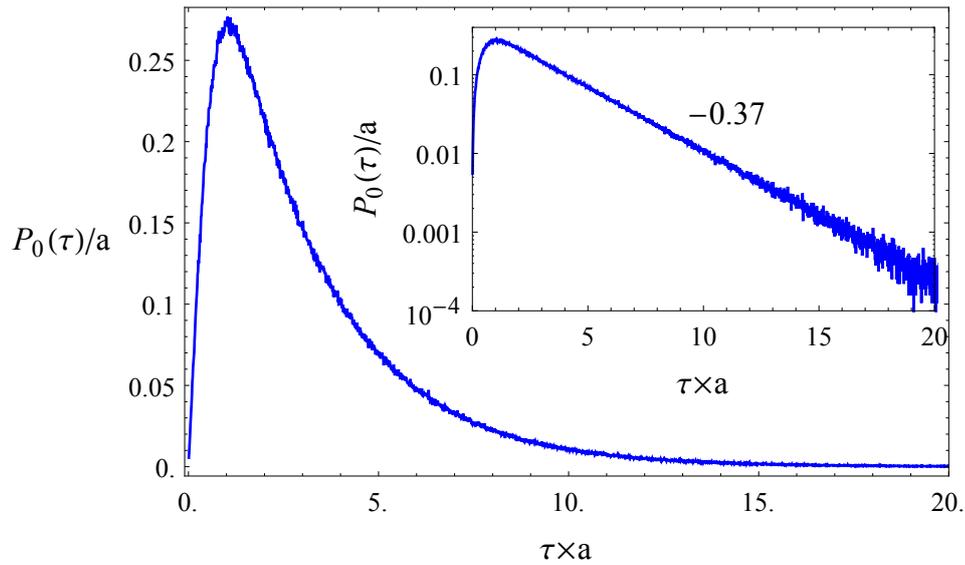
Figure 3.1: The normalised probability density function $P_0(\tau)/a$ of the zero-crossing interval τ of the Gaussian process with the exponentially bounded autocorrelation function $\rho_e(t)$ (3.2), is plotted as a function of $a\tau$. The inset log-linear plot indicates that the tail is of the exponential form $\exp(-A\tau)$, where $A \approx 0.37$. The figure is simulated with the time-scale length $a = 0.01$ and averaged over 5000 realisations with each up to 2^{18}.

3.3.1 Simulation results for the exponentially bounded autocorrelation function $\rho_e(t)$

Figure 3.1 shows the normalised probability density function $P_0(\tau)/a$ of the zero-crossing interval τ as a function of $a\tau$ for the Gaussian process with the exponentially bounded autocorrelation function $\rho_e(t)$ (3.2). The normalised probability density function $P_0(\tau)/a$ is plotted since the correlation length a is a scale parameter, which is shown in Appendix D. It can be seen that the probability density function starts from zero, then there is a peak located off-axis, implying zero-crossings are anti-bunched (repelled by each other). The inner figure shows the tail behaviour of the zero-crossing interval τ, which is plotted on a log-linear scale. The straight line shows that the tail is of exponential form $\exp(-A\tau)$, where A is about 0.37. Clearly, the end of the

tail shows the simulation noise.

Now we compare Figure 3.1 with Figure 2.1 in Chapter 2, which is obtained from the independence assumption. It can be seen that these two figures are satisfactorily close to each other, implying that the statistical independence approximation of zero-crossing intervals is *adequate*. This approximation also indicates that the correlations of intervals are so small that they can be neglected. To justify this fact, the correlations among zero-crossing intervals are shown in the next section in Figure 3.3 (d), and it is found the correlations are approximated to be zero.

The exponentially bounded autocorrelation function $\rho_e(t)$ decreases to zero quickly, implying that two values at different times of the process have little dependence on each other. Hence, it can be considered as producing short-term memory between the zero-crossings. As a consequence, it indicates that the independence assumption can be used to approximate correlations of zero-crossing intervals. One implication is that this assumption is still applicable if the autocorrelation function decays exponentially or even faster.

3.3.2   Simulation results for the power-law model $\rho_\gamma(t)$

This section shows simulation results of zero-crossing intervals of the Gaussian process with the autocorrelation function $\rho_\gamma(t)$, which is given by Equation (3.3). Then the results will be compared with that obtained in Section 2.4 of Chapter 2, which were analytically derived under the statistical independence assumption. The aim is to check the validation of the statistical independence approximation.

Probability density functions

Figure 3.2 shows the normalised probability density function $P_0(\tau)/a$ of the zero-crossing interval τ as a function of $a\tau$. From top to bottom, it corre-

sponds to $\gamma = 2$, 1 and $2/5$ respectively. Now compare Figure 3.2 with Figure 2.4 in Chapter 2, which is obtained from the independence assumption. Figure 3.2 shows that the probability density functions $P_0(\tau)$ have the similar shape and do not have power-law tails, however, Figure 2.4 shows that the tail of zero-crossing intervals is of the power-law form: $P_0(\tau) \sim \tau^{-(2+\gamma)}$ for large τ.

Figure 3.2 (a) shows that the tail is of the exponential form if $\gamma > 1$: because the inset plot is produced on a log-linear scale, and the straight line indicates that the tail is exponentially decaying $\exp(-A\tau)$, for large τ, where A is about 0.32.

Figure 3.2 (b) and (c) plot $P_0(\tau)/a$ against $a\tau$ for the cases $\gamma = 1$ and $\gamma = 2/5$. This regime $0 < \gamma \leq 1$ was already considered by Eichner et al. [39]. They claimed that given a Gaussian process with the power-law asymptote autocorrelation function $\rho(t) \sim t^{-\gamma}$ with $0 < \gamma \leq 1$, then the tail of the probability density function of the return intervals follows the stretched exponential. Specifically, they defined the return intervals as follows. Let $\{x_i\}$ denote a sequence of time series. An extreme event happens at i, if $x_i > q$ where q is some threshold value. The return interval then is defined as the time between the successive occurrence of extreme events. The problem they considered is very similar to the zero-crossing analysis discussed in this thesis if we put $q = 0$.
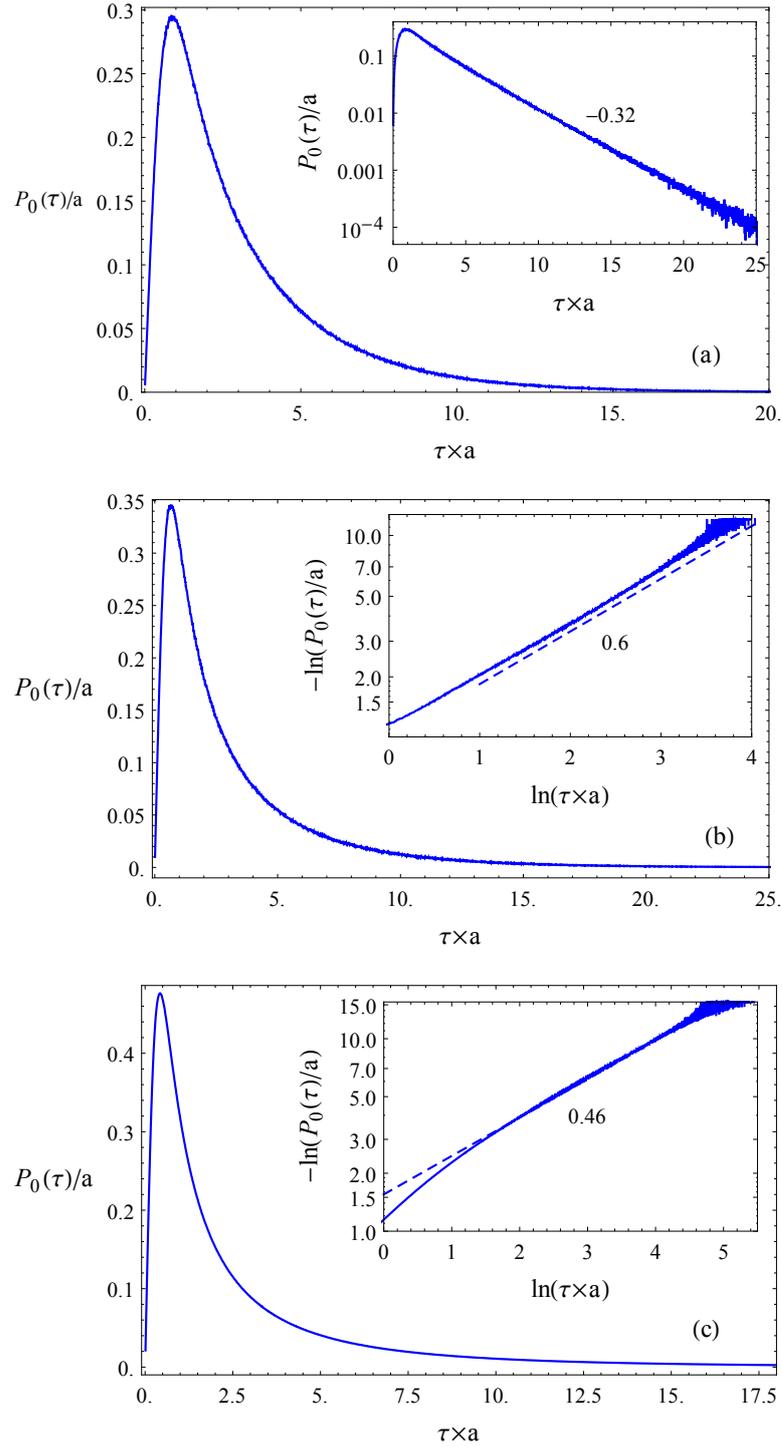
Figure 3.2: This figure shows the simulation results for the probability density function $P_0(\tau)/a$ of the zero-crossing interval τ given the power-law autocorrelation function $\rho_\gamma(t)$ (3.3). From top to bottom, it corresponds to $\gamma = 2$, 1 and $2/5$ respectively. The inner plots show the tail behaviour of the zero-crossing interval τ, which is different with the independence model shown in Figure 2.4 in Chapter 2. This figure is obtained by simulating with $a = 0.01$ and averaging over 10^5 realisations.

The inner plots of Figure 3.2 (b) and (c) show $-\ln(P_0(\tau)/a)$ as a function of $\ln(a\tau)$ in the log-linear fashion, and straight lines appear. These two plots seem to support the result of Eichner et al. [39], which claimed that $P_0(\tau) \sim \exp(-\tau^\eta)$, where $0 < \eta < 1$ is a constant. The thesis will argue that in spite of the apparent agreement with Eichner et al.'s results, this regime $0 < \gamma \leq 1$ does not represent a physically realizable Gaussian process because the power is infinite. Notwithstanding this, a computer 'experiment' with this autocorrelation function can be conducted, but it does not correspond to a realization of a valid Gaussian processes. This issue will be detailed in Chapter 4.

We conclude that for power-law bounded autocorrelation function $\rho_\gamma(t)$, the simulation results of zero-crossing intervals show different behaviours compared with that derived from the independence assumption shown in Section 2.4 of Chapter 2. This fact implies that simulations and analytical results are not consistent. Hence, the independent approximation to successive zero-crossing intervals should be rejected. Based on this fact, it is natural to consider and examine whether there exists correlations among zero-crossing intervals, which will be checked in the following section.

Correlations between zero-crossing intervals

This section calculates the correlations of the zero-crossing intervals. The aim is to examine the dependence between zero-crossing intervals.

Denote $\{r_i\}$, $i = 1, 2, \cdots, N$ as the lengths of zero-crossing intervals. That is r_1 represents the length of the first zero-crossing interval; r_2 is the length of the second zero-crossing interval, and so on. To study the correlations among zero-crossing intervals, the autocorrelation function of the zero-crossing intervals is calculated by

$$c(k) = \frac{1}{\sigma_{r_i}^2 (N - k)} \sum_{i=1}^{N-k} (r_i - \bar{r})(r_{i+k} - \bar{r}), \tag{3.5}$$

where $\sigma_{r_i}^2$ and $\bar{r}$ are the variance and mean of the interval data array $\{r_i\}$. In particular, when $k = 0$, $c(0)$ is unity. This definition is often encountered in time series analysis, for example [84].

The interpretation of $c(k)$ is as follows. $c(1)$ is the correlation between the ith and the $i+1$th zero-crossing intervals, $c(2)$ is the correlation between the ith and the $i+2$th zero-crossing intervals, and in general $c(k)$ measures the correlation between the ith and the $i + k$th zero-crossing intervals. If $c(k) \neq 0$, it means that two intervals are correlated. In simulations, $c(k)$ is calculated up to the lag 100 as it is sufficient to observe the trend of the correlations of zero-crossing intervals.

Figure 3.3 shows the correlations of zero-crossing intervals by calculating Equation (3.5) for $\gamma = 2$, 1 and $2/5$. It can be seen that the correlations $c(k)$ show the alternating decaying behaviour, and $c(1)$ is negative for all considered value γ. The correlation defined by Equation (3.5) is a measure of the linear dependence between two variables [85]. Hence, the negative value $c(1)$ implies that a zero-crossing interval and its successive one have the trend to move in the opposite directions, according to the definition (3.5).

The right panel of Figure 3.3 plots $c(k)$ against k on a log-log scale. The straight lines indicate that $c(k) \sim k^{-\delta}$, where $\delta > 0$ is a constant. It is found that δ is nearly the same as γ. For instance, when $\gamma = 1$, δ is about 1.1. The power-law behaviour of $c(k)$ indicates that zero-crossing intervals are also long-term correlated, and do not form the Markov chain as was assumed by McFadden [23].

Note that the value $c(k)$ is small and not significant for all shown examples. Therefore, it implies that the correlations of zero-crossing intervals will be contained in the high-order moments of $\{r_i\}$.

Figure 3.3 (d) shows the correlations of zero-crossing intervals for the exponentially bounded model $\rho_e(t)$ (3.2). It can be seen that $c(k)$ is small for all $k > 0$, implying that the independence assumption is a valid approximation
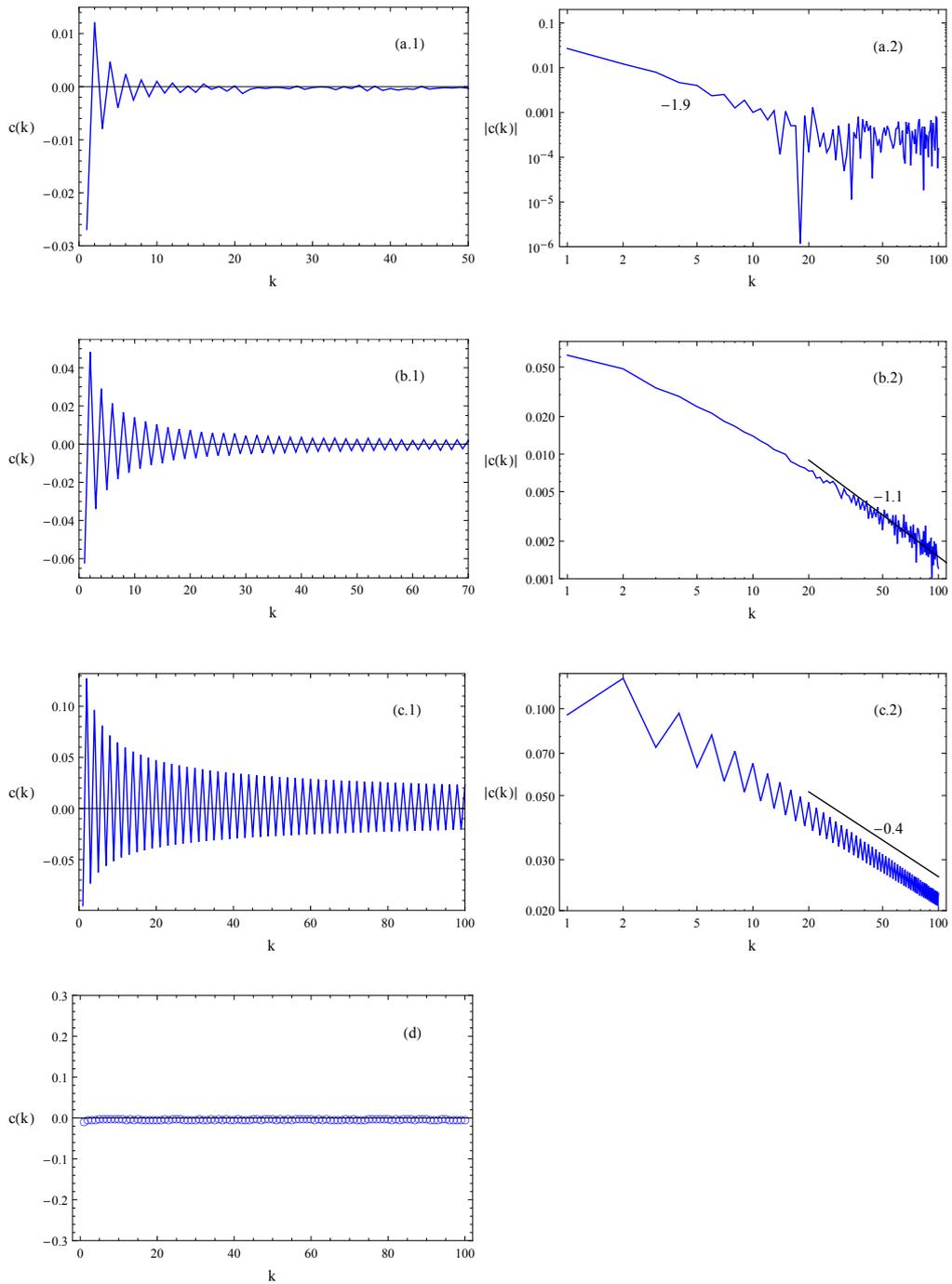
Figure 3.3: This figure shows the correlations of zero-crossing intervals given the power-law model $\rho_\gamma(t)$ (3.3). The correlations $c(k)$ are defined by Equation (3.5). Plots (a)-(c) correspond to $\gamma = 2, 1$ and $2/5$ respectively. It shows that the correlations have the alternating behaviour and are of power-law decaying form. Plot (d) shows the correlations of zero-crossing intervals for the exponentially bounded autocorrelation function $\rho_e(t)$ (3.2). It shows that the correlations are close to zero.

54

to the zero-crossing intervals.

3.3.3 Simulation results for the power-law model $\phi_\gamma(t)$

This section shows simulation results for zero-crossing intervals of the Gaussian process with the power-law bounded autocorrelation function $\phi_\gamma(t)$, which is given by Equation (3.4). Simulations will be compared with the analytical results derived from the independent assumption shown in Section 2.5 in Chapter 2. Furthermore, it will be seen that although $\phi_\gamma(t)$ and $\rho_\gamma(t)$ have the same power-law asymptote $t^{-\gamma}$ for large t, the exact structure of the autocorrelation function has effects on the initial value of the probability density function $P_0(\tau)$ of the zero-crossing interval τ.

Chapter 2 showed that the expansion of $\phi_\gamma(t)$ near the origin is

$$\phi_\gamma(t) = 1 - \frac{a^2}{2}t^2 + \frac{a^3}{2\gamma}|t|^3 + \frac{a^4(5\gamma^2 - 11)}{24\gamma^2}t^4 + O(|t|^5).$$

Unlike the power-law model $\rho_\gamma(t)$, which is smooth to all orders, the fourth derivative of $\phi_\gamma(t)$ at the origin is singular corresponding to the trace formed from a realization of the process having a derivative that is continuous but not differentiable. For this reason, the power-law model $\phi_\gamma(t)$ is referred as subfractal, which means zero-crossings could form a cluster [34]. Namely, the crossings could stay close to each other. To illustrate the behaviour of cluster, an example from a realisation of simulations is shown in black squares in Figure 3.4.

Probability density functions

Figure 3.5 shows the normalised probability density functions $P_0(\tau)/a$ of zero-crossing intervals as a function of $a\tau$ for the power-law model $\phi_\gamma(t)$ for the cases $\gamma = 2$, 1 and $2/5$ from top to bottom respectively. It can be seen that the shapes of $P_0(\tau)$ are richer than that for the power-law model
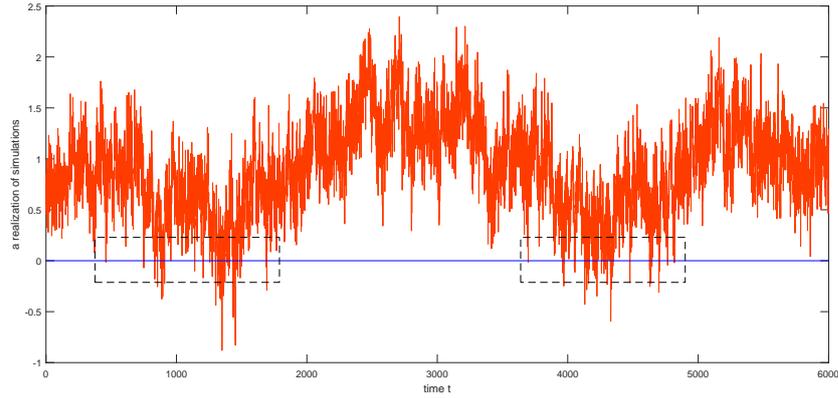
Figure 3.4: This figure illustrates the clusters formed by the zero-crossings from a realisation of simulations, shown in the two squares. In each square, the zero-crossings are close to each other, and there is space between two clusters. The power-law autocorrelation function $\phi_\gamma(t)$ is with the index $\gamma = 2$.

$\rho_\gamma(t)$, shown in Figure 3.2. Figure 3.5 indicates that the initial value $P_0(0)$ of the probability density function $P_0(\tau)$ of the zero-crossing interval τ is far away from zero for all considered value γ. This fact is different from that for the power-law model $\rho_\gamma(t)$ shown in Figure 3.2, where $P_0(0)$ is close to zero. Note that the initial value formula (2.41) in Chapter 2 is derived from the independence model but approaches to the simulation results, implying that the behaviour of $P_0'(0)$ can be approximated by Equation (2.42).

The inner plot of Figure 3.5 (a) is shown in a log-linear scale when $\gamma = 2$. The straight line indicates that the tail of the probability density function $P_0(\tau)$ of the zero-crossing interval τ is of exponential form $P_0(\tau) \sim \exp(-A\tau)$, where A is about 0.25. When $\gamma \leq 1$, the subfigures in Figure 3.5 (b) and (c) are produced by plotting $-\ln(P_0(\tau)/a)$ against $\ln(a\tau)$ in a log-linear fashion, and straight lines are presented. These results are similar to that shown for the power-law model $\rho_\gamma(t)$. Therefore, we conclude that the initial behaviour $P_0(0)$ is influenced by the full structure of the power-law autocorrelation function, and the simulation results of probability density functions of zero-crossing intervals show the same tail behaviours.
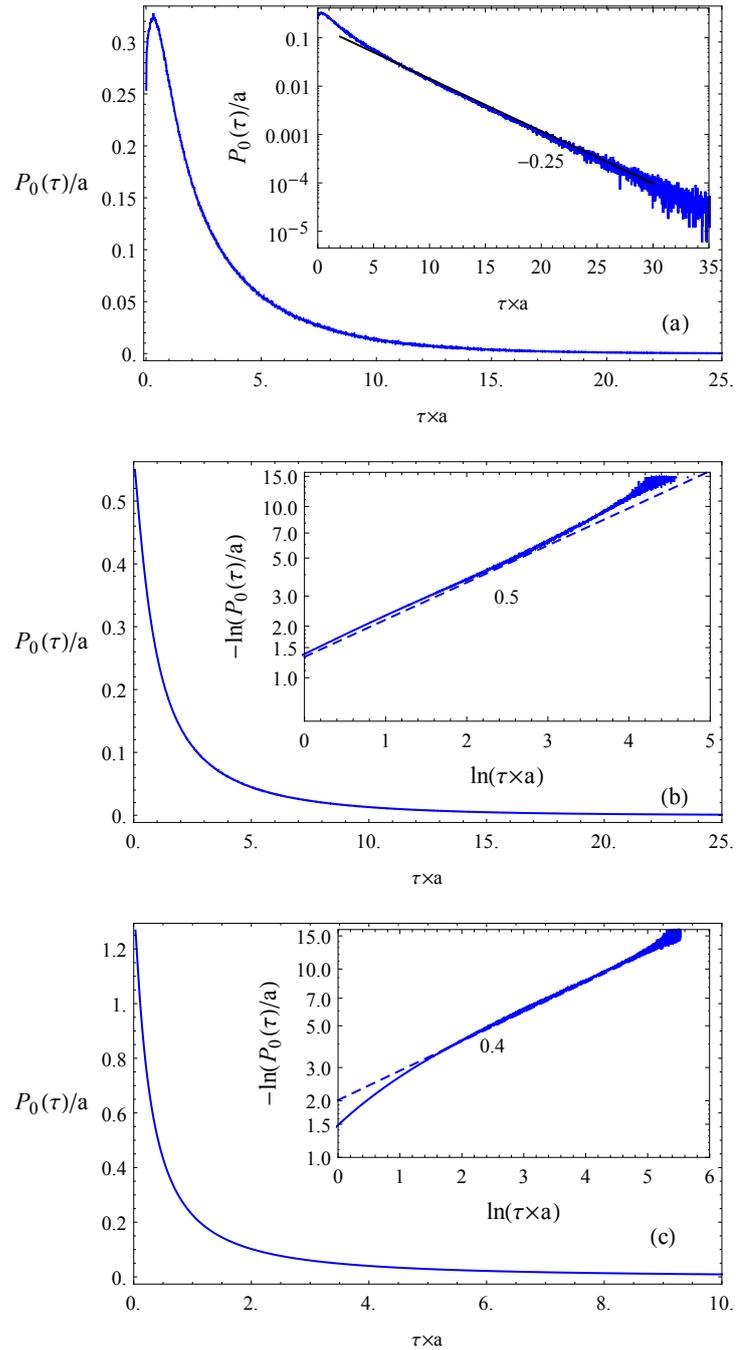
Figure 3.5: This figure shows the normalised probability density function $P_0(\tau)/a$ of zero-crossing intervals for the power-law model $\phi_\gamma(t)$. From top to bottom, it corresponds to $\gamma = 2, 1$ and $2/5$ respectively. The aim of this figure is to compare with Figure 3.2, which is obtained for the power-law model $\rho_\gamma(t)$. The obvious difference is that the initial value $P_0(0)$ is not zero, and $P_0(\tau)$ shows two shapes. This figure is simulated with $a = 0.01$ and averaging over 10^5 realisations.

Correlations of zero-crossing intervals

The correlations $c(k)$ of zero-crossing intervals are calculated by using Equation (3.5). Figure 3.6 shows the behaviour of $c(k)$ for the power-law model $\phi_\gamma(t)$. From top to bottom, it corresponds to $\gamma = 2$, 1 and $2/5$ respectively. It can be seen that the correlations $c(k)$ still show the alternating behaviour, and the absolute value $c(1)$ is not the largest. Comparing with Figure 3.3, it is found that the alternation is more intensive, indicating that the dependence of the zero-crossing intervals is stronger. The right panel of Figure 3.6 is plotted in a log-log scale. The straight lines imply that $c(k) \sim k^{-\delta}$, where δ is also shown. It is found that δ is very close to γ, especially when γ is small. We conclude that there is no obvious difference in behaviours of the correlations of the zero-crossing intervals for the considered power-law autocorrelation functions.

3.4   Summary

Simulation results for zero-crossing intervals of Gaussian processes were obtained in this chapter. The aim of this chapter is to test the validity of independence assumption between zero-crossing intervals.

For the exponentially bounded autocorrelation function $\rho_e(t)$, the independence assumption can be used to study zero-crossing intervals. Figure 3.1 shows the simulated probability density function of the zero-crossing interval τ. Comparing it with Figure 2.1 in Chapter 2, which is obtained from the independence assumption, it is found that they match well. Moreover, the correlations of zero-crossing intervals are shown in Figure 3.3 (d), which are close to zero, implying that there is less dependence between zero-crossing intervals. This fact indicates that if the autocorrelation function decays exponentially or even faster, the independence assumption is adequate.

For the power-law autocorrelation functions $\rho_\gamma(t)$ and $\phi_\gamma(t)$, however, the
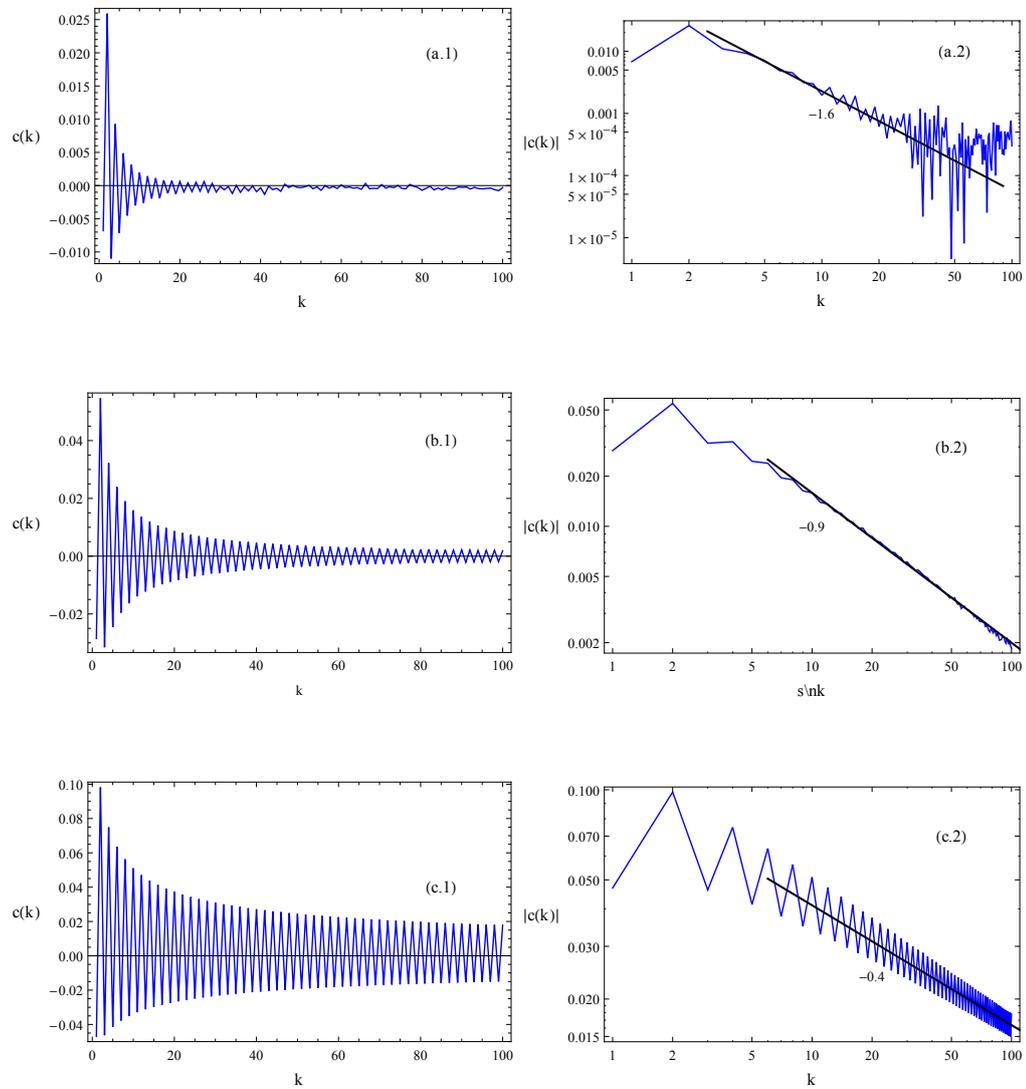
Figure 3.6: This figure shows the correlations $c(k)$ of zero-crossing intervals for the power-law model $\phi_\gamma(t)$. From top to bottom, it corresponds to $\gamma = 2$, 1 and $2/5$ respectively. The aim is to compare with Figure 3.3. It is found that correlations $c(k)$ of the zero-crossings intervals show the similar behaviour for both considered power-law autocorrelation functions.

independence assumption is not valid. The correlations $c(k)$ of zero-crossing intervals are not zero, and behave $c(k) \sim k^{-\delta}$, where δ is close to γ. This result was shown in Figure 3.3 and 3.6 respectively.

For considered power-law autocorrelation functions, the simulation results show that the tail of zero-crossing intervals is of exponential form when $\gamma > 1$. For the regime $0 < \gamma \leq 1$, the simulation results seem to support the work of Eichner et al. [39], which claimed that the tail is of stretched exponential type. This issue will be investigated in the following chapter.

The full structure of the power-law autocorrelation function affects the initial behaviour of the probability density function $P_0(\tau)$ of the zero-crossing interval τ, which is summarised in the following table.

	Shape of the density function $P_0(\tau)$	Initial value $P_0(0)$
$\rho_\gamma(t)$		0
$\phi_\gamma(t)$		$\neq 0$
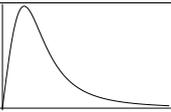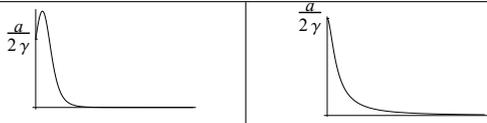
This table indicates that the density function $P_0(\tau)$ has various shapes and that the initial value $P_0(0)$ is different by changing the power-law autocorrelation function.

Chapter 4

Zero-crossing Intervals and Long-term Memory

4.1 Introduction

The work of Eichner et al. [39] was mentioned in Chapter 3, which claimed that when the autocorrelation function $\rho(t)$ of the Gaussian process has the asymptotic behaviour $\rho(t) \sim t^{-\gamma}$ for large t, then the tail of return intervals is of a stretched exponential $P_0(\tau) \sim \exp(-\tau^\gamma)$ for $0 < \gamma < 1$. This chapter first investigates this behaviour by considering the spectral density function of the autocorrelation function and the effect of the finite simulation length data. Taking these two factors into account, the chapter analyses properties of zero-crossing intervals given a cut-off power-law autocorrelation function. By using the cut-off model, it shows that the tail of the zero-crossing interval density function is of the exponential tail, not the stretched exponential tail.

4.2 Spectral density function

Eichner et al. did not specify the exact form of the power-law autocorrelation function used for their simulation, but the asymptotic behaviour of the

autocorrelation function is $\rho(t) \sim t^{-\gamma}$ for large t, which agrees with that used in this thesis. This section considers the spectral density function of the auto-correlation function to show that the simulation technique employed is not allowable for the $0 < \gamma \leq 1$ case.

The power spectral density function is defined as the Fourier transform of the autocorrelation function (Bendat [55], and Davenport and Root [80])

$$S(\omega) = \int_{-\infty}^{\infty} \rho(t) \mathrm{e}^{-i\omega t} \, \mathrm{d}t.$$

Then the inverse transform relation gives

$$\rho(t) = \frac{1}{2\pi} \int_{-\infty}^{\infty} S(\omega) \mathrm{e}^{i\omega t} \, \mathrm{d}\omega.$$

This Fourier transformation pair is valid as written if

$$\int_{-\infty}^{\infty} |\rho(t)| \, \mathrm{d}t < \infty.$$

More properties of $S(\omega)$ can be found in [55] and [80].

Now consider the spectral density function $S(\omega)$ of the power-law auto-correlation function $\rho_\gamma(t) = (1 + a^2 t^2/\gamma)^{-\gamma/2}$. Evaluating the Fourier transform of $\rho_\gamma(t)$ gives that

$$S(\omega) = \frac{\pi^{1/2} 2^{(3-\gamma)/2} \gamma^{(\gamma+1)/4}}{\Gamma(\gamma/2) a^{(\gamma+1)/2}} \, |\omega|^{\frac{\gamma-1}{2}} \, \mathrm{K}_{(1-\gamma)/2}(a^{-1} \gamma^{\frac{1}{2}} |\omega|),$$

where $\mathrm{K}_v(x)$ is the modified Bessel function [77]. The spectral density function $S(\omega)$ is positive for all ω, but is *not* finite at $\omega = 0$ for $0 < \gamma \leq 1$. This fact implies that the process is not physically realisable, since it has infinite power. The similar analysis can also be obtained for the power-law auto-correlation function $\phi_\gamma(t)$, since $\phi_\gamma(t)$ has the same asymptotic behaviour for large t.

On the other hand, the simulated Gaussian processes with the power-law

bounded autocorrelation functions are affected by the finite length of the data stream. The finite capacity or storage of the digital computer implies that, for autocorrelation functions with power-law tails, there will always be some truncation in the correlations [86]. This effectively introduces a cut-off or outer scale to the tail of the autocorrelation function. In other words, the power-law type correlations do not preserve for large correlation times. Hence, this fact indicates that in simulations, there exists an outer scale or a cut-off term embedded in power-law autocorrelation functions.

In response to these two points, the thesis claims the stretched exponential obtained by Eichner et al. [39] is not reasonable, because in the first place the simulated Gaussian processes with power-law autocorrelation functions for the regime $0 < \gamma \le 1$ are not physically realisable in practice, since it has infinite power, which is shown above. However, a computer 'experiment' with this autocorrelation function can be conducted, but it does not correspond to a realization of a valid Gaussian processes. These two points indicate that a cut-off term to the pure power-law autocorrelation function is needed, so as to truncate the infinite power and the effect of the finite data length. This means that the spectral density function of a cut-off power-law autocorrelation function will be finite for all $-\infty < \omega < \infty$. As a result of this analysis, the cut-off power-law autocorrelation function is considered in the following section. Given the cut-off autocorrelation function, it will be seen that there is *not* the stretched exponential tail, but the exponential tail.

4.3 The cut-off power-law autocorrelation function

Taking the infinite power and the finite storage of digital computers into consideration, this section evaluates a power-law bounded autocorrelation function but with a cut-off term. Then it can be shown that the spectral

density function is finite for all ω. It has to be noticed that the aim of the cut-off term is to make the process have the finite power and does not interfere with the power-law type correlations. This can be achieved by constructing an autocorrelation function that is effectively power-law in an intermediate regime (of arbitrary length), but contains an exponential cut-off in the far tail. Such a autocorrelation model, that is continuous, is

$$\rho_b(t) = (1 + a^2 t^2/\gamma)^{-\gamma/2} \exp\left(-\frac{t^2}{b^2}\right), \qquad (4.1)$$

where $b > 0$. To determine where the exponential behaviour takes in, we can solve the inequality

$$\left(1 + \frac{a^2 t^2}{\gamma}\right)^{-\gamma/2} \geq \exp\left(-\frac{t^2}{b^2}\right). \qquad (4.2)$$

This is a transcendental inequality, and can be solved by using the Newton-Raphson method [83]. The solution $t = t_c$ is where $\rho_b(t)$ transits from the power-law type to the exponential behaviour and depends on the value a, γ and b. Although $\rho_b(t) \sim \exp(-t^2)$ for large t and is not $t^{-\gamma}$, the larger the parameter b is, the more power-law type correlations are preserved. It will be seen later that even though the cut-off power-law autocorrelation function $\rho_b(t)$ is of Gaussian decay $\sim \exp(-t^2)$, but the tail of the probability density function $P_0(\tau)$ of the zero-crossing interval τ is still of exponential form. If $t < b$, $\rho_b(t)$ provides an intermediate power-law regime; but if $t \gg b$, $\rho_b(t)$ ensures convergence of the power spectrum for all ω and $\gamma > 0$. The cut-off model $\rho_b(t)$ shows the similar behaviour like the pure power-law autocorrelation function $\rho_\gamma(t)$ for sufficiently large values of b. It will be seen later that if $b = 1000$, results of the persistence exponent, either obtained from the power-law bounded autocorrelation function or from the power-law cut-off case, are closed to each other.

In simulations, the cut-off term can be of *any* type. This chapter assumes

that the cut-off term is $\exp(-t^2/b^2)$, not the pure exponential term $\exp(-t/b)$, because Equation (4.1) has the property that its expansion near the origin is

$$\rho_b(t) = 1 - \left(\frac{a^2}{2} + \frac{1}{b^2} \right) t^2 + \left(\frac{a^4}{8} + \frac{1}{2b^4} + \frac{a^2}{2b^2} + \frac{a^4}{4\gamma} \right) t^4 + O(t^6),$$

which implies that Rice's formula (2.25) is valid, and is close to that for the power-law model $\rho_\gamma(t)$, whose the crossing rate β is a/π. For the cut-off model (4.1), the zero-crossing rate is

$$\beta = \frac{1}{\pi} \sqrt{a^2 + \frac{2}{b^2}}, \tag{4.3}$$

which means that β is unaffected if $b \gg \sqrt{2}/a$. The following sections show the impact of the cut-off term on the persistence parameter, the variance and the probability density function of zero-crossing intervals.

The simulation method is the same as introduced in the previous chapter. In each realisation of the simulations, the correlation length a is 0.01, because of the same reason introduced in Chapter 3. Three different b values are used for comparison, which are $b = 250$, $b = 500$ and $b = 1000$ respectively. When analysing the independence model, the same parameters for a and b are used.

The persistence parameter

The persistence parameter θ is of interest in the thesis. Given the cut-off power-law autocorrelation function $\rho_b(t)$ (4.1), there are two ways to determine θ, which has been seen in Chapter 2 and 3. The first way is to calculate the pole of the zero-crossing interval probability density function in the Laplace space, according to the independence model (2.9) in Chapter 2. The other way is to obtain the persistence parameter θ from the simulation data, which was used in Chapter 3. This section first compares the persistence parameter θ obtained from these two separated methods, and the aim is to show the validity of the independence model for the zero-crossing intervals
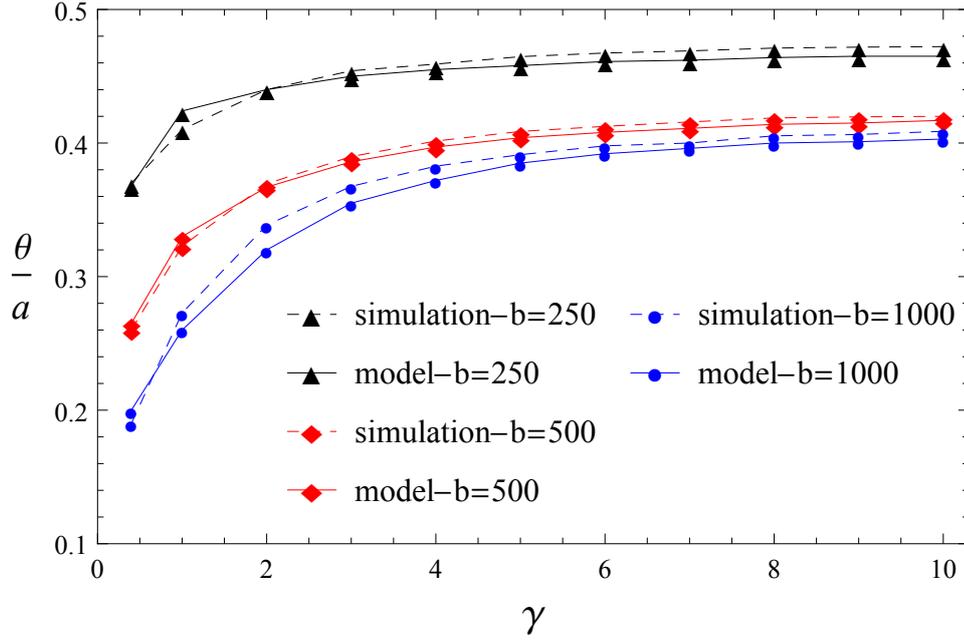
Figure 4.1: This figure shows the normalised persistence parameter θ/a as a function of γ for the cut-off power-law autocorrelation function $\rho_b(t)$ (4.1). The persistence parameter θ is determined from either the simulation data (dashed lines) or solving the pole of Equation (2.9) (solid lines) in Laplace space. It can be seen that there is a satisfactory agreement between the simulation results and the solutions from the independence model.

of the Gaussian process with the cut-off model $\rho_b(t)$.

The constant a is a scale parameter to the persistence parameter θ, which is shown in Appendix D, hence, Figure 4.1 shows the behaviour of the persistence parameter θ/a against γ for different values of b, which are calculated from either the independence model or the simulation data. It can be seen that the value of θ decreases with increasing b. For each b, the persistence parameter curves show a similar shape and increase to a constant value as γ increases. The agreement between the solid lines (the independence model) and the dashed lines (the simulation data) implies that the independence model of zero-crossing intervals can describe the asymptotic properties of the simulation results.

Now we compare the persistence parameter θ determined from the simu-

lation data for two autocorrelation functions. One is the pure power-law au-
tocorrelation function $\rho_\gamma(t)$ (3.3), and the other one is the cut-off power-law
autocorrelation function $\rho_b(t)$ (4.1). The purpose is to show how θ behaves
when $0 < \gamma \leq 1$. If θ exists, it implies that the tail of the zero-crossing inter-
vals is of exponential form. Figure 4.2 shows the persistence parameter θ/a
as a function of γ for both models. The three black curves are with $b = 250$
(square), $b = 500$ (diamond) and $b = 1000$ (down-triangle) respectively. The
red curve (circle) represents θ obtained from the power-law autocorrelation
function $\rho_\gamma(t)$. It is found that θ moves towards to the red curve with increas-
ing values of b. It can be seen that for $b = 1000$, θ is nearly identical to that
of the power-law model $\rho_\gamma(t)$ when $\gamma > 1$. This fact means that simulation
results are affected by the cut-off term in each realisation.

One important implication shown in Figure 4.2 is that the persistence
parameter θ exists and is finite when $0 < \gamma \leq 1$ for the cut-off power-law
autocorrelation function $\rho_b(t)$. The existence of θ means that the tail of the
probability density function $P_0(\tau)$ of the zero-crossing interval τ is of expo-
nential form, not the stretched exponential form. This argument is different
to that shown by Eichner et al. [39]. Note that for the pure power-law auto-
correlation function $\rho_\gamma(t)$, the analysis of the spectral density function in the
previous section shows that the process has infinite power and is not allow-
able for the cases $0 < \gamma \leq 1$. Hence, Figure 4.2 only shows the valid regime
of $\gamma > 1$ for the model $\rho_\gamma(t)$. The persistence parameter θ for the power-
law autocorrelation function $\phi_\gamma(t)$ is also plotted, and it shows the similar
behaviour like that for $\rho_\gamma(t)$, but θ is smaller.
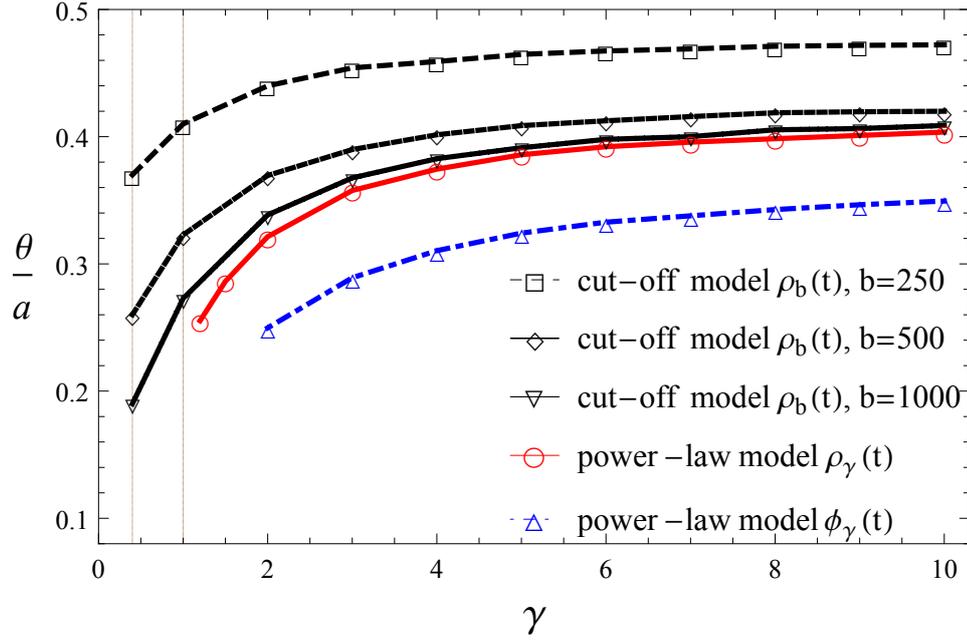
Figure 4.2: This figure compares the simulation results of the persistence parameter θ given the power-law autocorrelation function $\rho_\gamma(t)$ (red) and the cut-off power-law model $\rho_b(t)$ (black). Three different b values are compared. For the largest $b = 1000$, the black down-triangle is nearly the same to the red curve when $\gamma > 1$, and extends to where $\gamma < 1$. The two vertical lines are for $\gamma = 1$ and $\gamma = 2/5$ respectively. This figure indicates that for the regime of $0 < \gamma \leq 1$, the tail of the probability density function $P_0(\tau)$ of the zero-crossing interval τ is of exponential form finally, *not* a stretched exponential type. The persistence parameter θ for another power-law model $\phi_\gamma(t)$ is shown by the blue curve.

Variance of the zero-crossing interval τ

The previous section indicates that the tail of the zero-crossing interval τ is of exponential form, and the independence model could approximate the asymptotic behaviour of the simulation data. This section determines the variance σ^2 of the zero-crossing interval τ for the cut-off power-law model $\rho_b(t)$, and the aim is to compare with that for the pure power-law autocorrelation function $\rho_\gamma(t)$, which shows in Chapter 2 that the variance σ^2 is infinite
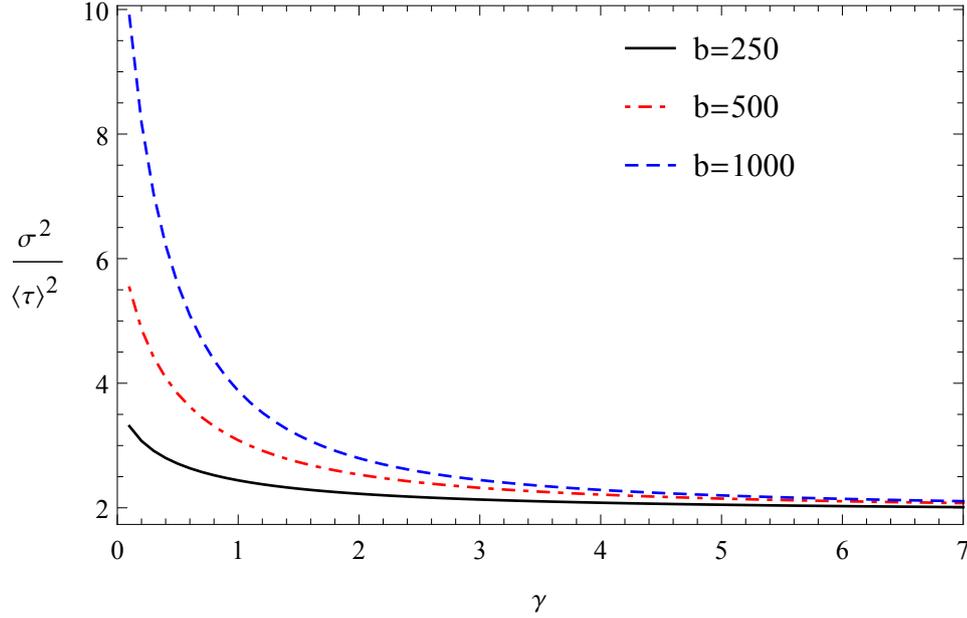
Figure 4.3: This figure plots the normalised variance $\sigma^2/\langle\tau\rangle^2$ of the zero-crossing intervals as a function of γ for the cut-off power-law autocorrelation function $\rho_b(t)$. It can be seen that all variances are finite for $\gamma > 0$, and this fact agrees with the existence of the persistence parameter θ shown in Figure 4.2.

when $\gamma \leq 1$. The normalised variance is considered again:

$$\frac{\sigma^2}{\langle\tau\rangle^2} = 2\beta \int_0^\infty R(t)\,\mathrm{d}t,$$

where here the zero-crossing rate β is given by Equation (4.3), and

$$R(t) = \frac{2}{\pi}\arcsin(\rho_b(t)).$$

Figure 4.3 shows the behaviour of the normalized variance $\sigma^2/\langle\tau\rangle^2$ of the zero-crossing intervals as a function of γ for the cut-off model $\rho_b(t)$ with different values of b. It can be seen that all curves show the similar behaviour, and the most important fact is that $\sigma^2/\langle\tau\rangle^2$ exists for all $\gamma > 0$. Hence, Figure 4.3 implies that the second moment of the zero-crossing interval τ exists and is finite, which is consistent with the existence of the persistence parameter θ shown in Figure 4.2. This result is different from that for the pure power-

law autocorrelation function $\rho_\gamma(t)$, which is shown in Figure 2.2 in Chapter 2, where $\sigma^2/\langle\tau\rangle^2$ diverges at $\gamma \leq 1$. One can conclude that the cut-off term makes the variance σ^2 become finite, which is reasonable in practice.

Probability density functions

Figure 4.4 shows the simulation results about the normalised probability density function $P_0(\tau)/a$ of the zero-crossing interval τ as a function of $a\tau$ for the cut-off power-law model $\rho_b(t)$. The shown examples are with the same index $\gamma = 2/5$. The blue-dashed curve is for $b = 500$, and the red-solid one is for $b = 1000$. It can be seen that the probability density functions have the similar shape but the peak for the case $b = 1000$ is slightly higher than the other one. Now compare this figure with Figure 3.2 (c) in Chapter 3, it is found that the shown probability density functions are close to each other. This fact implies that there is no obvious effect of the cut-off term on the shape of the probability density functions of the zero-crossing intervals for large b. The difference, however, is that the inner plot of Figure 4.4 shows that the tail of the zero-crossing interval τ is now of exponential form $P_0(\tau) \sim \exp(-A\tau)$, not the stretched exponential type, and the value of A is consistent with Figure 4.1 and 4.2.
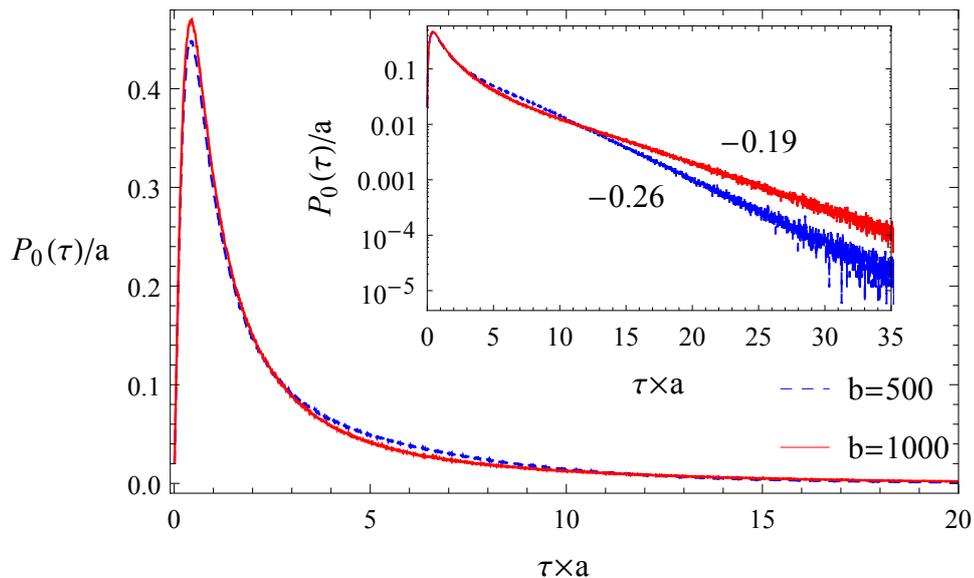
Figure 4.4: This figure shows the simulation results about the normalised probability density function $P_0(\tau)/a$ of the zero-crossing interval τ as a function of $a\tau$ for the cut-off power-law model $\rho_b(t)$, which is given by Equation (4.1). The value b is 500 and 1000 respectively. Here $a = 0.01$ and the index γ is $2/5$ for both cases. Comparing this with Figure 3.2 (c) in Chapter 3, we can see that the shape of the density function curves is close to each other, especially for large b, but the obvious difference is that the tail is of exponential form, not the stretched exponential type, which is claimed by Eichner et al. [39]. This figure is simulated by averaging over 10^5 realisations, each of length 2^{20}.

4.4   Summary

This chapter first investigated results obtained by Eichner et al. [39], which showed that the tail of the probability density function $P_0(\tau)$ of the zero-crossing interval τ is of the stretched exponential form for Gaussian processes with the power-law asymptote autocorrelation function $\rho(t) \sim t^{-\gamma}$ given $0 < \gamma \leq 1$. Taking the spectral density function of the autocorrelation function and the finite storage of the digital computer into consideration, this chapter claimed that the stretched exponential is not valid, because at the first place the process is not physically realisable, since it has infinite

power for the regime $0 < \gamma \leq 1$. Furthermore, the finite storage of the digital computer leads to the power-law correlations cannot sustain in the simulated processes for large correlated time lags, implying that there will always be some truncation in the correlations. These two facts imply that a cut-off power-law autocorrelation function is required in order to truncate the infinite power and the effect of the finite data length. Based on these two facts, the chapter secondly considered the case that the power-law bounded autocorrelation function $\rho_\gamma(t)$ provided with a cut-off term, namely, $\rho_b(t)$, which is given by Equation (4.1). The cut-off model $\rho_b(t)$ is effectively power-law in an intermediate regime (of arbitrary length), but contains an exponential cut-off in the far tail. The position $t = t_c$ where $\rho_b(t)$ transits from the power-law behaviour into the exponential type is obtained by solving the inequality (4.2) and depends on the value of b. Although $\rho_b(t)$ has a different decaying form $\exp(-t^2)$ for large t, the larger the parameter b is, the more power-law type correlations are preserved. Notice that the cut-off term can be of *any* type. The cut-off power-law autocorrelation model $\rho_b(t)$ was considered here because its second derivative near the origin is finite, which ensures the zero-crossing rate β exists and is finite. On the other hand, the spectral density function of $\rho_b(t)$ is always finite for all γ. Furthermore, the cut-off model $\rho_b(t)$ retains the same power-law correlations for large b, which agrees with $\rho_\gamma(t)$. This fact implies that we could investigate the influence of power-law bounded autocorrelations on the tail of zero-crossing intervals as long as the value b is large.

This chapter then shows that the zero-crossing intervals of the Gaussian process with the cut-off power-law autocorrelation function $\rho_b(t)$ can be determined from either the independence model or the simulation data by comparing the persistence parameter θ, which was shown in Figure 4.1. Then the chapter compared θ derived from two models: one is the power-law autocorrelation function $\rho_\gamma(t)$, and the other one is $\rho_b(t)$, which was shown in

Figure 4.2. It is found that for large b, θ agrees with each other. Specifically, the more importance is that θ exists for the regime $0 < \gamma \leq 1$ for the cut-off model $\rho_b(t)$, implying that the tail of the zero-crossing interval τ is of exponential form. This property is verified by plotting the full probability density function $P_0(\tau)$ of the zero-crossing interval τ, which was shown in Figure 4.4. The inner log-linear plot indicates that $P_0(\tau) \sim \exp(-A\tau)$, where A is consistent with the persistence parameter θ.

Chapter 5

Zero-Crossing Intervals of Symmetric Stable Processes

5.1 Introduction

The Gaussian distribution is a special case in the class of stable distributions. Therefore, it is natural to investigate the zero-crossing problem of the non-Gaussian stable process. Specifically, this chapter considers the zero-crossing intervals of the *symmetric* stable process because it will be seen later that the symmetric stable random variable has a simple characteristic function, which enables integrals to be performed. The first section of this chapter reviews a joint characteristic function introduced by Hopcraft and Jakeman [15], which is based on the single symmetric stable variable. With this joint characteristic function, it enables the clipped autocorrelation function $R(t)$ and the zero-crossing rate β to be generalised to the non-Gaussian stable case. As the Gaussian variable belongs to the stable variables, the similar method introduced in previous chapters can be used to explore the properties of the zero-crossing interval τ.

The symmetric stable process with the proposed joint characteristic function requires the *coherence* function, which plays the similar role to the au-

tocorrelation function of the Gaussian process, but is *not* the autocorrelation function, which will be seen later. The autocorrelation function defines the way in which the points of the Gaussian process are related to the other points, so does the coherence function of the symmetric stable process. We have already seen that the structure of the autocorrelation function affects the properties of zero-crossing intervals. Therefore, it is expected that the forms of the coherence function will influence zero-crossing intervals too.

It has been seen that the autocorrelation function has the expansion near the origin $\rho(t) = 1 - a^2 t^2/2 + O(t^3)$, which ensures that the zero-crossing rate β exists. Similarly, the expansion of the coherence function is also satisfied a particular structure near the origin, which is discussed later.

This chapter investigates zero-crossing intervals of the symmetric stable process with the exponential coherence function

$$\varphi_e(t) = \exp(-at), \tag{5.1}$$

where $a > 0$ is a time-scale parameter. Equation (5.1) decays to zero rapidly. Hence, it can be considered as a short-term memory function with the characteristic time-scale a.

Simulation of stable random variables is of a complex problem since they are lack of analytic expressions for their probability density functions. Hence, the problem of simulating sequences of stable random variables can be considered as another research area, and this thesis will not simulate non-independence stable random processes because of time limit for a PhD thesis. So the independence approximation is used to derive statistical properties of zero-crossing intervals, and the methodology is inherited from the Gaussian case shown in Chapter 2. Although the thesis does not consider simulations for the stable processes, the analytical results of zero-crossing intervals can be treated as an attempt and preparations for future work.

5.2 Zero-crossing formulae of symmetric stable processes

This section reviews a bivariate symmetric stable distribution introduced by Hopcraft and Jakeman [15]. With this joint distribution, it is possible to explore properties of zero-crossing intervals for the symmetric stable process.

The definition of symmetric stable distributions is introduced first. Then follows the bivariate symmetric stable distribution. Finally, two formulae for the clipped autocorrelation function $R(t)$ and the zero-crossing rate β are given. These two formulae are obtained by using the similar methods used in Chapter 2 for the Gaussian case.

5.2.1 Symmetric stable distributions

A random variable X belongs to the symmetric stable class of distributions if its characteristic function can be written as [42]:

$$C(\mu) = \int_{-\infty}^{\infty} m(x) \exp(i\mu x)\, dx$$

$$= \exp(-A|\mu|^{\nu}) \tag{5.2}$$

where $m(x)$ is the probability density function of X. The parameter $A > 0$ is a scale factor which measures the dispersion of the distribution. The exponent $\nu \in (0, 2]$ is called the stable index and describes heaviness of the tail. If ν takes values other than in this range, the probability density function $m(x)$ can be negative, so does not correspond to a valid probability density function. For all $\nu \in (0, 2]$, $m(x)$ is defined on $-\infty < x < \infty$.

The stable index ν is the most important parameter for the symmetric stable random variables because ν specifies the asymptotic behaviour of $m(x)$

for large x:

$$m(x) \sim \begin{cases} \frac{1}{|x|^{1+\nu}} & 0 < \nu < 2, \\ \exp(-x^2) & \nu = 2. \end{cases}$$

The probability density function $m(x)$ is obtained by Fourier inversion of Equation (5.2):

$$m(x) = \frac{1}{2\pi} \int_{-\infty}^{\infty} \exp(-\mathrm{i}x\mu) C(\mu) \, \mathrm{d}\mu.$$

For example, evaluating the above integral for $\nu = 1$ and 2 yields two simple and special cases of the symmetric stable distributions, namely the Cauchy ($\nu = 1$) distribution and the Gaussian ($\nu = 2$) distribution. The Cauchy probability density function is

$$m_C(x) = \frac{A}{\pi(x^2 + A^2)},$$

and the Gaussian probability density function is

$$m_G(x) = \frac{1}{\sqrt{4\pi A}} \exp(-\frac{x^2}{4A}).$$

If rewrite $m_G(x)$, we can verify that this Gaussian distribution has zero mean and variance $2A$, whereas neither mean nor variance exists for the Cauchy distribution.

A summary for known closed forms $m(x)$ is given in [48]. For a fuller review on the general stable distributions, key works include that Lévy [41], Samorodnitsky and Taqqu [42], and Zolotarev [44].

5.2.2   A bivariate distribution

This section reviews a special joint symmetric stable distribution, which was first proposed by Hopcraft and Jakeman [15]. With this distribution, it enables the clipped autocorrelation function $R(t)$ and the zero-crossing rate β for the symmetric stable process to be calculated.

Let $\{x(t), t \geq 0\}$ be a stationary Gaussian process with zero mean and unit variance. Then the probability density function of the single variable $x = x(t')$ is

$$f_1(x) = \frac{1}{\sqrt{2\pi}} e^{-x^2/2}, \tag{5.3}$$

and its characteristic function is obtained by Fourier transforming Equation (5.3):

$$C_1(\lambda) = \int_{-\infty}^{\infty} e^{i\lambda x} f_1(x)\, dx = \exp(-\frac{1}{2}\lambda^2), \tag{5.4}$$

which has the same type as (5.2) with $A = 1/2$.

Now consider the bivariate probability density function x and $y = x(t'+t)$:

$$f_2(x, y) = \frac{1}{\sqrt{(2\pi)^2(1 - \rho^2)}} \exp\left[-\frac{x^2 + y^2 - 2xy\rho(t)}{2(1 - \rho^2)}\right], \tag{5.5}$$

where $\rho(t) = \langle x(t')x(t' + t)\rangle$ is the autocorrelation function of the Gaussian process. With minor calculation, Equation (5.5) can be rewritten as a product of two single variable density functions (5.3):

$$f_2(x, y) = \frac{1}{\sqrt{1 - \rho^2}} f_1\left(\frac{y - \rho x}{\sqrt{1 - \rho^2}}\right) f_1(x). \tag{5.6}$$

Similarly, we can rewrite the joint characteristic function of x and y as a product of two single variable characteristic functions: Fourier transforming Equation (5.5) gives

$$C_2(\lambda, \mu; \rho) = \int_{-\infty}^{\infty}\int_{-\infty}^{\infty} e^{i(\lambda x + \mu y)} f_2(x, y)\, dx\, dy$$

$$= \exp\left[-\frac{1}{2}(\lambda^2 + 2\rho\lambda\mu + \mu^2)\right] \tag{5.7}$$

$$= C_1(\lambda + \mu\rho)C_1(\mu\sqrt{1 - \rho^2}). \tag{5.8}$$

Clearly, the common feature of Equation (5.6) and (5.8) is that they are expressed as the product of two single variable functions. The above calcu-

lation is for the Gaussian case $\nu = 2$, but it is possible to generalise into the non-Gaussian stable variables.

Let Equation (5.4) be replaced by (5.2), and replace $\rho(t)$ with $\varphi(t)$ (to distinguish from the autocorrelation function in Gaussian case), then (5.8) changes into

$$C_2(\lambda, \mu; \varphi) = \exp\left[-A(|\lambda + \varphi\mu|^\nu + (1 - \varphi^\nu)|\mu|^\nu)\right], \qquad (5.9)$$

where $\varphi(t)$ will be defined presently. $C_2(\lambda, \mu; \varphi)$ is the characteristic function of a bivariate stable distribution, and the general expression for the characteristic function of multivariate stable distributions can be found in [42] and [44]. The thesis concentrates on the two dimensional bivariate case which is appropriate for modeling two successive zero-crossing points. On the other hand, Equation (5.9) satisfies the conditions for any joint-characteristic functions:

$$C_2(\lambda, 0; \varphi) = C(\lambda) \qquad (5.10)$$

$$C_2(0, \mu; \varphi) = C(\mu) \qquad (5.11)$$

$$C_2(\lambda, \mu; 0) = C(\lambda)C(\mu) \qquad (5.12)$$

$$C_2(\lambda, \mu; 1) = C(\lambda + \mu). \qquad (5.13)$$

(5.10) and (5.11) show that the single-variable characteristic function can be obtained from the joint characteristic function. (5.12) and (5.13) indicate that the process is 'uncorrelated' or fully 'correlated' at two different times. Therefore, these equations indicate that $\varphi(t)$ plays the similar role to the autocorrelation function $\rho(t)$, whose value lies between $[0, 1]$. The function $\varphi(t)$, however, is *not* the autocorrelation function $\rho(t)$ appearing in the Gaussian process, and its meaning is defined by a suitable function later.

The derivation of the joint density function (5.6) in fact uses the Markov

property because one can derive the same result by considering the conditional joint probability density function. Hence, it implies the structure is time ordered. Notice that the thesis considers the zero-crossing problem with the finite zero-crossing rate β. If the process has the Markov property, then β is infinite [87]. The underlying process can be made invariant to time-ordering by a linear transformation.

Let (X, Y) denote the joint random variable with the characteristic function (5.9). Consider the random variable pair (W, Z) given by the linear transformation $W = cX + dY$ and $Z = eX + fY$ where

$$c = (1 + \varphi^\nu)^{-1/\nu}(1 - \varphi^2(1 - \varphi^\nu)^{-1/\nu})$$

$$d = (1 + \varphi^\nu)^{-1/\nu}(1 - \varphi^\nu)^{-1/\nu}\varphi$$

$$e = (1 + \varphi^\nu)^{-1/\nu}(1 - (1 - \varphi^\nu)^{-1/\nu})\varphi$$

$$f = (1 + \varphi^\nu)^{-1/\nu}(1 - \varphi^\nu)^{-1/\nu}.$$

Then the joint characteristic function of (W, Z) is

$$C_{WZ}(\omega, \gamma; \varphi) = \langle \exp(-i(\omega W + \gamma Z)) \rangle$$

$$= \langle \exp[i((c\omega + e\gamma)X + (d\omega + f\gamma)Y)] \rangle$$

$$= \exp\left[-\frac{A}{1 + \varphi^\nu}(|\omega + \varphi\gamma|^\nu + |\gamma + \varphi\omega|^\nu)\right].$$

In order to make it consistent with the symbols used in Equation (5.9), we write $C_{WZ}(\omega, \gamma; \varphi)$ as

$$C_2(\lambda, \mu; \varphi) = \exp\left[-\frac{A}{1 + \varphi^\nu}(|\lambda + \varphi\mu|^\nu + |\mu + \varphi\lambda|^\nu)\right], \qquad (5.14)$$

which also satisfies the conditions (5.10)-(5.13). Equation (5.14) is symmetric to the interchange of λ and μ, and is insensitive to the time ordering.

Let $\nu = 1$ and $\varphi = 1$, then Equation (5.14) reduces to $C_2(\lambda, \mu; 1) =$

$\exp[-A|\lambda + \mu|]$, which is the joint characteristic function for the bivariate Cauchy distribution [88]. If set $\nu = 2$ in (5.14) and compare with the joint-Gaussian density function (5.7), then we can identify the autocorrelation function as

$$\rho(t) = \frac{2\varphi(t)}{1 + \varphi^2(t)}, \tag{5.15}$$

which indicates that $\varphi(t)$ is not equal to $\rho(t)$, but is nevertheless a measure of the *coherence* between values adopted by the process at different times. If $t = 0$, then $\rho(t) = 1$, so $\varphi(0) = 1$. The autocorrelation function $\rho(t)$ tends to zero as $t \to \infty$, as does $\varphi(t)$. Hopcraft and Jakeman called $\varphi(t)$ as the 'coherence function'. The exact meaning in terms of a fractional structure function can be found in Appendix C.

The coherence function

The coherence function $\varphi(t)$ and the autocorrelation function $\rho(t)$ both measure the relations between values of the underlying process at different times. It must emphasise that $\varphi(t)$ is *not* $\rho(t)$, but they are related to each other by Equation (5.15). The coherence function $\varphi(t)$ can be of any type that falls between $[0, 1]$ and tends to zero for large t. When it comes to the zero-crossing analysis, however, the further restriction on the coherence function is required, which is shown in the following section.

5.2.3 Generalisation of Rice's formula

Hopcraft and Jakeman [15] evaluated Equation (2.22) and (2.23) in Chapter 2 by inverting (5.14), and showed that if $\varphi(t)$ has the expansion near the origin

$$\varphi(t) = 1 - at + O(t^2),$$

then the zero-crossing rate

$$\beta = \frac{4a\nu}{\pi^2} \int_0^1 dp\, \frac{p^{\nu-1}}{(1+p^\nu)^2} \ln \left| \frac{1+p}{1-p} \right|. \tag{5.16}$$

We can examine the validity of Equation (5.16) by comparing it with Rice's formula (2.25). Putting the expansions of $\varphi(t)$ and $\rho(t)$ near the origin

$$\varphi(t) = 1 - at + O(t^2)$$

$$\rho(t) = 1 - \frac{\rho''(0)}{2} t^2 + O(t^3)$$

into Equation (5.15) gives that

$$\varphi(t) \approx 1 - at + O(t^2) \approx 1 - \sqrt{-\rho''(0)}\, t + O(t^2).$$

Hence, one identifies the constant a for the Gaussian case. With $\nu = 2$ and $a = \sqrt{-\rho''(0)}$, Equation (5.16) yields

$$\beta = \frac{1}{\pi} \sqrt{-\rho''(0)},$$

which is in accord with Rice's formula (2.25).

5.2.4 Generalization of the Van Vleck theorem

To calculate the clipped autocorrelation function $R(t)$ for the symmetric stable process, the bivariate characteristic function $C_2(\lambda, \mu)$ (5.14) plays an important role, because its Fourier inverse defines the joint probability density function. Using the similar method which obtains the Van Vleck theorem (2.16) in Chapter 2, Hopcraft and Jakeman [15] showed that

$$R(t) = \frac{4[\varphi(t)]^\nu}{\pi^2} \int_0^\infty \frac{p^{\nu-1}}{1 + [\varphi(t)]^\nu p^\nu} \ln \left(\frac{1+p}{|1-p|} \right) dp, \tag{5.17}$$

which depends on the coherence function $\varphi(t)$ and the stable index ν. When $\nu = 2$ and $\rho = 2\varphi/(1+\varphi^2)$, Equation (5.14) reduces to the joint characteristic function of the Gaussian process, and then (5.17) becomes the Van Vleck theorem or the arcsine law (2.16).

The integral (5.17) has no closed forms except for the cases $\nu = 1$ and $\nu = 1/2$. When $\nu = 1$, Equation (5.17) is simplified:

$$R(t) = \frac{4\varphi(t)}{\pi^2} \int_0^\infty \frac{1}{1+\varphi p} \ln\left(\frac{1+p}{|1-p|}\right) \, \mathrm{d}p.$$

The above integral can be rearranged as follows:

$$R(t) = \frac{4}{\pi^2} \int_0^\infty \ln\left(\frac{1+p}{|1-p|}\right) \, \mathrm{d}\ln(1+\varphi p).$$

Then evaluating the p-integral from $[0,1]$ and $[1,\infty]$ respectively, one can obtain that

$$R(t) = \frac{4}{\pi^2} \int_0^\infty \log(1+\varphi p)\frac{2}{p^2-1} \, \mathrm{d}p.$$

Then it yields that

$$R(t) = 2 - \frac{2\,\Phi(\varphi^{-2}, 2, 2^{-1})}{\pi^2 \varphi} - \frac{8\log(\varphi)\coth^{-1}(\varphi)}{\pi^2}, \qquad (5.18)$$

where

$$\Phi(z, a, b) = \sum_{k=0}^\infty \frac{z^k}{(k+b)^a}$$

is the Lerch transcendent function [77].

When $\nu = 1/2$, Equation (5.17) reduces to

$$R(t) = \frac{4\sqrt{\varphi}}{\pi^2} \int_0^\infty \frac{1}{1+\sqrt{\varphi}\sqrt{p}} \frac{1}{\sqrt{p}} \ln\left(\frac{1+p}{|1-p|}\right) \, \mathrm{d}p.$$

The above integral can be rearranged as follows:

$$R(t) = \frac{8}{\pi^2} \int_0^\infty \ln\left(\frac{1+p}{|1-p|}\right) \, \mathrm{d}\ln(1+\sqrt{\varphi}\sqrt{p}).$$

We can simplify the above integral by considering the p-integral from $[0, 1]$ and $[1, \infty]$, which gives that

$$R(t) = \frac{8}{\pi^2} \int_0^\infty \ln(1 + \sqrt{\varphi}\sqrt{p}) \frac{2}{p^2 - 1} \, \mathrm{d}p.$$

Then we can write the integral as

$$R(t) = \frac{2}{\pi^2} \left(\pi(\pi - 4\operatorname{arccot}(\sqrt{\varphi})) + \frac{\Phi(\varphi^2, 2, 2^{-1})}{\varphi} + 4\operatorname{arccoth}(\varphi)\ln(\varphi) \right),$$

where $\Phi(z, a, b)$ is the Lerch transcendent function defined above.

5.3 Mean and variance of the zero-crossing interval τ

Two Equations (5.16) and (5.17) are used to investigate statistical properties of zero-crossing intervals of symmetric stable processes. The following sections consider zero-crossing intervals given the exponential coherence function $\varphi_e(t) = \exp(-at)$, which has the expansion $1 - at + O(t^2)$ near the origin, ensuring that the zero-crossing rate β is finite. The exponential coherence function $\varphi_e(t)$ is considered as it represents a short-term memory process, which is already seen for the Gaussian case. In practical problem, such a process is often found in river flows [58], ecology [59] and telecommunication networks [60]. Clearly, the autocorrelation function $\rho_e(t)$ in Chapter 2 is generated from $\varphi_e(t)$ by Equation (5.15).

We first evaluate the mean $\langle \tau \rangle$ and variance σ^2 of the zero-crossing interval τ, as these two basic quantities provide information about the average length and fluctuations of zero-crossing intervals.
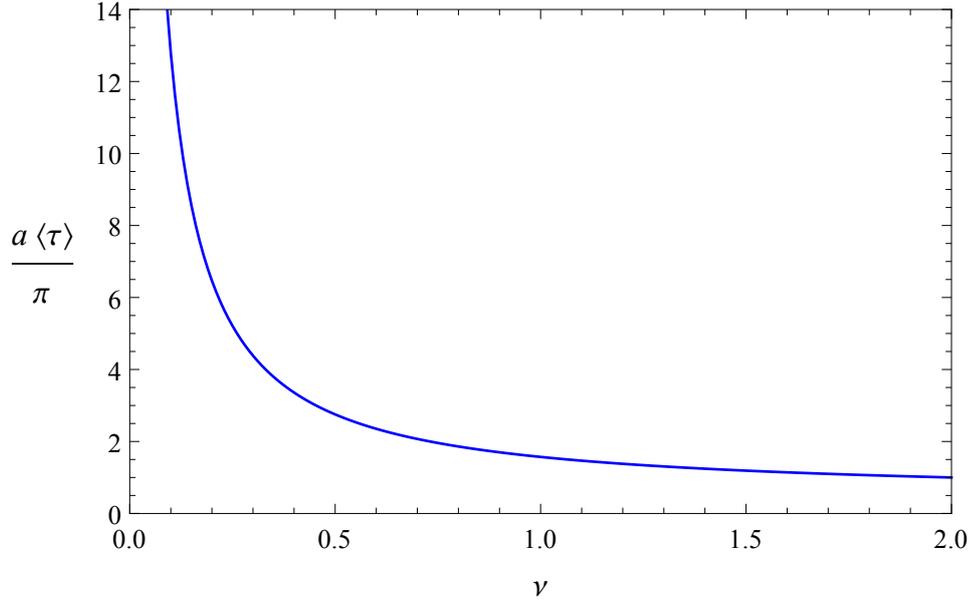
Figure 5.1: The normalised mean $a\langle\tau\rangle/\pi$ of the zero-crossing interval τ is plotted as a function of the stable index ν. It can be seen that the Gaussian case ($\nu = 2$) is the smallest compared with the non-Gaussian stable cases ($0 < \nu < 2$), and $a\langle\tau\rangle/\pi$ diverges as the stable index ν tends to 0.

5.3.1 Mean $\langle\tau\rangle$

It has been seen in Chapter 2 that $\langle\tau\rangle$ is the reciprocal of the zero-crossing rate β: $\langle\tau\rangle = 1/\beta$, where here β is given by Equation (5.16), which does not depend on the coherence function, and is a function of the stable index ν and the time-scale parameter a. Since Equation (5.16) exists for all $0 < \nu \leq 2$, then it implies that $\langle\tau\rangle$ is finite. For the Gaussian case, $\beta = a/\pi$, and then $\langle\tau\rangle$ is π/a. This fact suggests that an appropriate way to plot $\langle\tau\rangle$ is to normalise it to the Gaussian value. If $\nu = 1$, the zero-crossing rate is $2a/\pi^2$. For the others ν, the rate has to be evaluated numerically. If ν decreases to 0, the normalised mean behaves as

$$\frac{a\langle\tau\rangle}{\pi} \to \frac{4}{\pi\nu}, \quad \nu \to 0.$$

This behaviour indicates that for the non-Gaussian stable cases ($0 < \nu < 2$), $\langle\tau\rangle$ is infinite with vanishing ν.

Figure 5.1 shows the normalized mean $a\langle\tau\rangle/\pi$ as a function of the stable index ν. It can be seen that $a\langle\tau\rangle/\pi$ is the smallest for Gaussian case, and increases to infinity as $\nu \to 0$. One implication is that the number of zero-crossings of the Gaussian process is more than that for the non-Gaussian stable process in a similar interval of time. This property is caused by the heavy tails of the symmetric stable distributions, which means that the underlying process spends longer times away from the zero level and takes more time before returning. Since the returning time increases, it leads to the length between two successive zero-crossings becomes large, as seen in Figure 5.1.

5.3.2 Variance σ^2

The variance σ^2 of the zero-crossing interval τ is given by Equation (2.12):

$$\sigma^2 = \frac{2}{\beta} \int_0^\infty R(t)\, \mathrm{d}t,$$

where here $R(t)$ is given by (5.17). Unlike the mean $\langle\tau\rangle$, σ^2 depends not only on the stable index ν, but also on the coherence function $\varphi(t)$. To evaluate fluctuations of the zero-crossing intervals, the normalised variance is considered again:

$$\frac{\sigma^2}{\langle\tau\rangle^2} = 2\beta \int_0^\infty R(t)\, \mathrm{d}t, \tag{5.19}$$

which measures the fluctuations of the lengths of the zero-crossing intervals. If $\sigma^2/\langle\tau^2\rangle < 1$, then the fluctuations are considered to be weak, implying that the zero-crossing intervals are not dispersed significantly far away from its mean. Inserting $\varphi_e(t)$ (5.1) into Equation (5.19), then we have

$$\frac{\sigma^2}{\langle\tau\rangle^2} = \frac{8\beta}{\pi^2} \int_0^\infty \left\{ \int_0^\infty p^{\nu-1} \ln\left(\frac{1+p}{|1-p|}\right) \frac{1}{e^{a\nu t} + p^\nu}\, \mathrm{d}p \right\}\, \mathrm{d}t,$$

which is an improper double integral that cannot be evaluated analytically. Hence, the Composite Simpson Quadrature method [83] is used for the nu-

merical solution. By letting $u = a\nu t$ in the above integral, the constant a can be scaled out, so a is set to be 1 for calculation simplicity in the following section.

Figure 5.2 shows the behaviour of the normalised variance $\sigma^2/\langle\tau\rangle^2$ as a function of the stable index ν. It can be seen that $\sigma^2/\langle\tau\rangle^2$ is less than 1 for all ν, implying that the fluctuations of the lengths of the zero-crossing intervals are 'weak'. Furthermore, $\sigma^2/\langle\tau\rangle^2$ shows nearly a straight line, implying that it is approximately independent of the stable index ν. The accuracy of the numerical method can be examined by considering the behaviour of $\sigma^2/\langle\tau\rangle^2$ when $\nu \to 0$. For the exponential coherence function $\varphi_e(t)$, given by (5.1), the clipped autocorrelation function $R(t)$ is

$$R(t) = \frac{4}{\pi^2} \int_0^\infty \frac{p^{\nu-1}}{e^{a\nu t} + p^\nu} \ln\frac{1+p}{|1-p|} \, \mathrm{d}p. \tag{5.20}$$

Then integrating from zero to infinity gives that

$$\int_0^\infty R(t) \, \mathrm{d}t = \frac{4}{\pi^2} \int_0^\infty p^{\nu-1} \ln\frac{1+p}{|1-p|} \, \mathrm{d}p \int_0^\infty \frac{1}{e^{a\nu t} + p^\nu} \, \mathrm{d}t.$$

Evaluating the t-integral yields

$$\int_0^\infty R(t) \, \mathrm{d}t = \frac{4}{\pi^2 a\nu} \int_0^\infty \ln\frac{1+p}{|1-p|} \ln(1+p^\nu)\frac{\mathrm{d}p}{p}. \tag{5.21}$$

Let $\nu \to 0$, then Equation (5.21) has the limit

$$\int_0^\infty R(t) \, \mathrm{d}t \to \frac{2\ln 2}{a\nu}$$

and the zero-crossing rate β (5.16) becomes

$$\beta \to \frac{1}{4}a\nu. \tag{5.22}$$
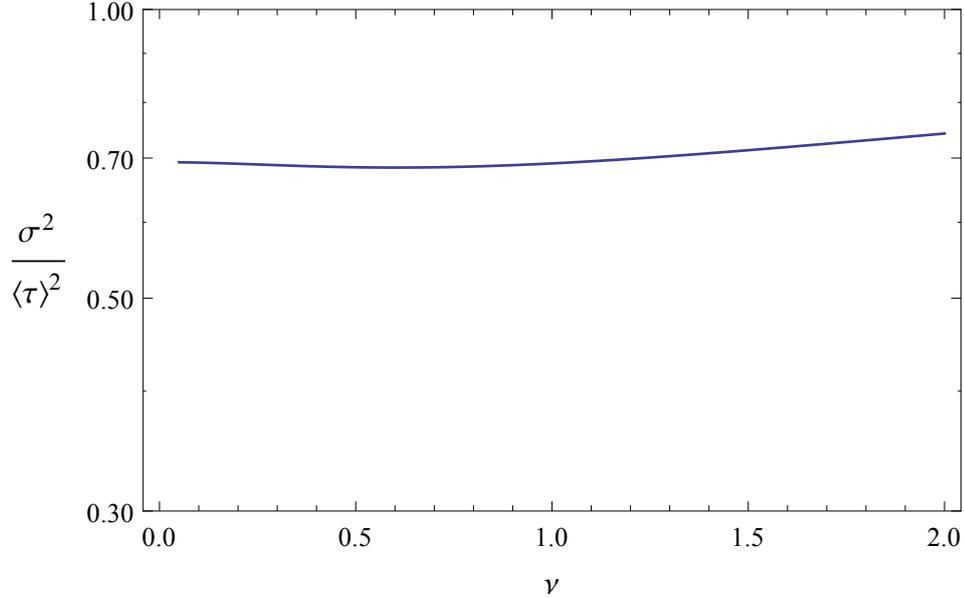
Figure 5.2: The normalised variance $\sigma^2/\langle\tau\rangle^2$ of the zero-crossing interval τ for the exponential coherence function $\varphi_e(t)$, which is given by Equation (5.1), is plotted as a function of the stable index ν. It can be seen that $\sigma^2/\langle\tau\rangle^2$ is less than 1 and shows less dependence on the stable index ν.

Now evaluating the normalised variance $\sigma^2/\langle\tau\rangle^2$ gives

$$\frac{\sigma^2}{\langle\tau\rangle^2} \to \ln 2 \approx 0.7$$

as $\nu \to 0$, which is consistent with Figure 5.2.

5.4 The persistence parameter

To determine the persistence parameter θ, we need to evaluate the pole in Equation (2.9) in Chapter 2: $1 - g(-\theta) = 0$, where $g(s) = \mathcal{L}\{R''(t)/(4\beta)\}$. In general, the closed forms for $g(s)$ are unknown, since the Laplace transform of $\mathcal{L}\{R''(t)/(4\beta)\}$ is complex: differentiating twice with respect to t in Equation (5.17), it gives that

$$R''(t) = \frac{4\,\nu\,\varphi^{\nu-2}}{\pi^2} \int_0^\infty \frac{U+W}{(1+\varphi^\nu p^\nu)^3} p^{\nu-1} \ln\left(\frac{1+p}{|1-p|}\right) \, \mathrm{d}p,$$

where

$$U = (\nu - 1 - p^\nu (1 + \nu)\varphi^\nu)(\varphi')^2$$

$$W = (1 + p^\nu \varphi^\nu)\varphi\varphi''.$$

Hence, the general expression for $g(s)$ is obtained by Laplace transforming $R''(t)/(4\beta)$:

$$g(s) = \frac{\nu}{\beta\pi^2} \int_0^\infty e^{-st}\, dt \int_0^\infty \frac{(U+W)\varphi^{\nu-2}}{(1 + \varphi^\nu p^\nu)^3} p^{\nu-1} \ln\left(\frac{1+p}{|1-p|}\right) dp.$$

However, for the exponential coherence function $\varphi_e(t) = \exp(-at)$, $g(s)$ can be obtained analytically for the cases $\nu = 1$ and $\nu = 1/2$. These two analytical expressions serve to benchmark the general numerical evaluations.

Closed-forms for $g(s)$

This section evaluates the Laplace transform of $R''(t)/(4\beta)$ if the symmetric stable process is with the exponential coherence function $\varphi_e(t)$. When $\nu = 1$, Equation (5.20) is

$$R(t) = \frac{4}{\pi^2} \int_0^\infty \frac{1}{e^{at} + p} \ln\left(\frac{1+p}{|1-p|}\right) dp. \tag{5.23}$$

Differentiating (5.23) twice with respect to t gives that

$$R''(t) = \frac{4}{\pi^2} a^2 e^{at} \int_0^\infty \frac{e^{at} - p}{(e^{at} + p)^3} \ln\left(\frac{1+p}{|1-p|}\right) dp.$$

For simplicity setting $c = \exp(at)$ and integrating by parts with respect to p, we obtain that

$$R''(t) = \frac{4}{\pi^2} a^2 c \left[\int_0^\infty \frac{2}{(p+c)(p^2-1)}\, dp - c \int_0^\infty \frac{2}{(p+c)^2(p^2-1)}\, dp \right].$$

Then integrating with respect to p gives that

$$R''(t) = \frac{4a^2}{\pi^2} \frac{at \coth(at) - 1}{\sinh(at)},$$

which can also obtain by differentiating twice with respect to t in Equation (5.18). Now Laplace transforming $R''(t)/(4\beta)$ yields

$$g(s) = \frac{2}{a} \left[\frac{a^2 + s^2}{a(a-s)^2} - \frac{s}{2a^2} \psi'(\frac{s-a}{2a}) \right]$$

where $\psi(\cdot)$ is the logarithmic derivative of the gamma function [77]

$$\psi(x) = \frac{\mathrm{d}}{\mathrm{d}x} \ln \Gamma(x) = \frac{\Gamma'(x)}{\Gamma(x)}.$$

When $\nu = 1/2$, we can obtain $g(s)$ by the similar method, details for which is shown in Appendix E. As for other stable indices, no analytical forms have been identified. It is shown in Appendix D that a is a scale parameter to θ, and θ can be rescaled by dividing a, hence, set $a = 1$ without loss of generality. These two analytical forms for $g(s)$ are used to find the persistence parameter θ, which is shown in the following section.

The persistence parameter θ for general ν

The persistence parameter θ is the pole of Equation (2.9) in Chapter 2, as seen before. In other words, θ is the root of Equation $1 - g(-\theta) = 0$, where $g(s) = \mathcal{L}\{R''(t)/(4\beta)\}$. By using Newton-Raphson method [83], we obtain the following results. When $\nu = 1$, it gives $\theta = 0.246$; when $\nu = 1/2$, θ is 0.145. These two solutions are served to verify the numerical method: the Composite Simpson Quadrature method [83] is used for evaluating the general cases ν. Figure 5.3 shows the scaled persistence parameter θ/a as a function of the stable index ν given the exponential coherence function $\varphi_e(t)$. For all ν, θ exists and is finite. It can be seen that the curve increases
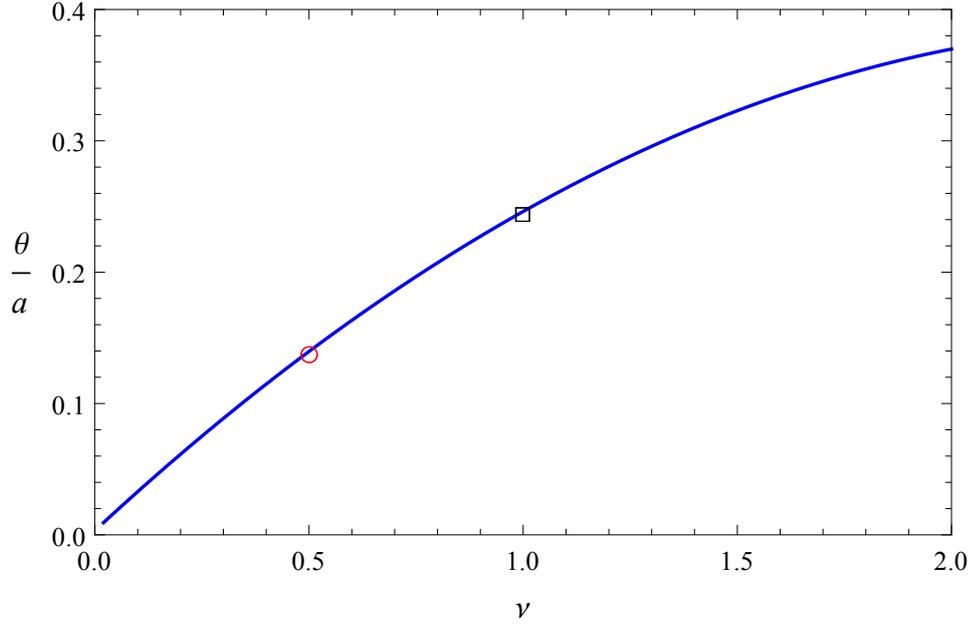
Figure 5.3: The scaled persistence parameter θ/a is plotted against the stable index ν for the exponential coherence function $\varphi_e(t)$, which is given by Equation (5.1). This figure implies that θ exists for all $0 < \nu \leq 2$. When $\nu = 2$ (Gaussian case), θ is the largest, indicating that the tail is less extended. For general ν, θ is determined by the numerical method. The square at $\nu = 1$ and the circle at $\nu = 1/2$ are obtained from the exact results.

monotonically from zero with increasing ν, implying the tail becomes steep. The square and the circle represent the $\nu = 1$ and $\nu = 1/2$ cases, respectively, which are obtained from the exact results. When $\nu = 2$, which corresponds to the Gaussian case, the persistence parameter θ is approximated to be 0.37. This result is consistent with that shown in Chapter 2 and 3 for the exponential autocorrelation function $\rho_e(t)$, where θ is directly evaluated from the Gaussian case. This fact implies that the autocorrelation function $\rho_e(t)$ is identified by the coherence function $\varphi_e(t)$, and for the case $\nu = 2$, if the persistence parameter θ exists, then it can be obtained from either the non-Gaussian stable or directly the Gaussian case.

5.5 Probability density functions

The two closed forms for $g(s) = \mathcal{L}\{R''(t)/(4\beta)\}$ for the cases $\nu = 1$ and $\nu = 1/2$ are used to obtain the probability density function $P_0(\tau)$ of the zero-crossing interval τ. We numerically invert the Laplace transform $p_0(s)$, which is given by Equation (2.9), through the Tablot method that is used many times in the previous chapters.

Figure 5.4 shows the probability density functions $P_0(\tau)$ of zero-crossing intervals of the symmetric stable process with the exponential coherence function $\varphi_e(t)$. Figure 5.4 (a) is for $\nu = 1$ and (b) plots for $\nu = 1/2$. It can be seen that all the probability density functions show the similar shape, and there is a maximum value for both curves. Furthermore, all curves emerge from the origin, and increase towards a peak, implying that zero-crossings are anti-bunched (repelled by each other).

To justify the persistence parameter θ is consistent with the tail behaviour of the zero-crossing intervals, the numerical data is plotted on the log-linear scale. All inner figures show a straight line, indicating that the probability density function $P_0(\tau)$ is of exponential form $\exp(-A\tau)$ for large τ. To be exact, the value A is 0.246 for $\nu = 1$, and is 0.145 for $\nu = 1/2$. These two slopes are the same as persistence exponents (the square and the circle) shown in Figure 5.3. This result confirms that the persistence parameter θ can be determined by the large τ behaviour of the probability density function $P_0(\tau)$ of the zero-crossing interval τ. Although the persistence parameter and the probability density functions are evaluated in different ways, their asymptotic values agree nevertheless.

Recall that Figure 2.1 in Chapter 2 shows the probability density function $P_0(\tau)$ of the zero-crossing interval τ with the exponentially bounded autocorrelation function $\rho_e(t)$, which is generated from the exponential coherence function $\varphi_e(t)$. Now we compare these two figures 5.4 and 2.1. It can be seen that all the probability density functions of the zero-crossing interval τ
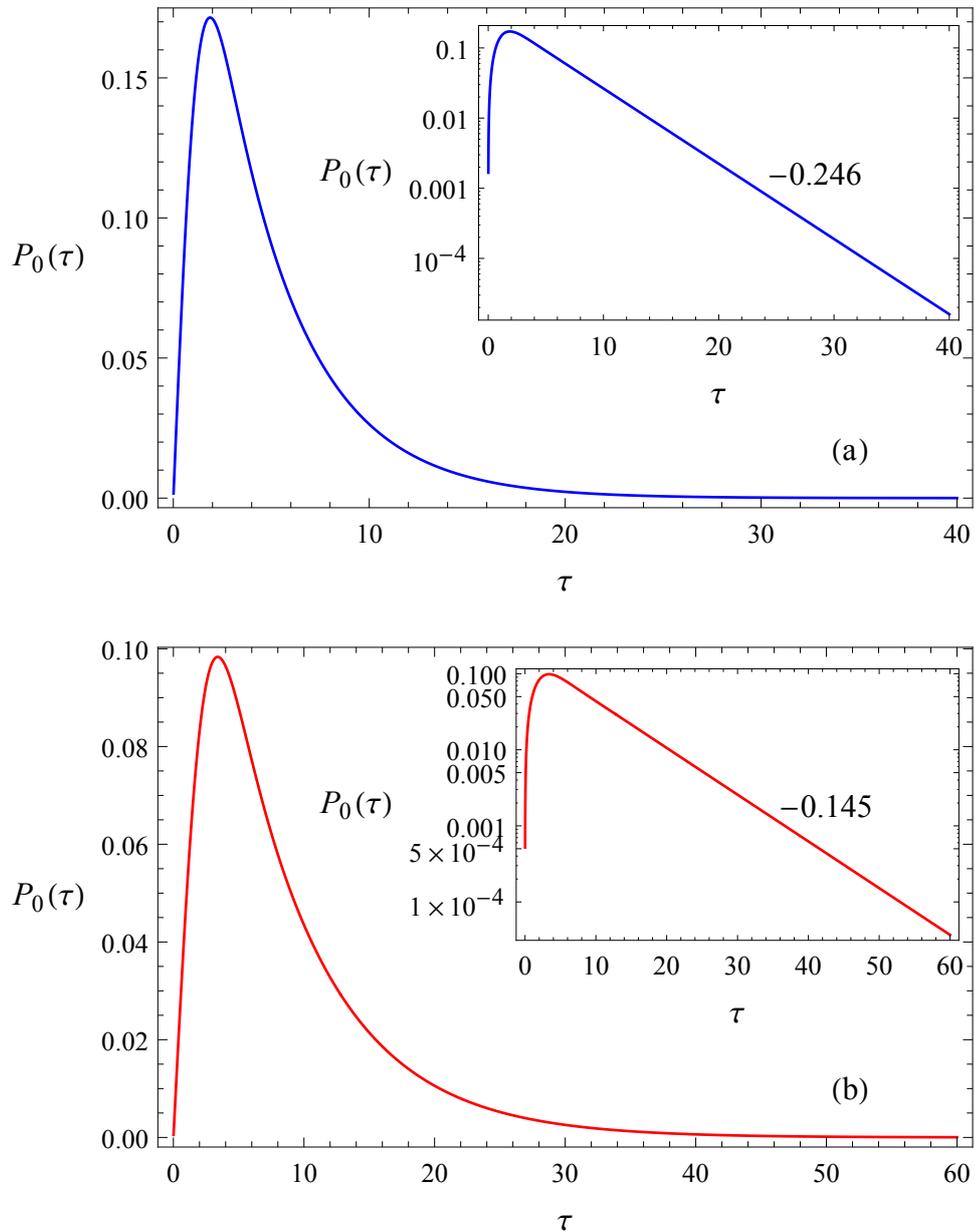
Figure 5.4: The probability density function $P_0(\tau)$ of the zero-crossing interval τ for the exponential coherence function $\varphi_e(t)$ with the stable index $\nu = 1$ (a) and $\nu = 1/2$ (b). $P_0(\tau)$ is obtained by using the Tablot method. The inner figures are plotted on a log-linear scale, and the straight lines imply that the tail of the zero-crossing interval τ is exponential. The slopes agree with the persistence parameter θ shown in Figure 5.3, which is marked by the square ($\nu = 1$) and the circle ($\nu = 1/2$).

show the similar behaviour, and the tail is of exponential form. However, for the non-Gaussian case, the index of the tail is smaller than that of the Gaussian case, implying that the tail of the zero-crossing interval τ is much extended. This is as expected since the probability density functions for the non-Gaussian stable random variables have long power-law tails.

5.6 Summary

This chapter has considered statistical properties of zero-crossing intervals of the symmetric stable process with the exponential coherence function $\varphi_e(t)$, which is given by Equation (5.1). Results are obtained by assuming that the successive zero-crossing intervals are independent. Although the thesis does not consider simulations for the stable processes, the analytical results of zero-crossing intervals can be treated as an attempt and preparations for future work.

It is found that the mean $\langle \tau \rangle$ of the zero-crossing interval τ does not depend on the coherence functions, but on the stable index ν, which is shown in Figure 5.1. For the Gaussian case, $\langle \tau \rangle$ is the smallest, but for the general ν, $\langle \tau \rangle$ increases as $\nu \to 0$, implying that the underlying symmetric stable process spends much more time away from the zero level. The normalised variance $\sigma^2/\langle \tau \rangle^2$ is determined by Equation (5.19), which is related to the coherence functions. Figure 5.2 shows that the fluctuations of $\sigma^2/\langle \tau \rangle^2$ are weak and approximately invariant with the stable index ν.

The persistence parameter θ is obtained by solving the equation for the pole of the Laplace transform of the zero-crossing interval probability density function: $1-g(-\theta) = 0$, where $g(s) = \mathcal{L}\{R''(t)/(4\beta)\}$. For the cases $\nu = 1$ and $\nu = 1/2$, the closed forms for $g(s)$ are obtained, which enable θ to be solved analytically. The solutions for θ provide a check for the numerical evaluations for other values of ν. The full behaviours of the persistence parameter θ are

plotted in Figure 5.3, which shows that θ is the largest for the Gaussian case, and agrees with the analytical result.

The probability density function $P_0(\tau)$ of the zero-crossing interval τ for selected stable indices ν was also obtained, which is shown in Figure 5.4. All the probability density functions show the similar shape, and the tail of the zero-crossing interval τ is of exponential form $P_0(\tau) \sim \exp(-A\tau)$, where A is identical to the persistence parameter θ.

Chapter 6

Zero-crossing Intervals and Power-law Coherence Functions

6.1 Introduction

Zero-crossing intervals of the symmetric stable process with the exponential coherence function $\varphi_e(t) = \exp(-at)$ were considered in Chapter 5. This chapter continues the same problem, but with the power-law coherence function

$$\varphi_\gamma(t) = (1 + at/\gamma)^{-\gamma}, \tag{6.1}$$

and the cut-off power-law coherence function

$$\varphi_b(t) = (1 + at/\gamma)^{-\gamma} \exp\left(-\frac{t}{b}\right). \tag{6.2}$$

$\varphi_\gamma(t)$ is considered because it has the power-law asymptote $\varphi_\gamma(t) \sim t^{-\gamma}$ for large t, hence Equation (6.1) implies that the underlying process has long-term coherence, similar to the Gaussian process with the power-law autocorrelation function, whose zero-crossing intervals show various properties. The cut-off model $\varphi_b(t)$ is considered because we have already seen the effects of the cut-off term on the zero-crossing intervals for the Gaussian case. These

two coherence functions are motivated by results of zero-crossing intervals of Gaussian processes.

The main purpose of this chapter is to derive statistical properties of zero-crossing intervals given the independence assumption since it is the only theory which is available. It has been seen that Gaussian variables are a special case in the stable random variables. Hence, it is expected to see that given the stable process with the power-law decaying coherence function and the independent assumption, the tail of the probability density function $P_0(\tau)$ of the zero-crossing interval τ is of power-law type and the persistence exponent θ does not exist. These two results will be shown in this chapter later. Due to the difficulty of simulating stable processes, which was stated in Chapter 5, this chapter still does not compare with the simulation results. However, if there exists the simulated stable process with the power-law type coherence function; and based on the fact that the Gaussian random variable belongs to the class of stable random variables, it is expected to obtain the analogous simulation results for the non-Gaussian stable cases. Namely, the simulation results show that the independence approximation between successive zero-crossing intervals is not satisfied, and the tail of the probability density function $P_0(\tau)$ of the zero-crossing interval τ is of exponential from, which were already met in the Gaussian case with the power-law autocorrelation functions shown in Chapter 3.

The chapter first shows the results of zero-crossing intervals for the power law model $\varphi_\gamma(t)$, then for the cut-off model $\varphi_b(t)$. Quantities to be calculated include the mean $\langle \tau \rangle$, the variance σ^2, the probability density function $P_0(\tau)$ of the zero-crossing interval τ, and the persistence parameter θ when exists.

6.2 Power-law coherence function $\varphi_\gamma(t)$

The expansion of $\varphi_\gamma(t)$, which is given by Equation (6.1), near the origin is $1 - at + O(t^2)$. This fact confirms the existence of the zero-crossing rate β for the symmetric stable process, introduced in Chapter 5. Appendix D shows that the constant a is a scale parameter, so in the following section, set $a = 1$ for computational simplicity.

6.2.1 Mean and variance of the zero-crossing interval τ

For the symmetric stable process, the zero-crossing rate β is given by Equation (5.16), which does not depend on the coherence function. Hence, the mean $\langle\tau\rangle$ of the zero-crossing interval τ is $1/\beta$, which is shown in Figure 5.1 in Chapter 5.

The variance σ^2 is given by Equation (2.12), and the normalised variance is considered again

$$\frac{\sigma^2}{\langle\tau\rangle^2} = \frac{8\beta}{\pi^2} \int_0^\infty p^{\nu-1} \ln\left(\frac{1+p}{|1-p|}\right) \mathrm{d}p \int_0^\infty \frac{1}{(1 + at/\gamma)^{\gamma\nu} + p^\nu} \mathrm{d}t, \qquad (6.3)$$

which does not converge if $\gamma\nu \leq 1$. Figure 6.1 shows the behaviour of $\sigma^2/\langle\tau\rangle^2$ as a function of ν, which is obtained by numerically evaluating Equation (6.3). The Composite Simpson Quadrature method [83] is used. Two examples for γ are illustrated. All shown curves display similar behaviours, and $\sigma^2/\langle\tau\rangle^2$ is finite when $\nu > 1/\gamma$. For small γ, which is characterised the memory of the power-law coherence function $\varphi_\gamma(t)$, $\sigma^2/\langle\tau\rangle^2$ shows strong fluctuations.

Comparing with Figure 5.2 in Chapter 5, which shows the behaviour of $\sigma^2/\langle\tau\rangle^2$ for the exponential coherence function $\varphi_e(t) = \exp(-at)$, it can be seen that the fluctuations of the lengths of zero-crossing intervals are much stronger for the power-law coherence function $\varphi_\gamma(t)$ as $\gamma\nu \to 1$.
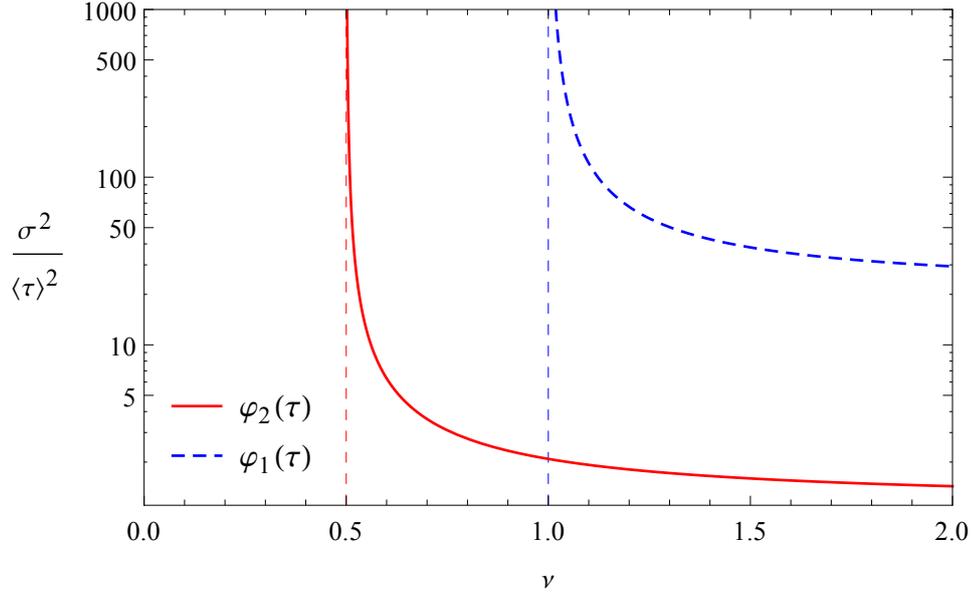
Figure 6.1: This figure plots the normalised variance $\sigma^2/\langle\tau\rangle^2$ for the power-law coherence function $\varphi_\gamma(t)$ (6.1). Two examples are illustrated. The red-solid one is $\gamma = 2$, and the dashed-blue is for $\gamma = 1$. The normalised variances lie above each other with decreasing γ, implying fluctuations of the lengths of intervals become stronger as γ declines. The two vertical lines are threshold values when the variance becomes infinite at $\gamma\nu \leq 1$.

6.2.2 The persistence parameter θ

The persistence parameter θ is obtained by solving the pole of Equation (2.9) in Chapter 2. That is, to determine θ satisfying $1 - g(-\theta) = 0$, where $g(s) = \mathcal{L}\{R''(t)/(4\beta)\}$. Inserting $\varphi_\gamma(t)$ into Equation (5.17) in Chapter 5 and differentiating twice with respective to t, the large t behaviour of $R''(t)$ is obtained by expanding the integrand around $p = 1$, which gives that

$$R''(t) \sim \frac{1}{(1 + at/\gamma)^{2+\gamma\nu}}, \quad t \to \infty. \tag{6.4}$$

By using the similar analysis introduced in Chapter 2, the behaviour (6.4) implies that there does *not* exist the persistence parameter θ. Furthermore, it means that the tail of the probability density function of the zero-crossing in-

terval τ is of power-law type: $P_0(\tau) \sim \tau^{-(2+\gamma\nu)}$ for large τ. The tail behaviour involves the stable index ν, which is inherited from the stable distribution, and the index γ appearing in the power-law coherence function $\varphi_\gamma(t)$; the factor 2 ensures that the mean $\langle\tau\rangle$ of the zero-crossing interval τ exists. This result is consistent with the fact that if $\gamma\nu > 1$, the variance is finite, which agrees with Figure 6.1.

6.2.3 The initial value $P_0(0)$

This section determines the initial value $P_0(0)$, as it is related to the behaviour of zero-crossings (anti-bunched or bunched), which we have already seen in Chapter 2. The initial value theorem [76]

$$\lim_{\tau \to 0} P_0(\tau) = \lim_{s \to \infty} s\, p_0(s)$$

is used again, but the calculation is slightly complex for the non-Gaussian stable case. To simplify the analysis in the following sections, we first introduce a class of integrals that frequently occurs, which is defined through:

$$J_{m,n} = \int_0^\infty \frac{q^{m\nu-1}}{(1+q^\nu)^n} \ln \frac{1+q}{|1-q|}\, \mathrm{d}q, \tag{6.5}$$

where the stable index $0 < \nu \leq 2$, and both $m \geq 1$ and $n \geq 1$ are integers. For example, the zero crossing β (Equation (5.16)) can be written as

$$\beta = \frac{2a\nu}{\pi^2} J_{1,2}.$$

There is a degree of degeneracy in the integrals for special combinations of m and n. The integral $J_{m,n}$ can be simplified as follows. First write

$$J_{m,n} = \int_0^1 \frac{q^{m\nu-1}}{(1+q^\nu)^n} \ln \frac{1+q}{1-q}\, \mathrm{d}q + \int_1^\infty \frac{q^{m\nu-1}}{(1+q^\nu)^n} \ln \frac{q+1}{q-1}\, \mathrm{d}q.$$

Chapter 6

The substitution $q = 1/q$ in the second integral of the right hand side allows the integral to be performed yielding

$$J_{m,n} = \int_0^1 \frac{q^{m\nu-1}(1 - q^{n\nu-2m\nu})}{(1 + q^\nu)^n} \ln \frac{1+q}{1-q} \, dq,$$

which has the following relationship:

$$J_{m,2m} = 2J_{m,2m+1},$$

$$J_{m,2m+1} = J_{m+1,2m+1},$$

$$J_{m+1,2(m-1)} = J_{m,2m-1}.$$

Now consider properties of the Laplace transform. The large s behaviour of $\mathcal{L}\{R''(t)\}$ corresponds to the small t behaviour of $R''(t)$. Thus writing

$$R''(t) = k_0 + k_1 t + k_2 t^2 + \cdots,$$

then

$$\mathcal{L}\{R''(t)\} = \frac{k_0}{s} + \frac{k_1}{s^2} + \frac{2k_2}{s^3} + \cdots,$$

where

$$k_0 = \frac{4(a\nu)^2}{\pi^2} \left\{ 2J_{1,3} - (1 - \frac{1}{\gamma\nu})J_{1,2} \right\}$$

and

$$k_1 = \frac{a^3\nu^2}{\gamma} \left(-4J_{1,3} - 2\gamma\nu(J_{1,4} - 2J_{2,4}) + \left(1 - \frac{1}{\gamma\nu}\right)(2J_{1,2} + \gamma\nu(J_{1,3} - J_{2,3})) \right)$$

with the integral $J_{m,n}$ is defined by Equation (6.5). Therefore the expansion for $g(s)$ is of the form

$$g(s) = \frac{g_0}{s} + \frac{g_1}{s^2} + \cdots.$$

101

Chapter 6

By the initial-value theorem and $g(s) = \mathcal{L}\{R''(t)/4\beta\}$, we can obtain that

$$P_0(0) = \frac{a\nu}{2} \left[2\frac{J_{1,3}}{J_{1,2}} - \left(1 - \frac{1}{\gamma\nu} \right) \right].$$

Hence, the initial value $P_0(0)$ has the simple form

$$P_0(0) = \frac{a}{2\gamma}. \tag{6.6}$$

This result shows that the value of $P_0(0)$ is non-zero for the power-law coherence function $\varphi_\gamma(t)$. Note that let $\gamma \to \infty$, then $\varphi_\gamma(t) \to \varphi_e(t) = \exp(-at)$, and the initial value $P_0(0) \to 0$, which agrees with Figure 5.4 in Chapter 5.

Using the initial value theorem twice, we can obtain $P_0'(0)$ as well:

$$P_0'(0) = \lim_{s \to \infty} s \left(s \left(\frac{g_0}{s} + \frac{g_1}{s^2} + \cdots \right) - P_0(0) \right) = g_1.$$

That is

$$P_0'(0) = (a\nu)^2 \left(\frac{2J_{2,4} - J_{1,4}}{J_{1,2}} - \frac{1}{(\gamma\nu)^2} \right). \tag{6.7}$$

The sign of $P_0'(0)$ is determined by terms in parentheses in (6.7). It is found that if $\gamma\nu > 1.4$, then $P_0'(0)$ is positive, which indicates that zero-crossings are anti-bunched (repelled by each other). Otherwise, $P_0'(0)$ is negative, implying zero-crossings are bunched (attracted to each other). The behaviour of $P_0'(0)$ indicates that $P_0(0)$ is non-zero, which agrees with Equation (6.6). The combinations of $\gamma\nu$ for which makes $P_0'(0)$ positive are plotted in Figure 6.2. The shaded region shows that $P_0'(0)$ is positive, and two examples of combinations of $\gamma\nu$ are also shown. The red-dashed line is for $\gamma\nu = 3$, which represents the positive sign of $P_0'(0)$, and the blue dashed is for $\gamma\nu = 1$, which is an example for the negative $P_0'(0)$.

To check this analysis, two examples of the probability density functions $P_0(\tau)$ of zero-crossing intervals are shown in the following section. In Figure 6.2, the star is for the combination $\gamma = 2$ and $\nu = 3/2$ and the triangle is for
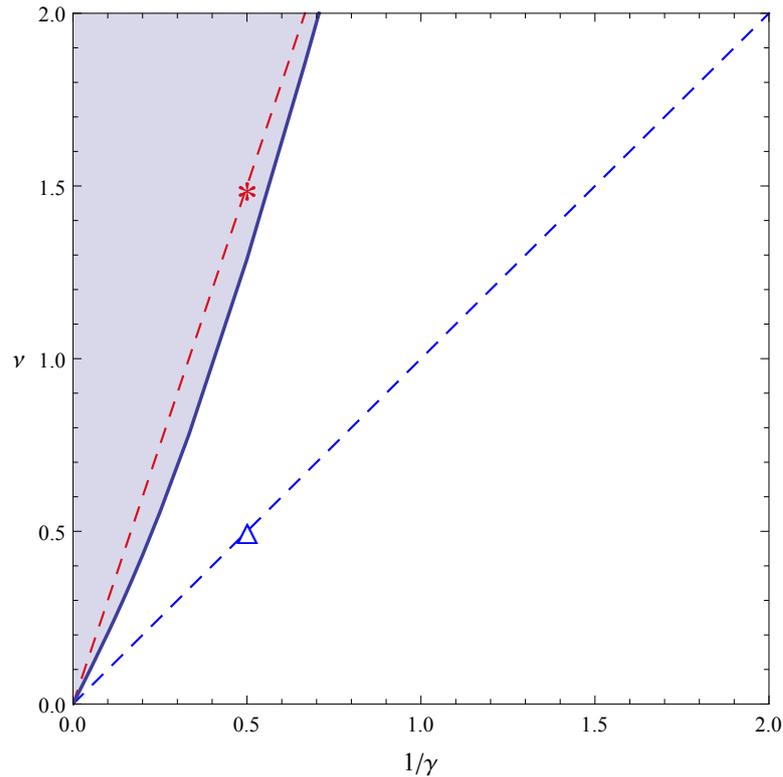
Figure 6.2: This figure plots the sign of $P_0'(0)$, which is determined by combinations of $\gamma\nu$. The value $P_0'(0)$ indicates the behaviour of zero-crossings. The shaded region represents for $P_0'(0) > 0$. The red dashed line is for $\gamma\nu = 3$, and the blue dashed is for $\gamma\nu = 1$. The symbols are the locations of examples of the probability density functions: the star is for $\gamma = 2$ and $\nu = 3/2$ and the triangle is for $\gamma = 2$ and $\nu = 1/2$.

$\gamma = 2$ and $\nu = 1/2$. In these two cases, it is expected that the initial value $P_0(0)$ is determined by Equation (6.6), and one of the probability density functions $P_0(\tau)$ increases from the origin, and the other one decreases.

6.2.4 Probability density functions

This section shows the probability density function $P_0(\tau)$ of the zero-crossing interval τ for the symmetric stable process with the power-law coherence function $\varphi_\gamma(t)$. The closed forms for $g(s) = \mathcal{L}\{R''(t)/(4\beta)\}$ are not easy to determine, so the approximated function $G(s)$ to $g(s)$ is used, which has already been seen in Chapter 2. The exact forms for $G(s)$ are shown in Appendix F. All probability density functions are obtained from the numerical

inversion of the Laplace transform with the independence assumption.

The first example is with the combination value $\gamma\nu = 1$, where $\gamma = 2$ and $\nu = 1/2$. Since $\gamma\nu = 1$, it implies that the variance and high-order moments of the zero-crossing interval τ are infinite. The probability density function $P_0(\tau)$ is shown in Figure 6.3 (a). It can be seen that $P_0(\tau)$ begins with the initial value $P_0(0) = a/(2\gamma)$ and monotonically decays to zero. This behaviour implies that zero-crossings are bunched. The behaviour $P_0'(0) < 0$ can be traced back to the blue-dashed line in Figure 6.2, which is marked by the triangle. The location of the triangle indicates that the value $P_0'(0)$ is negative, implying that $P_0(\tau)$ decreases from the origin, in agreement with Figure 6.3. The inset plot of Figure 6.3 (a) is on a double-logarithmic scale, indicating that the tail is of power-law form $P_0(\tau) \sim \tau^{-(2+\gamma\nu)}$ for large τ, which is consistent with what was deduced in Section 6.2.2.

The second example is the combination $\gamma\nu = 3$, for which the variance of the zero-crossing interval τ is finite, but the high-order moments are not. Figure 6.3 (b) shows the probability density function $P_0(\tau)$ of zero-crossing intervals with $\gamma = 2$ and $\nu = 3/2$. It can be seen that the initial value $P_0(0)$ is still $P_0(0) = a/(2\gamma)$, however, there is an obvious difference compared with the $\gamma\nu = 1$ case: $P_0(\tau)$ increases from the initial value, implying that $P_0'(0)$ is positive. This behaviour refers the red-dashed line in Figure 6.2. The star represents for $\gamma = 2$ and $\nu = 3/2$, and its location means that $P_0'(0)$ is positive, which is in agreement with Figure 6.3 (b). The inner double-logarithmic plot in Figure 6.3 (b) confirms that the tail of the zero-crossing interval τ is also of power-law form $P_0(\tau) \sim \tau^{-(2+\gamma\nu)}$ for large τ.

6.3 Power-law cut-off coherence function $\varphi_b(t)$

The cut-off power-law autocorrelation function $\rho_b(t)$ was used to investigate zero-crossing intervals of Gaussian processes in Chapter 4. This section is to
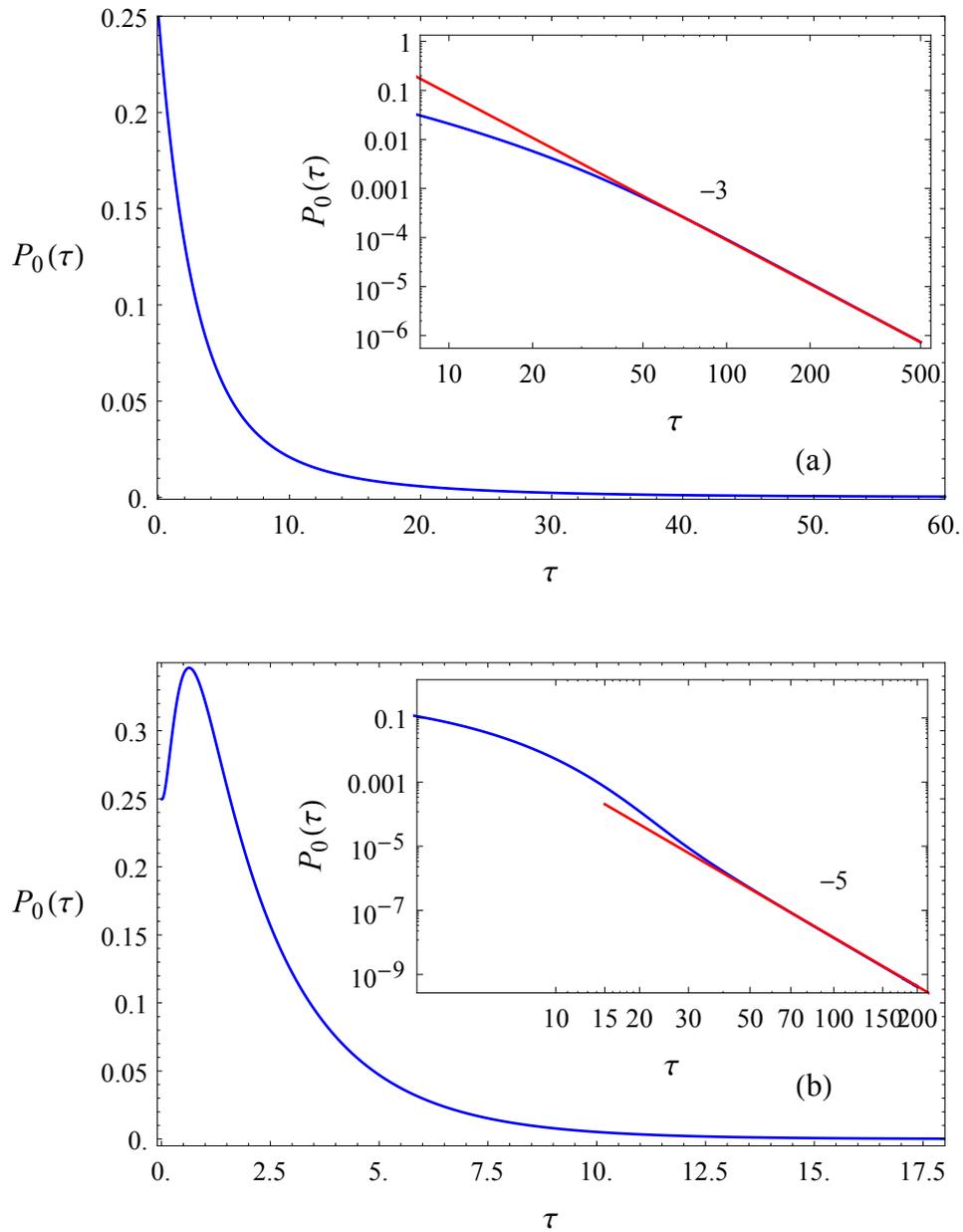
Figure 6.3: This figure shows the probability density function $P_0(\tau)$ of the zero-crossing interval τ for the power-law coherence function $\varphi_\gamma(t)$. Figure (a) is for $\gamma\nu = 1$ with $\gamma = 2$ and $\nu = 1/2$, and (b) is for $\gamma\nu = 3$ with $\gamma = 2$ and $\nu = 3/2$. All density functions have the initial value $a/(2\gamma)$, but the sign of $P_0'(0)$ is different. The behaviour of $P_0'(0)$ agrees with Figure 6.2, where the triangle denotes the case with $\gamma = 2$ and $\nu = 1/2$, and the star represents the case with $\gamma = 2$ and $\nu = 3/2$.

complete the cut-off power-law theory corresponding to the power-law coherence function. That is to show the behaviour of the zero-crossing intervals if the symmetric stable process has the cut-off power-law coherence function $\varphi_b(t)$, given by Equation (6.2), which has the expansion near the origin

$$\varphi_b(t) = 1 - \left(a + \frac{1}{b}\right) t + O(t^2).$$

As a result, it implies that the zero-crossing rate changes into

$$\beta = \frac{2\nu}{\pi^2} \left(a + \frac{1}{b}\right) J_{1,2}, \tag{6.8}$$

where $J_{1,2}$ is the integral given by Equation (6.5). Clearly, Equation 6.8 is similar to the original zero-crossing rate for large b.

The following sections evaluate relevant properties of the zero-crossing intervals. The choice of the parameter $b > 0$ is arbitrary. The main aim of this section is to show that with the cut-off term $\exp(-t/b)$, the probability density function $P_0(\tau)$ of zero-crossing intervals is *not* of power-law form, and the persistence parameter θ exists. Hence, two examples for $b = 10$ and $b = 5$ are considered in the following sections, as it is sufficient to compare the effect of b on the zero-crossing intervals.

6.3.1 Mean and variance of zero-crossing intervals

Mean $\langle \tau \rangle$

The mean $\langle \tau \rangle$ of the zero-crossing interval τ is still $1/\beta$, where now the zero-crossing rate β is given by Equation (6.8). Comparing with the usual zero-crossing rate given by Equation (5.16), the difference is that the scale parameter changes from a to $a + 1/b$. Hence, the behaviour of $\langle \tau \rangle$ is little affected and is similar to that shown in Figure 5.1 in Chapter 5.

Chapter 6

Variance σ^2

The normalised variance is considered again, which now is given as

$$\frac{\sigma^2}{\langle\tau\rangle^2} = \frac{8\beta}{\pi^2} \int_0^\infty p^{\nu-1} \ln\left(\frac{1+p}{|1-p|}\right) \mathrm{d}p \int_0^\infty \frac{1}{(1+at/\gamma)^{\gamma\nu}\mathrm{e}^{\nu t/b} + p^\nu} \, \mathrm{d}t. \quad (6.9)$$

The above integral does converge for all γ and ν as can be demonstrated by using the comparison test:

$$\int_0^\infty \frac{1}{(1+at/\gamma)^{\gamma\nu}\mathrm{e}^{\nu t/b} + p^\nu} \, \mathrm{d}t < \int_0^\infty \frac{1}{\mathrm{e}^{\nu t/b} + p^\nu} \, \mathrm{d}t,$$

where the right-hand side integral is finite. Comparing Equation (6.9) with Equation (6.3), which is the normalised variance for the power-law coherence model $\varphi_\gamma(t)$, the difference is that the variance is always finite and exists for the cut-off coherence model $\varphi_b(t)$.

The normalised variance (Equation (6.9)) is evaluated numerically, and Figure 6.4 shows the normalised variance $\sigma^2/\langle\tau\rangle^2$ as a function of the stable index ν for the cut-off power-law coherence model $\varphi_b(t)$. The two blue curves are for the case $\gamma = 1$, where $b = 10$ is the dashed one, and $b = 5$ is the solid one; and the two red curves stand for the case $\gamma = 2$ with $b = 10$ (dashed) and $b = 5$ (solid).

These four curves show the similar behaviour, which decreases from small ν and eventually becomes insensitive to for large values of ν. For fixed γ, the variance is large for large b. For fixed b, the variance is large for small γ. These properties imply that both γ and b have effects on the variance of the zero-crossing interval τ.

Now compare Figure 6.4 with Figure 6.1. The red curve in Figure 6.1 is for the pure power-law coherence function $\varphi_\gamma(t)$ with $\gamma = 2$, which shows that the variance is infinite at $\nu = 1/2$, but the two red curves for $\gamma = 2$ in Figure 6.4 indicate that it is finite for all ν. The similar result is obtained for the case $\gamma = 1$. These facts confirm that the cut-off term affects the
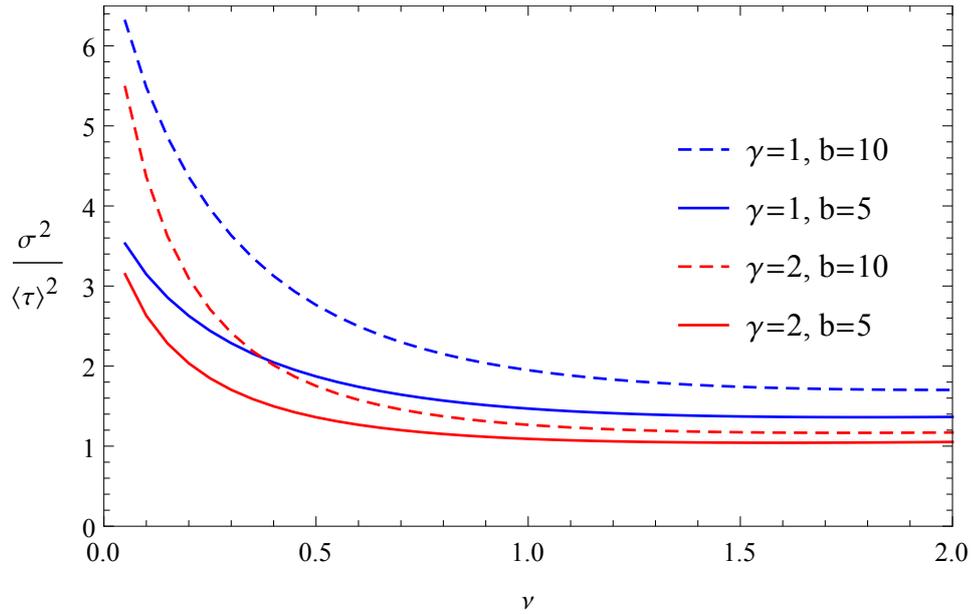
Figure 6.4: This figure plots the normalised variance $\sigma^2/\langle\tau\rangle^2$ of zero-crossing intervals against the stable index ν for the cut-off power-law coherence model $\varphi_b(t)$. The two red curves are for the case $\gamma = 2$ with $b = 10$ (dashed) and $b = 5$ (solid); and the two blue ones are for the case $\gamma = 1$ with $b = 10$ (dashed) and $b = 5$ (solid). Comparing with Figure 6.1, the aim is to show that the variance is finite if the power-law coherence model $\varphi_\gamma(t)$ has the exponential cut-off term $\exp(-t/b)$ even b is large.

properties of zero-crossing intervals, and its variance becomes a finite value for arbitrary γ and ν.

6.3.2 The persistence parameter θ

The persistence parameter θ is of interest in this thesis. It has been seen that given the independence assumption and the power-law coherence function $\varphi_\gamma(t)$, there does not exist θ. This fact, however, is not true for the cut-off power-law coherence function $\varphi_b(t)$.

To determine the persistence parameter θ, we need to evaluate the pole in Equation (2.9) in Chapter 2: $1 - g(-\theta) = 0$, where $g(s) = \mathcal{L}\{R''(t)/(4\beta)\}$. However, the closed forms for $g(s)$ are not known in general, so the Laplace transform has to be evaluated numerically. Note that for the cut-off power-

law coherence function $\varphi_b(t)$, the zero-crossing rate is given by Equation (6.8), then the Composite Simpson Quadrature method [83] is used again. Figure 6.5 shows the persistence parameter θ as a function of ν for selected γ and b. It has to be mentioned that now there *exists θ,* which is different from that for the power-law coherence function $\varphi_\gamma(t)$. The existence of θ leads to the tail of the zero-crossing interval τ changing to the exponential form.

The shown values for γ and b can be divided into two groups. The first group (blue) includes $(\gamma = 1, b = 10)$ and $(\gamma = 1, b = 5)$, and the second group (red) is $(\gamma = 2, b = 10)$ and $(\gamma = 2, b = 5)$. It can be seen that all curves start from zero, and increase as the stable index ν increases. Each group shows that the persistence parameter θ depends on the value b. If γ is fixed, then θ becomes small when b is large. This fact means that the exponential tail is less significant, and the power-law tail takes over, as shown in the previous section. If b is fixed, then θ increases as γ increases. This fact is because $(1 + at/\gamma)^{-\gamma}$ tends to $\exp(-at)$ as $\gamma \to \infty$. The symbols are used to indicate the tail index of the zero-crossing interval τ in the following section.
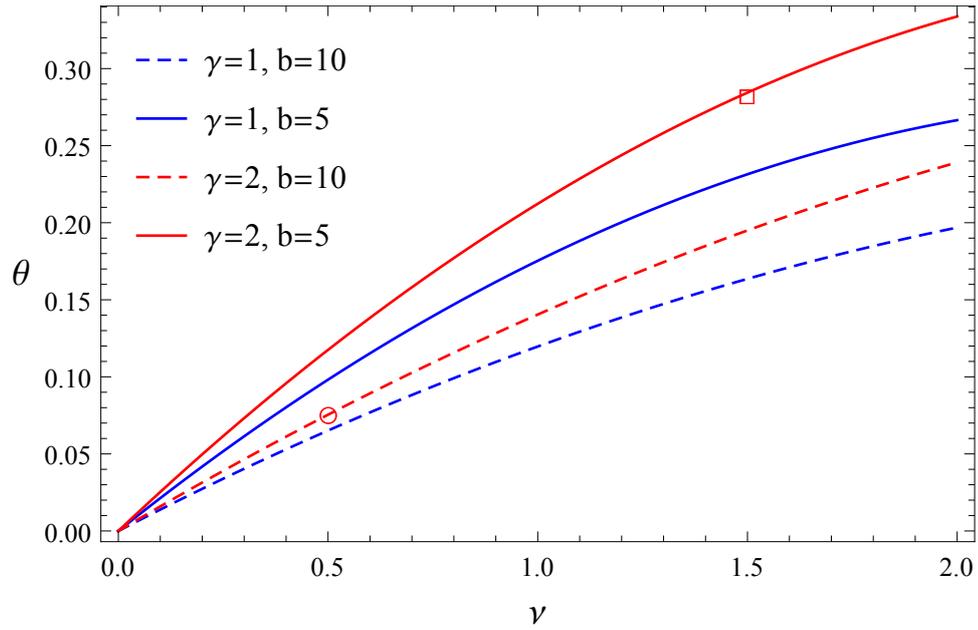
Figure 6.5: This figure plots the persistence parameter θ against the stable index ν for the cut-off power-law coherence function $\varphi_b(t)$. Four examples are shown, and all curves start from zero. The aim of this figure is to demonstrate that given the cut-off term $\exp(-t/b)$, θ is finite and exists for all ν and γ. This behaviour is *different* from that for the pure power-law coherence model $\varphi_\gamma(t)$, for which θ does not exist.

6.3.3   The probability density function

This section shows the probability density function $P_0(\tau)$ of the zero-crossing interval τ for the symmetric stable process with the cut-off power-law coherence function $\varphi_b(t)$. The density functions are obtained by using the Talbot method as before. The closed forms for $g(s) = \mathcal{L}\{R''(t)/(4\beta)\}$ are not known in general, so the asymptotic analysis is used to obtain the approximation function $G(s)$ to $g(s)$, which combines the large and small behaviour of $\mathcal{L}\{R''(t)/(4\beta)\}$, as seen in Chapter 2. By using the similar analysis introduced in the previous section, it is found that for the cut-off power-law coherence model $\varphi_b(t)$, we have

$$R''(t) \sim \frac{e^{-\nu t/b}}{(1 + at/\gamma)^{\gamma\nu}}$$

for large t. Note that this large t behaviour is different from that for the power-law model $\varphi_\gamma(t)$, which is shown in Equation (6.4). Furthermore, this asymptotic behaviour indicates that the tail of the zero-crossing interval τ has the form $P_0(\tau) \sim (1 + a\tau/\gamma)^{-\gamma\nu} \exp(-\nu\tau/b)$ for large τ. The exact forms of the function $G(s)$ are given in Appendix F.

Figure 6.6 shows two examples of the probability density function $P_0(\tau)$ of the zero-crossing interval τ given the cut-off power-law coherence function $\varphi_b(t)$. Figure (a) is with the combination $\gamma\nu = 3$, where $\gamma = 2$, $\nu = 3/2$ and $b = 5$; and Figure (b) is with $\gamma\nu = 1$, where $\gamma = 2$, $\nu = 1/2$ and $b = 10$. The inset plots are produced on a log-linear scale, and straight lines are shown, implying the tail is of exponential form. Comparing with Figure 6.3, we conclude that the tail is not the power-law type, even though the combination of $\gamma\nu$ is the same. This fact implies that the cut-off term affects the nature of the zero-crossing interval τ. The index of the tail can refer to Figure 6.5, which agrees with the locations of the square and the circle respectively.

6.4   Summary

This chapter considers zero-crossing intervals of symmetric stable processes with the power-law coherence function $\varphi_\gamma(t)$ (6.1) and the cut-off power-law coherence function $\varphi_b(t)$ (6.2) respectively given the independence assumption, which is the only available theory to analyse zero-crossing intervals. Although the thesis does not consider simulations for the stable processes, the analytical results of zero-crossing intervals can be treated as an attempt and preparations for future work.

For the power-law coherence function $\varphi_\gamma(t)$, it is found that the mean $\langle \tau \rangle$ of the zero-crossing interval τ is finite, but the variance σ^2 does depend on the combinations of $\gamma\nu$. If $\gamma\nu \leq 1$, then σ^2 is infinite. As a consequence,
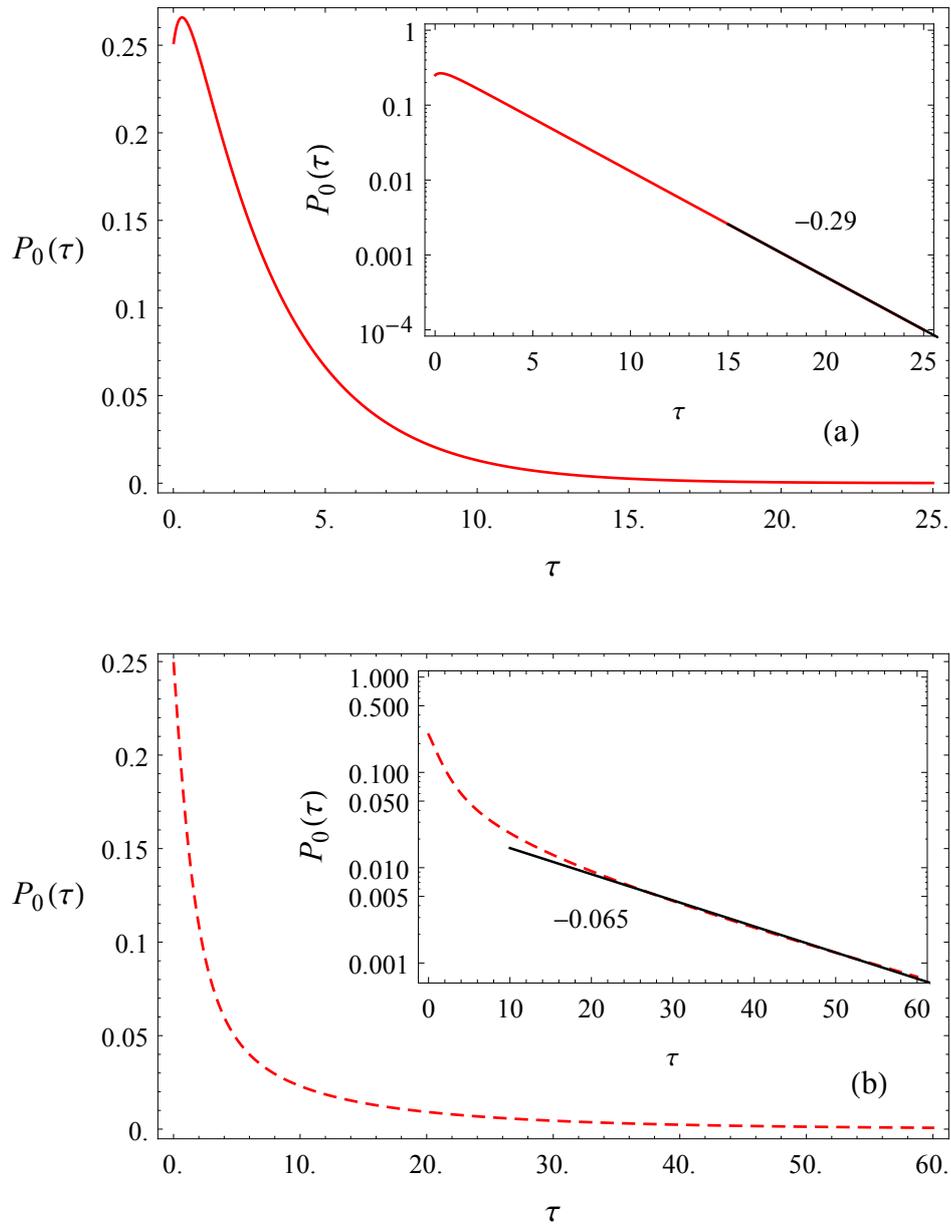
Figure 6.6: This figure shows the probability density function $P_0(\tau)$ of zero-crossing intervals for the symmetric stable process with the cut-off power-law coherence model $\varphi_b(t)$. The aim of this figure is to show that given the cut-off term $\exp(-t/b)$, the tail is of exponential form, not the power-law form as was shown in Figure 6.3. Plot (a) is with $\gamma = 2$, $b = 5$ and $\nu = 3/2$ (corresponding to $\gamma\nu = 3$); and Plot (b) is with $\gamma = 2$, $b = 10$ and $\nu = 1/2$ (corresponding to $\gamma\nu = 1$). The index of the tail agrees with the symbols in Figure 6.5. The square is for Plot (a), and the circle is for Plot (b).

it indicates that there does not exist the persistence parameter θ, and the probability density function $P_0(\tau)$ does not have an exponential tail. The analysis shows that the tail is of power-law form $P_0(\tau) \sim \tau^{-(2+\gamma\nu)}$ for large τ, which implies that the zero-crossing interval τ is influenced by the stable index ν and the value γ adopted from $\varphi_\gamma(t)$. This confirms the fact that σ^2 is infinite if $\gamma\nu \leq 1$.

The cut-off power-law coherence function $\varphi_b(t)$ is considered, which is motivated by the cut-off power-law autocorrelation function of the Gaussian process shown in Chapter 4. The cut-off term $\exp(-t/b)$ in $\varphi_b(t)$ does affect the properties of zero-crossing intervals. It is found that the large b has a small effect on the zero-crossing rate. More important is that the variance σ^2 of the zero-crossing interval τ becomes finite for all γ and ν, which is shown in Figure 6.4. Another difference is that the persistence parameter θ exists, implying the tail is of exponential form. The behaviour of θ is shown in Figure 6.5, which increases monotonously from zero, but depends on the value b. Two examples of the probability density functions of the zero-crossing intervals are shown. The combinations of $\gamma\nu$ are the same as those used for the pure power-law coherence function $\varphi_\gamma(t)$, but now the tail of the zero-crossing interval τ is of exponential form, not the power-law.

Chapter 7

Conclusion

This thesis has considered zero-crossing intervals of Gaussian and symmetric stable processes. The main aim is to explore the probability density function $P_0(\tau)$ of the zero-crossing interval τ, and to determine the persistence parameter θ, which describes the asymptotic behaviour of $P_0(\tau)$.

Chapter 2 used the independence approximation to analytically investigate zero-crossing intervals of Gaussian processes with three different autocorrelation functions. The independence assumption is a gross approximation, but is a simple and analytically tractable choice. The independence results can serve as the benchmark to the simulation results. If the simulation results, which were shown in Chapter 3, does not agree with the analytical results, it implies we must reject the independence approximation of successive zero-crossing intervals. The first one is the exponentially bounded autocorrelation function $\rho_e(t)$. It is found that the mean $\langle \tau \rangle$ of the zero-crossing interval τ is π/a, where a is a time-scale constant appeared in $\rho_e(t)$, and the variance σ^2 of τ is a finite value. The persistence parameter θ is calculated by solving the pole of the Laplace transform of $P_0(\tau)$. Moreover, the probability density function $P_0(\tau)$ is obtained by using the Tablot method. It is found that $P_0(\tau)$ is of exponential form, whose index is the same as the persistence parameter θ.

The two power-law autocorrelation functions $\rho_\gamma(t)$ and $\phi_\gamma(t)$ were then considered, where $\gamma > 0$ is the power-law index. It is found that results of zero-crossing intervals have certain features in common. The mean $\langle \tau \rangle$ of τ is also π/a, but the variance σ^2 varies according to the value of γ. Given the independent approximation, the analytical calculation shows that for both power-law autocorrelation functions, the variance σ^2 is a finite value if $\gamma > 1$, and does not exist if $0 < \gamma \le 1$. As a consequence, it leads to a change in the tail behaviour of the probability density function $P_0(\tau)$ of the zero-crossing interval τ. Moreover, it was analytically shown that there does not exist the persistent parameter θ. Furthermore, it was also shown that $P_0(\tau)$ is of power-law form $\tau^{-(2+\gamma)}$ for large τ. For these two power-law autocorrelation functions, the difference, however, lies in the initial value $P_0(0)$. For the model $\rho_\gamma(t)$, $P_0(0)$ is always zero, but for $\phi_\gamma(t)$, it is not and depends on the value γ.

Chapter 3 and 4 aim to examine the validity of the independence approximation by comparison with the simulations. It is found that for the exponentially bounded autocorrelation function $\rho_e(t)$, the simulated probability density function $P_0(\tau)$ of the zero-crossing interval τ is close to that obtained from the independence model. This fact implies that the independence assumption is *adequate*. Furthermore, this thesis also examined the correlations of zero-crossing intervals. It was found that the correlations of zero-crossings intervals were were very close to zero.

For the power-law autocorrelation functions $\rho_\gamma(t)$ and $\phi_\gamma(t)$, however, the simulations show that the independence assumption is not valid, which implies that we cannot use the independent results shown in Chapter 2 to model statistical properties of zero-crossing intervals. It was also found that the correlations of the zero-crossing intervals show the alternating behaviour, and is power-law correlated. The fact implies that the correlations of zero-crossing intervals cannot be neglected. On the other hand, although there

exists the disagreement between the simulation results and the analytical results, the analytical derivation methods used in Chapter 2 can be used to explore other interested autocorrelation functions.

The simulation results for the power-law bounded autocorrelation functions $\rho_\gamma(t)$ and $\phi_\gamma(t)$ showed similar behaviours. It was found that the tail of the zero-crossing interval τ is of exponential from when $\gamma > 1$. For the regime $0 < \gamma \leq 1$, the thesis claimed that the simulation results were not physically realisable at the first place, because the spectral density function $S(\omega)$ of the power-law bounded autocorrelation functions is not finite at $\omega = 0$. This property implies that the process has infinite power, which is not physically realisable. Notwithstanding with, a computer 'experiment' with such autocorrelation function can be conducted, but it does not correspond a realization of a valid Gaussian process. To remedy this behaviour, the thesis investigated the power-law autocorrelation function $\rho_\gamma(t)$ provided with a cut-off term. That is the cut-off power-law autocorrelation function $\rho_b(t)$, where b determines the correlation length of the cut-off term. Although the asymptotic behaviour of the cut-off model $\rho_b(t)$ is different from the power-law autocorrelation function $\rho_\gamma(t)$, the model $\rho_b(t)$ truncates the infinite power. Furthermore, the model $\rho_b(t)$ takes the finite data length into consideration, because the power-law type correlations do not always sustain in the simulated processes for large correlated time lags due to the finite capacity or storage of the digital computer. The cut-off autocorrelation function was considered, because the thesis required to construct an autocorrelation function that is effectively power-law in an intermediate regime (of arbitrary length), but contain an exponential cut-off in the far tail. The value b has to be large, because the aim of the cut-off term is to make the process have the finite power and does not interfere with the power-law type correlations. If b increases, the cut-off model $\rho_b(t)$ is close to $\rho_\gamma(t)$. Furthermore, the cut-off time $t = t_c$ can be solved and deicides where the autocorrelation function

$\rho_b(t)$ transits from the power-law type to exponential behaviour. Then it is found that for large b, the simulated probability density functions are very close to that for the pure power-law function $\rho_\gamma(t)$, but the tail of the zero-crossing intervals is of exponential form. It has to be noted that Eichiner et al. [89] claimed that the tail of the probability density function $P_0(\tau)$ of the zero-crossing interval τ is of the stretched exponential, but it has to be mentioned that the simulated processes he used is of infinite power, which is not practically realizable at the first place.

In Chapter 5, zero-crossing intervals of symmetric stable processes with the exponential coherence function $\varphi_e(t)$ were investigated. The methodology is inherited from the Gaussian case. Results of this chapter were obtained under the independence assumption of successive zero-crossing intervals. It is expected to derive the analogous results that the independence approximation is valid, because the exponential coherence function of symmetric stable processes corresponds to the exponentially bounded autocorrelation of Gaussian processes, where the independence assumption was shown to be valid. It was found that the zero-crossing interval τ has the exponential tail and the initial value $P_0(0)$ is 0. Note that the behaviour is the same as the exponentially bounded autocorrelation function $\rho_e(t)$, which in fact is generated from $\varphi_e(t)$. The mean $\langle \tau \rangle$ of the zero-crossing interval τ is larger than that for the Gaussian case because of the heavy tails of the stable distributions. The normalised variance $\sigma^2/\langle \tau \rangle^2$ is less than 1 and nearly independent of the stable index ν, indicating that the interval length has less fluctuations. The persistence parameter θ for general ν is also considered. It is found that θ increases from zero when ν increase from 0 to 2, implying the tail of probability density functions of zero-crossing intervals is much extended. When $\nu = 2$, the persistence parameter θ agrees with each other, either calculating from $\rho_e(t)$ of the Gaussian case or $\varphi_e(t)$ of the stable case. The probability density functions of the zero-crossing intervals are shown for $\nu = 1/2$ and

1. Both show the similar shape, and the tail indices are the same as the persistence parameter θ. Note that results shown in this chapter were derived from the independent approximation. As Gaussian random variables belong to the stable random variables, and the independent assumption is satisfied to explore zero-crossing intervals of Gaussian processes with the exponentially bounded autocorrelation function as shown in previous chapters, it is expected to obtain the similar results that the independent assumption is also valid to investigate zero-crossing intervals of stable processes with exponentially bounded coherence functions, because such type coherence functions decay to zero sufficiently quick, which indicates that the correlations between zero-crossing intervals are negligible.

Chapter 6 showed statistical properties of zero-crossing intervals of symmetric stable processes with either the power-law coherence function $\varphi_\gamma(t)$ or the cut-off power-law coherence function $\varphi_b(t)$ under the independence assumption. The cut-off type coherence function $\varphi_b(t)$ was investigated, because it corresponds to the cut-off power-law autocorrelation function $\rho_b(t)$ in the Gaussian case, which was considered in Chapter 4. For the power-law model $\varphi_\gamma(t)$, the persistence parameter θ does not exist, and the tail of the zero-crossing intervals τ is of power-law form $P_0(\tau) \sim \tau^{-(2+\gamma\nu)}$ for large τ, which depends on the stable index ν, as well as the memory index γ. This fact implies that the zero-crossing interval τ is related to the underlying symmetric stable process and the power-law coherence function. For the cut-off model $\varphi_b(t)$, zero-crossing intervals show different features. Note that $\varphi_b(t)$ is close to $\varphi_\gamma(t)$ if b is large. It is found that the persistence parameter θ exists, and the tail of τ is of exponential form. The cut-off power-law coherence function $\varphi_b(t)$ was considered, as it is parallel with the cut-off power-law autocorrelation function $\rho_b(t)$ in the Gaussian case. The results in this chapter were derived from the independent assumption and can serve as benchmark to the simulation results, which can be considered as the further work. How-

ever, it is expected to see that given the power-law bounded coherence function and a valid simulation algorithm, the independent approximation is not satisfied to model statistical properties of zero-crossing intervals, which is similar to that of Gaussian processes with power-law bounded autocorrelation function.

7.1   Further Work

Chapter 2 has examined only the positive autocorrelation functions, but one could consider the oscillatory autocorrelation function. The simulation results of Chapter 3 and 4 indicate that the correlations of the zero-crossing intervals are *not* significant, implying that the dependence of the zero-crossing intervals may be determined by higher order correlations.

In Chapter 5 and 6, it considered zero-crossing intervals of symmetric stable processes with different coherence functions given the independence assumption; however, the results are required to compare with simulations. That is how to simulate the non-independence symmetric stable process with a specific coherence function. Then it will be possible to explore the validity of the independence assumption.

Another quantity that may be calculated is to determine the probability $p(n, t)$ that finds exactly n zeros in the given interval $(t', t' + t)$. The function $p(n, t)$ is important because it can also be used to determine the probability density function $P_0(\tau)$ of the zero-crossing interval τ.

To model the correlations of successive zero-crossing intervals, McFadden [23] generalized the independence model by defining $p_n(s) = a_n(s)p_0^{n+1}(s)$, where assuming $\{a_n(s)\}$ possess all the information about correlations. It is felt that the best hope for further progress lies in the invention of $\{a_n(s)\}$ from the simulation data. Then the following equation may be summed up

in n

$$g(s) = \sum_{n=0}^{\infty} (-1)^n a_n(s) p_0^{n+1}(s),$$

so that one could express $p_0(s)$ in terms of $g(s)$ and $\{a_n(s)\}$. Then the inverse Laplace transform of $p_0(s)$ could show the tail behaviour, which agrees with the simulation data.

$$g(s) = \sum_{n=0} -120$$

Appendix A

Relations of zero-crossing intervals

These equations (2.3)-(2.5) can be derived by considering the probabilities of particular events. That is

$$p(n, \tau) = \Pr[\text{find } n \text{ crossings in the interval } (t, t + \tau)]$$
$$= \Pr[\text{find } n \text{ crossings in } (t, t + \tau) \text{ and none in } (t + \tau, t + \tau + \mathrm{d}\tau)]$$
$$+ \Pr[\text{find } n \text{ crossings in } (t, t + \tau) \text{ and one in } (t + \tau, t + \tau + \mathrm{d}\tau)].$$

Note that the last term, which was considered by McFadden [23], is the probability of the event finding n crossings in $(t, t+\tau)$ and one in $(t+\tau, t+\tau+\mathrm{d}\tau)$, not the event finding $n-1$ crossings in $(t, t+\tau)$ and one in $(t+\tau, t+\tau+\mathrm{d}\tau)$ because of the total probability. Similarly, McFadden wrote

$$p(n, \tau + \mathrm{d}\tau) = \Pr[\text{find } n \text{ points in the interval } (t, t + \tau + \mathrm{d}\tau)]$$
$$= \Pr[\text{find } n \text{ points in } (t, t + \tau) \text{ and none in } (t + \tau, t + \tau + \mathrm{d}\tau)]$$
$$+ \Pr[\text{find } n - 1 \text{ points in } (t, t + \tau) \text{ and one in } (t + \tau, t + \tau + \mathrm{d}\tau)].$$

Then McFadden assumed that $p(n, \tau)$ is continuous and wrote the difference as

$$p(n, \tau + \mathrm{d}\tau) - p(n, \tau) \approx p'(n, \tau)\, \mathrm{d}\tau.$$

Thus it follows that

$$p'(n, \tau)\, \mathrm{d}\tau = \Pr[\text{find } n-1 \text{ points in } (t, t+\tau) \text{ and one in } (t+\tau, t+\tau+\mathrm{d}\tau)]$$
$$- \Pr[\text{find } n \text{ points in } (t, t+\tau) \text{ and one in } (t+\tau, t+\tau+\mathrm{d}\tau)].$$

$$(\text{A.1})$$

Take the second term on the right-hand side of Equation (A.1) as an example, McFadden wrote this expression as

$$\Pr[\text{no more than } n \text{ points in } (t, t+\tau) \text{ and one in } (t+\tau, t+\tau+\mathrm{d}\tau)]$$
$$- \Pr[\text{no more than } n-1 \text{ points in } (t, t+\tau) \text{ and one in } (t+\tau, t+\tau+\mathrm{d}\tau)].$$

$$(\text{A.2})$$

The probability that there are no more than n zeros in $(t, t+\tau)$ is the probability that the time to the nth zero is greater than τ, i.e.

$$\int_{\tau}^{\infty} P_n(v)\, \mathrm{d}v.$$

Then Equation (A.2) becomes

$$\beta \mathrm{d}\tau \int_{\tau}^{\infty} P_n(v)\, \mathrm{d}v - \beta \mathrm{d}\tau \int_{\tau}^{\infty} P_{n-1}(v)\, \mathrm{d}v. \qquad (\text{A.3})$$

Similar consideration to the first term on the right-hand side of Equation (A.1) gives that

$$\beta \mathrm{d}\tau \int_{\tau}^{\infty} P_{n-1}(v)\, \mathrm{d}v - \beta \mathrm{d}\tau \int_{\tau}^{\infty} P_{n-2}(v)\, \mathrm{d}v. \qquad (\text{A.4})$$

Inserting Equations (A.3) and (A.4) into Equation (A.1), and assuming the second derivative $p''(n, \tau)$ exists and provided that for $n = 0$ and $n = 1$, $P_n(\tau) = 0$, then Equations (2.3), (2.4) and (2.5) are the results.

Appendix B

Moments of zero-crossing intervals

From the definition of the Laplace transform, the moments of the zero-crossing interval τ may be obtained from the derivatives of the transform $p_0(s)$, evaluated at $s = 0$. If the function $p_0(s)$ and $g(s)$ are regular functions of s, then the expansions of $g(s)$ and $p_0(s)$ near the origin are

$$p_0(s) = 1 - \langle\tau\rangle s + \langle\tau^2\rangle s^2/2 - \cdots , \tag{B.1}$$

$$g(s) = g(0) + g'(0)s + g''(0)s^2/2 + \cdots .$$

The above expansion for $p_0(s)$ implies that all the moments for τ exist, however, it is not always this case because the expansion of $p_0(s)$ will be affected by the type of the autocorrelation function $r(t)$ of the underlying process $x(t)$. For example, if $r(t)$ is of power-law form and $x(t)$ is a Gaussian process, then the expansion of $p_0(s)$ has another form. This issue is seen in Chapter 2.

Three constants in the expansion of $g(s)$ can be identified [23]. Now consider $g(0)$ first. For sufficiently small t, we have $R(t) \approx 1 + R'(0)t$, then the probability that $x(t')$ and $x(t' + t)$ are of opposite sign is $[1 - R(t)]/2$

([23]). For small t, this probability becomes the expected number of zeros per unit time multiplied by t,

$$\beta t = \frac{1}{2}[1 - R(t)],$$

therefore $R'(0) = -2\beta$. If $R(t)$ and its derivative vanish at infinity, then

$$
\begin{aligned}
g(0) &= \int_0^\infty \frac{R''(t)}{4\beta} \, \mathrm{d}t \qquad \text{(by parts)} \\
&= -\frac{1}{4\beta} R'(0) \\
&= \frac{1}{2}.
\end{aligned}
$$

Note from (2.9), this result confirms that $p_0(0) = 1$, which states that $P_0(\tau)$ is correctly normalised. The value of $g'(0)$ and $g''(0)$ can be calculated using integration by parts. For example,

$$
\begin{aligned}
g'(0) &= -\int_0^\infty t \frac{R''(t)}{4\beta} \, \mathrm{d}t \\
&= -\frac{1}{4\beta} \int_0^\infty t \, \mathrm{d}R'(t) \\
&= -\frac{1}{4\beta} \left[tR'(t)|_0^\infty - \int_0^\infty R'(t) \, \mathrm{d}t \right] \\
&= -\frac{1}{4\beta} \left[tR'(t)|_0^\infty - R(t)|_0^\infty \right] \\
&= -\frac{1}{4\beta}
\end{aligned}
$$

where it is assumed that $tR'(t) \to 0$ as $t \to \infty$, and

$$
\begin{aligned}
g''(0) &= \frac{1}{4\beta} \int_0^\infty t^2 R''(t) \, \mathrm{d}t \\
&= \frac{1}{4\beta} \left[t^2 R''(t) \big|_0^\infty - \int_0^\infty 2t R'(t) \, \mathrm{d}t \right] \\
&= \frac{1}{4\beta} \left[t^2 R''(t) \big|_0^\infty - 2 \left[t R(t) \big|_0^\infty - \int_0^\infty R(t) \, \mathrm{d}t \right] \right] \\
&= \frac{1}{2\beta} \int_0^\infty R(t) \, \mathrm{d}t,
\end{aligned}
$$

where it is assumed that $tR(t) \to 0$ and $t^2 R'(t) \to 0$ as $t \to \infty$.

Substituting the expansion of $g(s)$ near the origin into Equation (2.9) and using $g(0)$, $g'(0)$ and $g''(0)$, it is found, by matching coefficients of the powers of s, the first and second moment can be identified:

$$
\langle \tau \rangle = \frac{1}{\beta},
$$

and

$$
\langle \tau^2 \rangle = \frac{2}{\beta} \int_0^\infty R(t) \, \mathrm{d}t + \frac{1}{\beta^2}.
$$

The expression for the mean $\langle \tau \rangle$ of the zero-crossing interval τ verifies the heuristic argument as shown before. With the second moment, the variance σ^2 of the zero-crossing interval τ is

$$
\sigma^2 = \frac{2}{\beta} \int_0^\infty R(t) \, \mathrm{d}t.
$$

Appendix C

Interpretation of the coherence function

The interpretation of the coherence function $\varphi(t)$ can be determined through the fractional structure function of the process. Let $m(x)$ denote the probability density function of a single symmetric stable random variable, and $m_2(x, y)$ denote the joint probability density function for two symmetric stable random variables. The fractional moment of a stable random variable can be defined as

$$\langle |X|^\gamma \rangle = \int_{-\infty}^{\infty} \mathrm{d}x \, |x|^\gamma \, m(x),$$

where $-1 < \gamma < \nu$ in order for the integral to converge. Extending this to a process, the structure function is defined to gauge the difference between two values x and y at different times:

$$S_\nu^\gamma(A, \varphi) = \langle |X - Y|^\gamma \rangle = \int_{-\infty}^{\infty} \mathrm{d}x \int_{-\infty}^{\infty} \mathrm{d}y \, |x - y|^\gamma m_2(x, y; \varphi),$$

provided $-1 < \gamma < \nu$. To evaluate $\langle |X|^\gamma \rangle$ and $S_\nu^\gamma(A, \varphi)$, one can express the joint probability density functions $m(x)$ and $m_2(x, y)$ in terms of the characteristic function (5.2) and (5.14). One commonly seen example of the structure function is obtained from the zero-mean Gaussian process with the

variance σ^2:

$$S_2^2(\sigma, \rho) = 2\sigma^2(1 - \rho).$$

For the Gaussian case $\nu = 2$, γ lies in the range $-1 < \gamma < \infty$ and $m_2(x, y)$ is given by (5.5).

In order to identify the general relationship between the autocorrelation function and the coherence function, Hopcraft and Jakeman [15] calculated

$$S_2^{-1/2}(A, \varphi) = \frac{\Gamma(1/4)}{\sqrt{2\pi\sigma}} \frac{1}{(1 - \rho)^{1/4}}$$

and

$$S_\nu^{-1/2}(A, \varphi) = \frac{1}{\nu(2A)^{1/(2\nu)}} \sqrt{\frac{2}{\pi}} \Gamma\left(\frac{1}{2\nu}\right) \left(\frac{1 + \varphi^\nu}{(1 - \varphi)^\nu}\right)^{\frac{1}{2\nu}},$$

as these two quantities can be expressed in the closed forms and used to find the relationship between the autocorrelation function $\rho(t)$ and the coherence function $\varphi(t)$ without losing generality [15]. Then they *defined* a relation between the coherence function φ and a notional quantity $\tilde{\varphi}$ by comparing $S_2^{-1/2}(A, \varphi)$ and $S_\nu^{-1/2}(A, \varphi)$:

$$\frac{1}{(1 - \tilde{\varphi})^{1/4}} = \left(\frac{1 + \varphi^\nu}{(1 - \varphi)^\nu}\right)^{\frac{1}{2\nu}},$$

yielding

$$\tilde{\varphi}(t) = 1 - \left(\frac{(1 - \varphi)^\nu}{1 + \varphi^\nu}\right)^{2/\nu}. \tag{C.1}$$

Equation (C.1) implies the nonlinear relationship between the coherence function $\varphi(t)$ and a notional quantity $\tilde{\varphi}(t)$. The notional quantity $\tilde{\varphi}(t)$ can be interpreted as the fractional correlation function expressed by the coherence function, and this fractional correlation function turns into the usual autocorrelation function $\rho(t)$ for the Gaussian process by setting $\nu = 2$ in

Equation (C.1), giving

$$\tilde{\varphi}(t) = \rho(\tau) = \frac{2\varphi(t)}{1 + \varphi^2(t)},$$

which is already seen in Equation (5.15). Equation (C.1) also shows that the coherence function $\varphi(t)$ is the fractional moments for the process, hence it indicates that the coherence function is *not* the autocorrelation function. However, by letting $\nu = 2$ in Equation (C.1), it can be used to identify the autocorrelation function $\rho(t)$ by the coherence function $\varphi(t)$.

Appendix D

The time-scale parameter a

This appendix shows that the time-scale constant a appeared in the autocorrelation function $\rho(t)$ and the coherence function $\varphi(t)$ is a scale parameter to the persistence factor θ and to the probability density function $P_0(\tau)$ of the zero-crossing interval τ.

Consider the Laplace transform of $\mathcal{L}\{R''(t)/(4\beta)\}$. Since $R(t)$ can be expressed in terms of either $\rho(t)$ or $\varphi(t)$ depended on the underlying process, therefore $R(t)$ can be thought as a function of the parameter a as well, that is $R(at)$. Now differentiating twice with respect to t and taking the Laplace transform, it gives that

$$g(s) = \mathcal{L}\left\{\frac{R''(t)}{4\beta}\right\} = \frac{a^2}{4\beta}\int_0^\infty R''(at)\mathrm{e}^{-st}\,\mathrm{d}t. \tag{D.1}$$

Set $\eta = at$, then Equation (D.1) becomes

$$g(s) = \frac{a}{4\beta}\int_0^\infty R''(\eta)\mathrm{e}^{-\xi\eta}\,\mathrm{d}\eta,$$

where $\xi = s/a$. If the persistence factor θ exists, one can obtain it by solving equation $1 - g(-\theta) = 0$, which means that

$$\theta = -\frac{s}{a}.$$

This implies that the constant a is a scale parameter to the persistence factor θ. Furthermore, the Laplace transform $p_0(s)$ of the probability density function is expressed as a function of $g(s)$, implying that a is also a scaled parameter to $P_0(\tau)$.

Appendix E

Another closed-form for $g(s)$

This Appendix evaluates the Laplace transform of $R''(t)/(4\beta)$ given the exponentially bounded coherence function $\varphi_e(t) = \exp(-at)$ when the stable index $\nu = 1/2$. It has been seen that

$$g(s) = \mathcal{L}\left\{\frac{R''(t)}{4\beta}\right\},$$

where

$$R(t) = \frac{4}{\pi^2} \int_0^\infty \frac{(\varphi(t))^\nu \, p^{\nu-1}}{1 + (\varphi(t))^\nu \, p^\nu} \ln\left(\frac{1+p}{|1-p|}\right) \mathrm{d}p.$$

Substitute $\varphi_e(t)$ into $R(t)$, we have

$$R(t) = \frac{4}{\pi^2} \int_0^\infty \frac{p^{\nu-1}}{\mathrm{e}^{a\nu t} + p^\nu} \ln\left(\frac{1+p}{|1-p|}\right) \mathrm{d}p.$$

If $\nu = 1/2$, then

$$R(t) = \frac{4}{\pi^2} \int_0^\infty \frac{1}{\mathrm{e}^{at/2} + \sqrt{p}} \frac{1}{\sqrt{p}} \ln\frac{1+p}{|1-p|} \mathrm{d}p.$$

Differentiating twice with respect to t, one has

$$R''(t) = \frac{a^2}{\pi^2} \mathrm{e}^{at/2} \int_0^\infty \frac{\mathrm{e}^{at/2} - \sqrt{p}}{(\mathrm{e}^{at/2} + \sqrt{p})^3} \frac{1}{\sqrt{p}} \ln\frac{1+p}{|1-p|} \mathrm{d}p.$$

For simplicity, let $c = e^{at/2}$ and evaluate the above integral, it gives

$$R''(t) = \frac{4a^2}{\pi^2} \frac{1}{\sinh(at)} \left[1 - at \coth(at) + \frac{\pi}{\sinh(at)} (\sinh(\frac{at}{2}))^3 \right] \qquad \text{(E.1)}$$

Taking the Laplace Transform of Equation (E.1), it yields that

$$\begin{aligned} g(s) &= \mathcal{L} \left\{ \frac{R''(t)}{4\beta} \right\} \\ &= \frac{1}{12\beta\pi^2(a-s)^2} \Big[\pi^2 s^3 - 2a(6 + (\pi - 3)\pi)s^2 + a^2\pi(\pi - 12)s \\ &\quad + 6a^3(\pi - 2) + 6s(a-s)^2 \mathrm{A}(s) \Big] \end{aligned}$$

where the function $\mathrm{A}(s)$ is

$$\mathrm{A}(s) = \pi \left[H_1 \left(\frac{2s - 3a}{4a} \right) - H_1 \left(\frac{2s - a}{4a} \right) \right] - H_2 \left(\frac{s - 3a}{2a} \right),$$

where

$$H_1(x) = \psi(1 + x) + \delta,$$
$$H_2(x) = H_1(x) + 2^{-x},$$

where $\psi(x)$ is the digamma function and the constant $\delta = 0.5772\cdots$ is the Euler-Mascheroni constant [77].

Appendix F

The asymptotic approximation function G(s)

This appendix shows the asymptotic approximated functions $G(s)$, which are used for numerically inverting Laplace transform. The exponential integral function is defined as [77]

$$E_n(s) = \int_1^\infty e^{-st} t^{-n} \, dt.$$

For the Gaussian processes with the power-law autocorrelation function $\rho_\gamma(\tau)$, $G(s)$ is given below.

1. For $\gamma = 2$:
$$G(s) = \frac{0.39 + 6e^s E_4(s)}{4.79 + 5.25s + 0.86s^2}.$$

2. For $\gamma = 1$:
$$G(s) = \frac{0.03 + e^s E_3(s)}{1 + 0.64s + 0.05s^2}.$$

3. For $\gamma = 2/5$:
$$G(s) = \frac{0.15 + 0.23e^s E_{2.4}(s)}{0.64 + 0.31s + 0.06s^2}.$$

The above three $G(s)$ are used to produced the probability density functions shown in Figure 2.4 in Chapter 2.

For symmetric stable processes with the power-law coherence function $\varphi_\gamma(\tau)$, $G(s)$ is given below.

1. For $\gamma = 2$ and $\nu = 1/2$:

$$G(s) = \frac{0.25 + 0.15\mathrm{e}^{10s}E_3(10s)}{0.65 + s}.$$

2. For $\gamma = 2$ and $\nu = 3/2$:

$$G(s) = \frac{0.25 + 6.56\mathrm{e}^{1.8s}E_5(1.8s)}{2.12 + s}.$$

These two $G(s)$ are used to produce the probability density functions shown in Figure 6.3 in Chapter 6.

For the symmetric stable processes with the cut-off power-law coherence function $\varphi_b(\tau)$, $G(s)$ is given below.

1. For $\gamma = 2$, $b = 5$ and $\nu = 3/2$:

$$G(s) = \frac{1 + 2.7^{0.3+s}E_3(0.3 + s)}{2.8 + 4s}.$$

2. For $\gamma = 2$, $b = 10$ and $\nu = 1/2$:

$$G(s) = \frac{2 + 2.7^{0.05+s}E_1(0.05 + s)}{9.2 + 8s}.$$

These two $G(s)$ are used to produce the probability density functions shown in Figure 6.6 in Chapter 6.

Bibliography

[1] Emil Julius Gumbel. *Statistics of extremes*. Courier Corporation, 2012.

[2] Mark Kac. On the average number of real roots of a random algebraic equation (ii). *Proceedings of the London Mathematical Society*, 2(1):390–408, 1948.

[3] Stephen O Rice. Mathematical analysis of random noise. *Bell System Technical Journal*, 23(3):282–332, 1944.

[4] Stephen O Rice. Mathematical analysis of random noise. *Bell System Technical Journal, The*, 24(1):46–156, 1945.

[5] Robert F Pawula. Analysis of an estimator of the center frequency of a power spectrum. *Information Theory, IEEE Transactions on*, 14(5):669–676, 1968.

[6] Elias Masry. The recovery of distorted band-limited stochastic processes. *Information Theory, IEEE Transactions on*, 19(4):398–403, 1973.

[7] Stanley M Cobb. The distribution of intervals between zero crossings of sine wave plus random noise and allied topics. *Information Theory, IEEE Transactions on*, 11(2):220–233, 1965.

[8] SO Rice. Intervals between periods of no service in certain satellite communication systemsâĂŤanalogy with a traffic system. *Bell System Technical Journal*, 41(5):1671–1690, 1962.

[9] Nelson M Blachman. Fm reception and the zeros of narrow-band gaussian noise. *Information Theory, IEEE Transactions on,* 10(3):235–241, 1964.

[10] F Shayeganfar, M Hölling, J Peinke, and M Reza Rahimi Tabar. The level crossing and inverse statistic analysis of german stock market index (dax) and daily oil price time series. *Physica A: Statistical Mechanics and its Applications,* 391(1):209–216, 2012.

[11] Michael S Longuet-Higgins. The distribution of intervals between zeros of a stationary random function. *Philosophical Transactions of the Royal Society of London A: Mathematical, Physical and Engineering Sciences,* 254(1047):557–599, 1962.

[12] Michael S Longuet-Higgins. On the intervals between successive zeros of a random function. In *Proceedings of the Royal Society of London A: Mathematical, Physical and Engineering Sciences,* volume 246, pages 99–118. The Royal Society, 1958.

[13] Ian F Blake and William C Lindsey. Level-crossing problems for random processes. *Information Theory, IEEE Transactions on,* 19(3):295–315, 1973.

[14] Paul Lévy. Théorie des erreurs. la loi de gauss et les lois exceptionnelles. *Bulletin de la Société mathématique de France,* 52:49–85, 1924.

[15] KI Hopcraft and E Jakeman. On the joint statistics of stable random processes. *Journal of Physics A: Mathematical and Theoretical,* 44(43):435101, 2011.

[16] EV Bulinskaya. On the mean number of crossings of a level by a stationary gaussian process. *Theory of Probability & Its Applications,* 6(4):435–438, 1961.

[17] Kiyosi Ito et al. The expected number of zeros of continuous stationary gaussian processes. *Journal of Mathematics of Kyoto University*, 3(2):207–216, 1963.

[18] N Donald Ylvisaker. The expected number of zeros of a stationary gaussian process. *The Annals of Mathematical Statistics*, 36(3):1043–1046, 1965.

[19] Richard Barakat. Level crossing statistics of aperture integrated isotropic speckle. *JOSA A*, 5(8):1244–1247, 1988.

[20] MR Leadbetter. On the distributions of the times between events in a stationary stream of events. *Journal of the Royal Statistical Society. Series B (Methodological)*, pages 295–302, 1969.

[21] E Wong. Some results concerning the zero-crossings of gaussian noise. *SIAM Journal on Applied Mathematics*, 14(6):1246–1254, 1966.

[22] JA McFadden. The axis-crossing intervals of random functions. *Information Theory, IRE Transactions on*, 2(4):146–150, 1956.

[23] JA McFadden. The axis-crossing intervals of random functions–ii. *Information Theory, IRE Transactions on*, 4(1):14–24, 1958.

[24] William Feller. *An Introduction to Probability Theory and Its Applications: Volume One*. John Wiley & Sons, 1950.

[25] Bernard Derrida, Vincent Hakim, and Reuven Zeitak. Persistent spins in the linear diffusion approximation of phase ordering and zeros of stationary gaussian processes. *Physical review letters*, 77(14):2871, 1996.

[26] Clément Sire, Satya N Majumdar, and Andreas Rüdinger. Analytical results for random walk persistence. *Physical Review E*, 61(2):1258, 2000.

[27] TW Burkhardt. Semiflexible polymer in the half plane and statistics of the integral of a brownian curve. *Journal of Physics A: Mathematical and General*, 26(22):L1157, 1993.

[28] Satya N Majumdar. Persistence in nonequilibrium systems. *arXiv preprint cond-mat/9907407*, 1999.

[29] Satya N Majumdar and Clément Sire. Survival probability of a gaussian non-markovian process: application to the t= 0 dynamics of the ising model. *Physical review letters*, 77(8):1420, 1996.

[30] David Slepian. The one-sided barrier problem for gaussian noise. *Bell System Technical Journal*, 41(2):463–501, 1962.

[31] M Kac. Probability theory: its role and its impact. *SIAM Review*, 4(1):1–11, 1962.

[32] Harald Cramér and M Ross Leadbetter. *Stationary and related stochastic processes: Sample function properties and their applications*. Courier Dover Publications, 2013.

[33] Herbert Steinberg, Peter M Schultheiss, Conrad A Wogrin, and Felix Zweig. Short-time frequency measurement of narrow-band random signals by means of a zero counting process. *Journal of Applied Physics*, 26(2):195–201, 1955.

[34] JM Smith, KI Hopcraft, and E Jakeman. Fluctuations in the zeros of differentiable gaussian processes. *Physical Review E*, 77(3):031112, 2008.

[35] C-K Peng, J Mietus, JM Hausdorff, S Havlin, H Eugene Stanley, and AL Goldberger. Long-range anticorrelations and non-gaussian behavior of the heartbeat. *Physical review letters*, 70(9):1343, 1993.

[36] Eva Koscielny-Bunde, Armin Bunde, Shlomo Havlin, and Yair Goldreich. Analysis of daily temperature fluctuations. *Physica A: Statistical Mechanics and its Applications*, 231(4):393–396, 1996.

[37] CK Peng, SV Buldyrev, AL Goldberger, S Havlin, F Sciortino, M Simons, HE Stanley, et al. Long-range correlations in nucleotide sequences. *Nature*, 356(6365):168–170, 1992.

[38] Eduardo G Altmann and Holger Kantz. Recurrence time analysis, long-term correlations, and extreme events. *Physical Review E*, 71(5):056106, 2005.

[39] Jan F Eichner, Jan W Kantelhardt, Armin Bunde, and Shlomo Havlin. Statistics of return intervals in long-term correlated records. *Physical Review E*, 75(1):011128, 2007.

[40] Piero Olla. Return times for stochastic processes with power-law scaling. *Physical Review E*, 76(1):011122, 2007.

[41] Paul Lévy. *Calcul des probabilités*, volume 9. Gauthier-Villars Paris, 1925.

[42] Gennady Samoradnitsky and Murad S Taqqu. *Stable non-Gaussian random processes: stochastic models with infinite variance*, volume 1. CRC Press, 1994.

[43] Stamatis Cambanis, Gennady Samorodnitsky, and Murad S Taqqu. *Stable processes and related topics: a selection of papers from the Mathematical Sciences Institute workshop, January 9-13, 1990*, volume 25. Birkhauser, 1991.

[44] Vladimir M Zolotarev. *One-dimensional stable distributions*, volume 65. American Mathematical Soc., 1986.

[45] Raya Feldman and Murad Taqqu. *A practical guide to heavy tails: statistical techniques and applications*. Springer Science & Business Media, 1998.

[46] Stefan Mittnik, Marc S Paolella, and Svetlozar T Rachev. Diagnosing and treating the fat tails in financial returns data. *Journal of Empirical Finance*, 7(3):389–416, 2000.

[47] John P Nolan. *Stable distributions*, volume 1177108605. ISBN, 2012.

[48] Wai Ha Lee. *Continuous and discrete properties of stochastic processes*. PhD thesis, University of Nottingham, 2010.

[49] John C Frain. *Studies on the Application of the Alpha-stable Distribution in Economics*. Trinity College, 2009.

[50] Per Bak, Chao Tang, and Kurt Wiesenfeld. Self-organized criticality. *Physical review A*, 38(1):364, 1988.

[51] Nobuko Fuchikami and Shunya Ishioka. Statistics of level crossing intervals. In *Second International Symposium on Fluctuations and Noise*, pages 29–37. International Society for Optics and Photonics, 2004.

[52] David Vernon Widder. The laplace transform. 1946. *Zbl0139*, 29504, 1959.

[53] Maurice Stevenson Bartlett. *An introduction to stochastic processes: with special reference to methods and applications*. CUP Archive, 1978.

[54] David Middleton, Institute of Electrical, and Electronics Engineers. *An introduction to statistical communication theory*, volume 960. McGraw-Hill New York, 1960.

[55] Julius S Bendat and Allan G Piersol. *Random data: analysis and measurement procedures*, volume 729. John Wiley & Sons, 2011.

[56] Maurice Bertram Priestley. Spectral analysis and time series. 1981.

[57] GEP Box, GM Jenkins, and GC Reinsel. Forecasting and control. time series analysis, 1994.

[58] Jose D Salas. Analysis and modeling of hydrologic time series. *Handbook of hydrology*, 19:1–72, 1993.

[59] Anthony R Ives, Karen C Abbott, and Nicolas L Ziebarth. Analysis of ecological time series with arma (p, q) models. *Ecology*, 91(3):858–871, 2010.

[60] Abdelnaser Adas. Traffic models in broadband networks. *IEEE Communications Magazine*, 35(7):82–89, 1997.

[61] Gennady Samorodnitsky and Murad S Taqqu. Linear models with long-range dependence and with finite or infinite variance. In *New directions in time series analysis*, pages 325–340. Springer, 1993.

[62] Jan Beran. *Statistics for long-memory processes*, volume 61. CRC press, 1994.

[63] RF Voss and J Clarke. 1/f noise in speech and music. *Nature*, 258:317–318, 1975.

[64] Holger Hennig, Ragnar Fleischmann, Anneke Fredebohm, York Hagmayer, Jan Nagler, Annette Witt, Fabian J Theis, and Theo Geisel. The nature and perception of fluctuations in human musical rhythms. *PloS one*, 6(10):e26457, 2011.

[65] Daniel J Levitin, Parag Chordia, and Vinod Menon. Musical rhythm spectra from bach to joplin obey a 1/f power law. *Proceedings of the National Academy of Sciences*, 109(10):3716–3720, 2012.

[66] Philip Charles Ingrey. *Optical limits in Left-Handed Media*. PhD thesis, University of Nottingham, 2010.

[67] Keith Iain Hopcraft, Eric Jakeman, and Kevin D Ridley. *The Dynamics of Discrete Populations and Series of Events*. Taylor & Francis, 2014.

[68] Jason Marko Smith. *Discrete properties of continuous, non-Gaussian random processes*. PhD thesis, University of Nottingham, 2007.

[69] Alan M Cohen. *Numerical methods for Laplace transform inversion*, volume 5. Springer Science & Business Media, 2007.

[70] AD Wunsch. Complex variables with applications. 2004.

[71] J Abate and PP Valkó. Multi-precision laplace transform inversion. *International Journal for Numerical Methods in Engineering*, 60(5):979–993, 2004.

[72] RA Spinelli. Numerical inversion of a laplace transform. *SIAM Journal on Numerical Analysis*, 3(4):636–649, 1966.

[73] Kristopher L Kuhlman. Review of inverse laplace transform algorithms for laplace-space numerical approaches. *Numerical Algorithms*, 63(2):339–355, 2013.

[74] Alan Talbot. The accurate numerical inversion of laplace transforms. *IMA Journal of Applied Mathematics*, 23(1):97–120, 1979.

[75] Subhash Chandra Malik and Savita Arora. *Mathematical analysis*. New Age International, 1992.

[76] Murray R Spiegel. *Laplace transforms*. McGraw-Hill New York, 1965.

[77] Milton Abramowitz and Irene A Stegun. *Handbook of mathematical functions: with formulas, graphs, and mathematical tables*, volume 55. Courier Corporation, 1964.

[78] Hernán A Makse, Shlomo Havlin, Moshe Schwartz, and H Eugene Stanley. Method for generating long-range correlations for large systems. *Physical Review E*, 53(5):5445, 1996.

[79] Donald B Percival. Simulating gaussian random processes with speci-fied spectra. *Computing Science and Statistics*, pages 534–534, 1993.

[80] Wilbur B Davenport, William L Root, et al. *An introduction to the theory of random signals and noise*, volume 159. McGraw-Hill New York, 1958.

[81] Aldo H Romero and Jose M Sancho. Generation of short and long range temporal correlated noises. *Journal of Computational Physics*, 156(1):1–11, 1999.

[82] Makse Hernán, Havlin Shlomo, Stanley H Eugene, and Schwartz Moshe. Novel method for generating long-range correlations. *Chaos, Solitons & Fractals*, 6:295–303, 1995.

[83] William H Press. *Numerical recipes 3rd edition: The art of scientific computing*. Cambridge university press, 2007.

[84] Ruey S Tsay. *Analysis of financial time series*, volume 543. John Wiley & Sons, 2005.

[85] George Casella and Roger L Berger. *Statistical inference*, volume 2. Duxbury Pacific Grove, CA, 2002.

[86] Chung-Kang Peng, Shlomo Havlin, Moshe Schwartz, and H Eugene Stanley. Directed-polymer and ballistic-deposition growth with corre-lated noise. *Physical Review A*, 44(4):R2239, 1991.

[87] JA McFadden. The axis crossings of a stationary gaussian markov pro-cess. *Information Theory, IRE Transactions on*, 7(3):150–153, 1961.

[88] Thomas S Ferguson. A representation of the symmetric bivariate cauchy distribution. *The Annals of Mathematical Statistics*, pages 1256–1266, 1962.

[89] Jan F Eichner, Jan W Kantelhardt, Armin Bunde, and Shlomo Havlin. Extreme value statistics in records with long-term persistence. *Physical Review E*, 73(1):016130, 2006.